

Three membered rings as probes in the activity based protein profiling

Dissertation zur Erlangung des Doktorgrades
der Fakultät für Chemie
der Technischen Universität München

von M. Sc. Maximilian Pitscheider
geboren am 05.07.1983
in München

Technische Universität München
Lehrstuhl für organische Chemie II

Three membered rings as probes in the activity based protein profiling

Maximilian Friedrich Pitscheider

Vollständiger Abdruck der von der Fakultät für Chemie der Technischen
Universität München zur Erlangung des akademischen Grades eines
Doktors der Naturwissenschaften
genehmigten Dissertation.

Vorsitzender: Univ.-Prof. Dr. Johannes Buchner

Prüfer der Dissertation:

1: Univ.-Prof. Dr. Stephan A. Sieber

2: Univ.-Prof. Dr. Thomas Brück

Die Dissertation wurde am 27.11.2011 bei der Technischen Universität
München eingereicht und durch die Fakultät für Chemie am 08.12.2011
angenommen.

Meiner Familie

Danksagung

An erster Stelle danke ich meinem Betreuer Prof. Dr. Stephan A. Sieber für die interessante und vielfältige Themenstellung, die exzellenten Arbeitsbedingungen und die große wissenschaftliche Freiheit. Seine große Begeisterungsfähigkeit für das Thema, die stetige Motivation und seine Unterstützung während meiner gesamten Promotionszeit haben entscheidend zum Erfolg dieser Arbeit beigetragen. Vielen Dank auch für die Möglichkeit, durch die Teilnahme an einer Vielzahl von Konferenzen meinen wissenschaftlichen Horizont zu erweitern.

Den Mitgliedern der Prüfungskommission danke ich für ihre Bemühungen und den zeitlichen Aufwand bei der Evaluierung der Arbeit. Prof. Dr. Thomas Brück danke ich recht herzlich für die Übernahme des Koreferats.

Frau Kerstin Kurz und Frau Mona Wolff danke ich für die hervorragende Hilfsbereitschaft bei allen bürokratischen und organisatorischen Fragen und der unverzichtbaren Hilfe im Laboralltag. Den Mitarbeitern der NMR-Spektroskopie Dr. David Stephenson und Claudia Dubler an der LMU und dem Verantwortlichen für die small molecule Massenspektrometrie an der TU, Herrn Burghard Cordes danke ich für die schnelle Aufnahme von NMR- und Massenspektren.

Meiner arbeitskreisinternen Kooperationspartnerin Dr. Nina Mäusbacher danke ich herzlich für ihren unermüdlichen Engagement bei der homologen Überexpression und den Knock-out Studien. Sie übernahm dabei die genetischen Arbeiten bis hin zur Transformierung und ohne ihren großartigen Einsatz und die zahlreichen fruchtbaren Diskussionen wäre dieses Projekt so nicht möglich gewesen.

Frau Dr. Katrin Lorenz-Baath möchte ich in die freundliche und geduldige Einweisung in die Arbeitsmethoden der Zellkultur danken. Ich hoffe ich habe nicht allzuvielen Infektionen eingeschleppt.

Dem gesamten Arbeitskreis, meinen Freunden und liebgewonnenen Kollegen aus drei Jahren und zwei Universitäten möchte ich herzlichst für die entspannte und gemeinschaftliche Atmosphäre im Labor und den zahlreichen außeruniversitären Aktivitäten danken. Ohne die stete Hilfsbereitschaft bei kleineren und größeren Problemen sowie die zahlreichen fachlichen Diskussionen und den Rückhalt, der mich in so mancher Situation aufgefangen hat, wäre diese Arbeit nicht entstanden. Dies gilt nicht nur für Ronald Orth, Thomas Böttcher und Isabell Staub, den Kollegen der ersten Stunde, sondern auch für die Mitglieder des neuen Kreises an der TU, Tanja Wirth, Oliver Battenberg, Jürgen Eirich, Dr. Mathew Nodwell, Georg Rudolf, Franziska Mandl, Mathias Leidl, Dr. Katrin Lorentz-Baath, Maximilian Koch und Maria Damen. Danke für jede Frotzelei, jeden Kalauer und jedes Feierabendbier. Viel Erfolg in eurer weiteren Laufbahn. Macht es einfach!

Meinen Bachelorstudenten Lissa Princz und Matthias Westphal sowie meinen Forschungspraktikanten Tanja Wirth, Tanja Ossiander, Erwin Wiesemayer und Amelie Koch danke ich für ihre hohe Einsatzbereitschaft und Motivation beim Bearbeiten der Projekte. Vielen Dank auch an unsere langjährige wissenschaftliche Hilfskraft Mathias Leidl, dessen hilfsbereite und humorvolle Art nicht mehr aus dem Arbeitskreis wegzudenken sind.

Ebenso bedanken möchte ich mich für die stete Unterstützung meiner Eltern Petra und Karl Pitscheider während meines gesamten Studiums und der Promotionszeit. Euer Zuspruch hat mir stets Kraft gegeben. Dies gilt auch für meine Geschwister Johannes Hönlinger und Susanne Harper und meiner Schwägerin Doris Witt die bei einem Glas Wein immer ein offenes Ohr für mich hatten. Ihr seid die beste Familie, die man sich wünschen kann!

Mein letzter und größter Dank geht an meine Frau Almut Pitscheider, die in jedem Augenblick unserer Beziehung für mich da war und mich aufgebaut hat. Ich danke dir von Herzen für die Geduld, wenn es des Öfteren ein bis zwei Stunden länger als versprochen gedauert hat, oder wenn die Arbeit nicht in der Uni blieb. Du hast mir stets geholfen das Ziel im Auge zu behalten. Eine bessere Unterstützung und eine bessere Partnerin an meiner Seite kann ich mir nicht vorstellen.

Introductory remark

Parts of this thesis have been published in international journals.

Table of Contents

1	Summary	1
2	Zusammenfassung	7
3	Introduction	13
3.1	The return of an old foe	13
3.2	Proteomics	17
3.3	Activity-based protein profiling	18
3.3.1	General	18
3.3.2	Basic design of an ABPP probe	19
3.3.3	Tag free-ABPP	21
3.3.4	Course of a tag free-ABPP experiment	22
3.3.5	Identification of proteins by mass-spectrometry (MS)	24
3.4	Natural products in ABPP	27
3.5	Scope of this work	28
4	Results	31
4.1	Synthesis	31
4.1.1	Cyclopropanes	31
4.1.1.1	General	31
4.1.1.2	Synthetic strategy	33
4.1.2	Oxiranes	34
4.1.2.1	General	34
4.1.2.2	Synthetic strategy	37
4.1.3	Thiiranes	41
4.1.3.1	General	41
4.1.3.2	Synthetic strategy	43
4.1.4	Aziridines	45
4.1.4.1	General	45
4.1.4.2	Synthetic strategy	48
4.2	Summary	50

Table of Contents

4.3 Stability	50
4.4 Proteomics	54
4.5 Assays	64
4.5.1 Minimal inhibitory concentration	64
4.5.2 Toxicity to eucaryotic cells	66
4.6 Target verification by recombinant overexpression	68
4.6.1 General	68
4.6.2 Heterologous overexpression in <i>E. coli</i>	69
4.7 Mechanism of action	73
4.7.1 Fatty acid biosynthesis	73
4.7.2 Genetic Knockout	74
4.7.3 Homologous overexpression	76
4.7.4 Point mutation	80
4.8 Summary	83
5 Experimental section	85
5.1 Organic chemistry	85
5.1.1 Materials	85
5.1.1.1 General	85
5.1.1.2 TLC Stains	86
5.1.2 Synthesis	87
5.1.2.1 Ethyl (<i>2R,3R</i>) oxirane-2,3-dicarboxylate, (1)	87
5.1.2.2 Ethyl (<i>2R,3R</i>) 3-(<i>N</i> -propargylaminocarbonyl) oxirane-2-carboxylate (2 , OxyEt)	87
5.1.2.3 (<i>2R,3R</i>) 3-(<i>N</i> -propargylaminocarbonyl) oxirane-2-carboxylic acid (3)	88
5.1.2.4 Butyl (<i>2R,3R</i>) 3-(<i>N</i> -propargylaminocarbonyl) oxirane-2-carboxylate (4 , OxyBut)	89
5.1.2.5 Hexyl (<i>2R,3R</i>) 3-(<i>N</i> -propargylaminocarbonyl) oxirane-2-carboxylate (5 , OxyHex)	90
5.1.2.6 Octyl (<i>2R,3R</i>) 3-(<i>N</i> -propargylaminocarbonyl) oxirane-2-carboxylate (6 , OxyOc)	91
5.1.2.7 Dodecyl (<i>2R,3R</i>) 3-(<i>N</i> -propargylaminocarbonyl) oxirane-2-carboxylate (7 , OxyDode)	92
5.1.2.8 Benzyl (<i>2R,3R</i>) 3-(<i>N</i> -propargylaminocarbonyl) oxirane-2-carboxylate (8 , OxyBenz)	93

5.1.2.9	Allyl (<i>2R,3R</i>) 3-(<i>N</i> -propargylaminocarbonyl) oxirane-2-carboxylate (9 , OxyAll)	94
5.1.2.10	Ethyl (<i>2S,3S</i>) 3-(<i>N</i> -propargylaminocarbonyl) thiirane-2-carboxylate (10 , ThiEt)	95
5.1.2.11	Butyl (<i>2S,3S</i>) 3-(<i>N</i> -propargylaminocarbonyl) thiirane-2-carboxylate (11 , ThiBut)	96
5.1.2.12	Hexyl (<i>2S,3S</i>) 3-(<i>N</i> -propargylaminocarbonyl) thiirane-2-carboxylate (12 , ThiHex)	97
5.1.2.13	Octyl (<i>2S,3S</i>) 3-(<i>N</i> -propargylaminocarbonyl) thiirane-2-carboxylate (13 , ThiOc)	98
5.1.2.14	Dodecyl (<i>2S,3S</i>) 3-(<i>N</i> -propargylaminocarbonyl) thiirane-2-carboxylate (14 , ThiDode)	99
5.1.2.15	Benzyl (<i>2S,3S</i>)-3-(<i>N</i> -propargylaminocarbonyl) thiirane-2-carboxylate (15 , ThiBenz)	100
5.1.2.16	Allyl (<i>2S,3S</i>)-3-(<i>N</i> -propargylaminocarbonyl) thiirane-2-carboxylate (16 , ThiAll)	101
5.1.2.17	General procedure for the preparation of the aziridine probes:	102
5.1.2.18	(<i>E</i>)-ethyl 4-oxo-4-(prop-2-yn-1-ylamino)but-2-enoate (17 , MichEt)	102
5.1.2.19	Ethyl (<i>2R*,3R*</i>)-3-(<i>N</i> -propargylaminocarbonyl) aziridine-2-carboxylate (18 , AziEt)	103
5.1.2.20	(<i>E</i>)-4-oxo-4-(prop-2-yn-1-ylamino)but-2-enoic acid (19)	104
5.1.2.21	(<i>E</i>)-octyl 4-oxo-4-(prop-2-yn-1-ylamino)but-2-enoate (20 , MichOc)	105
5.1.2.22	(<i>E</i>)-benzyl 4-oxo-4-(prop-2-yn-1-ylamino)but-2-enoate (21 , MichBenz)	106
5.1.2.23	Octyl (<i>2R*,3R*</i>) 3-(<i>N</i> -propargylaminocarbonyl) aziridine-2-carboxylate (22 , AziOc)	107
5.1.2.24	Benzyl (<i>2R*,3R*</i>)-3-(<i>N</i> -propargylaminocarbonyl) aziridine -2-carboxylate (23 , AziBenz)	108
5.1.2.25	Diethyl cyclopropane-1,2-dicarboxylate (24)	108
5.1.2.26	2-(ethoxycarbonyl)cyclopropane-carboxylic acid (25)	109

Table of Contents

5.1.2.27	1-ethyl 2-hex-5-yn-1-yl cyclopropane-1,2-dicarboxylate (26 , CycloEt)	109
5.2	Biochemistry	111
5.2.1	Microbiology	111
5.2.1.1	Materials	111
5.2.1.1.1	Bacteria	111
5.2.1.1.2	Antibiotic stocks	111
5.2.1.1.3	Media	112
5.2.1.1.4	Agar plates	113
5.2.1.2	Methods	113
5.2.1.2.1	Cryostocks	113
5.2.1.2.2	Competent cells	114
5.2.2	Cell culture	117
5.2.2.1	Materials	117
5.2.2.1.1	Buffers	117
5.2.2.2	Methods	117
5.2.2.2.1	Cultivation and splitting	117
5.2.2.2.2	Counting	118
5.2.2.2.3	MTT Assay	119
5.2.3	Genomics	121
5.2.3.1	Materials	121
5.2.3.1.1	Buffers	121
5.2.3.1.2	Enzymes	122
5.2.3.2	Plasmids	122
5.2.3.2.1	Size standards	123
5.2.3.2.2	Primers	123
5.2.3.3	Methods	127
5.2.3.3.1	Extraction of genomic DNA	127
5.2.3.3.2	PCR	127
5.2.3.3.3	Agarose gelectrophoresis	133
5.2.3.3.4	Gateway cloning	134
5.2.3.3.5	Ligation independent cloning	137
5.2.3.3.6	Ligation	138
5.2.3.3.7	Transformation	139
5.2.3.3.8	Site directed mutagenesis	141

5.2.3.3.9	Gene knockout	143
5.2.3.3.10	Gene overexpression	147
5.2.4	Proteomics	149
5.2.4.1	Materials	149
5.2.4.1.1	Devices	149
5.2.4.1.2	Buffers	149
5.2.4.1.3	Fluorescent dyes, ligands and linkers for click-chemistry	152
5.2.4.2	Methods	153
5.2.4.2.1	SDS-PolyAcrylamid-Gel Electrophoresis (SDS-Page)	153
5.2.4.2.2	Coomassie-staining	155
5.2.4.2.3	Bradford Assay	155
5.2.4.2.4	Preparation of proteomes	156
5.2.4.2.5	Heat control	157
5.2.4.2.6	Analytic proteome labeling <i>in vitro</i>	157
5.2.4.2.7	Analytic proteome labeling <i>in situ</i>	158
5.2.4.2.8	Preparative proteome labeling <i>in situ</i>	158
5.2.4.2.9	Bioinformatics	161
	Curriculum vitae	163
	Publications	165
	List of abbreviations	167
	Bibliography	171

1 Summary

Due to the rapid development of multiresistant pathogenic bacteria during the last 50 years, infectious diseases pose a serious threat to public health. In the U.S., infections with multiresistant bacteria account for a higher death toll than e.g. HIV.^[1] At the same time, the arsenal of effective antibacterial drugs is dwindling. The employment of a very limited number of different drugs, which target just a handful of bacterial processes, facilitate the adaptation of bacteria to these drugs. Therefore, the quest for novel lead structures and the discovery of yet unexplored biochemical pathways which could be used in the fight against multiresistant bacteria has returned to the focus of the scientific community. In the last years, one key technology emerged and excelled in these investigations. This interdisciplinary method, called activity-based protein profiling (ABPP) uses small reactive molecules as probes which specifically bind to the active sites of their target enzymes (see Figure 1.0.0.1).

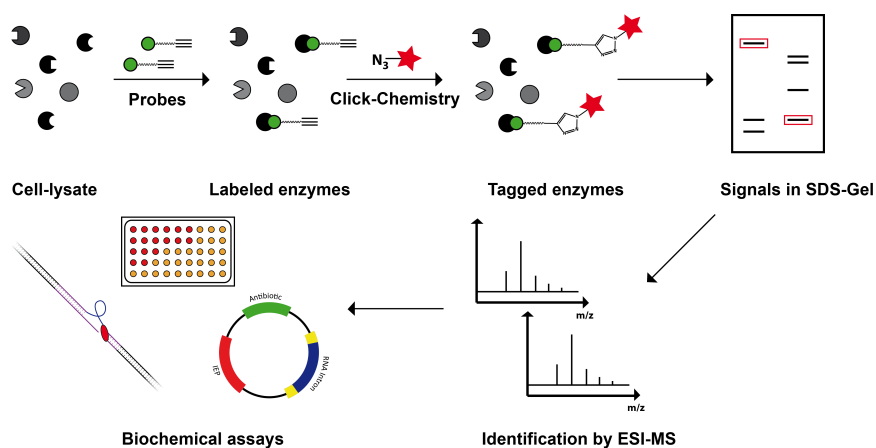


Figure 1.0.0.1: *Schematic overview of an ABPP experiment*

By fusing the labeled enzymes with a fluorescent tag, these enzymes can be visualized in complex proteomes by in-gel fluorescent scans and subsequently identified via mass spectrometry. If the identified targets are pathogenesis-related or part of cellular processes which are vital for the bacterium, the deployed probe is likely to show antibacterial properties. Additional biochemical assays, like minimal inhibitory concentration- or proteolysis-assays, can then be applied to determine the pharmacological potential of the compound (e.g. antibiotic activity, toxicity, etc.).

The scope of the present thesis, was to investigate the antibacterial potential of three membered rings and to identify their enzymatic targets in bacteria. Therefore we synthesized a small library of compounds containing three membered ring systems. The structural layout of all probes was based on one scaffold related to the protein-reactive natural product E-64, originally isolated from *Aspergillus japonicus*. The library consists of substituted homo-(cyclopropane) as well as heterocyclic probes (aziridine, oxirane, thiirane), which were used in a comparative study to analyze their biological activity (see Figure 1.0.0.2).

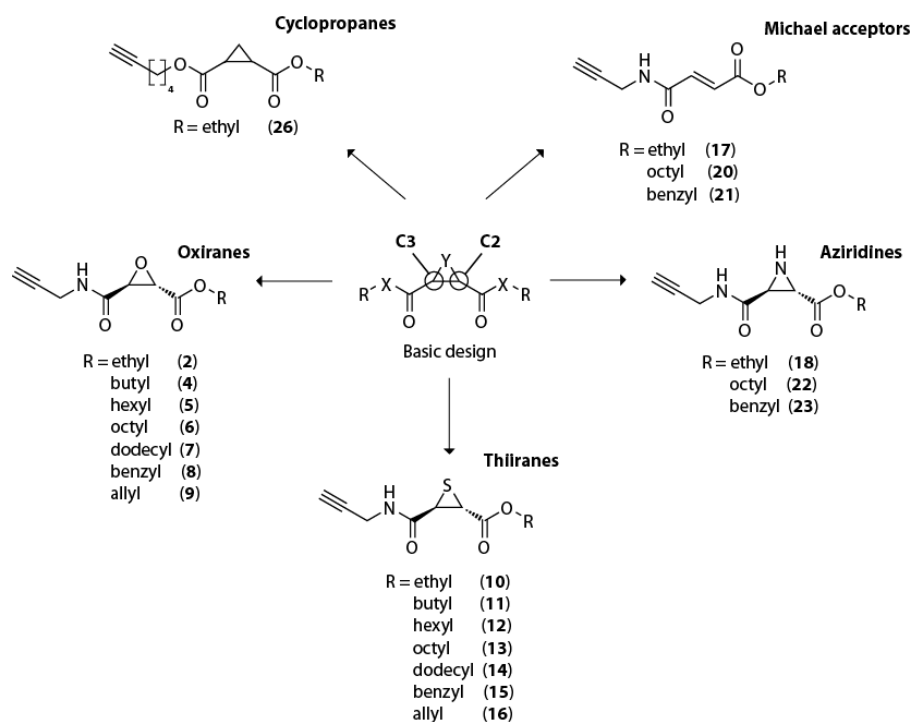


Figure 1.0.0.2: *Library of synthesized probes*

The only difference between the individual molecules of the compound library was the chemical composition of the cycles. This allowed to compare the proteome reactivities of the probes based on these differences. To maximize enzyme coverage, the compound library was established with a number of probes carrying a variety of decorations in the C2 position. Small (ethyl-, allyl-) and longer (octyl-) aliphatic residues as well as an aromatic residue (benzyl-) were used to increase fitting of the different probes with the active sites of structurally diverse enzymes.

The compound library was applied to living bacteria to investigate the enzymatic targets of different probes. After incubation, the cells were lysed and separated via SDS-PAGE (Sodium-Dodecylsulfate-Gelelectrophoresis). A subsequent in-gel fluorescent scan visualized all enzymes labeled by the different probes. As expected, the probes displayed a variation in activity and selectivity, as a function of the core motif as well as the decorations. The oxirane and thiirane probes proved to label enzymes selectively in concentrations as low as 50 μM (see Figure 1.0.0.3).

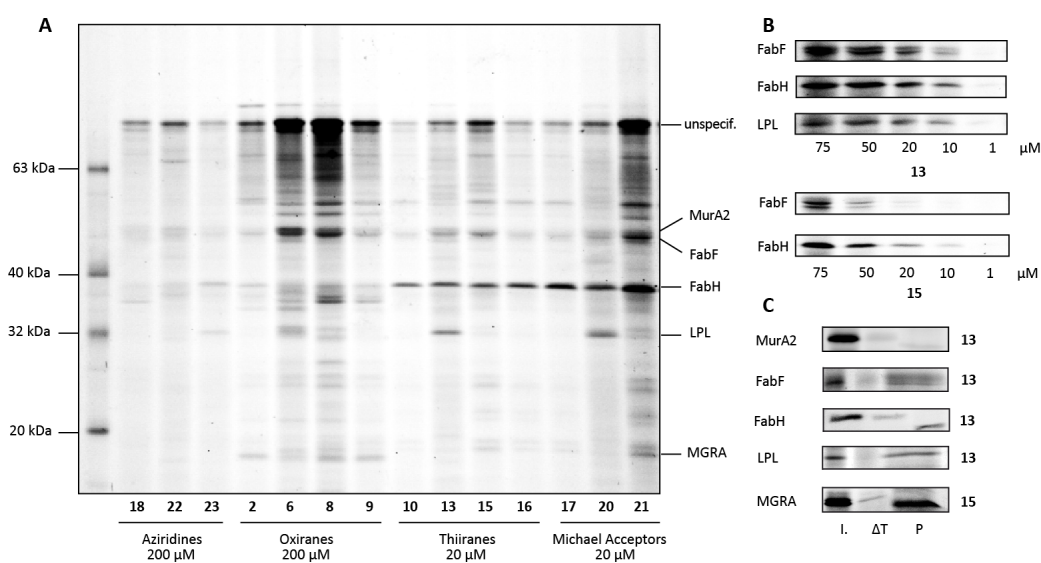


Figure 1.0.0.3: In situ probe labeling in *S. aureus* *Mu50* at optimal concentrations (A) derived by dose down experiments (B). Verification of mass spec identification via labeling of recombinant proteins (C)

The analysis of the targets of the oxirane and thiirane probes by HPLC-MS (High-Pressure Liquid-Chromatography coupled Mass Spectrometry), led to the identification of two vital enzymes (Fatty-Acid-Biosynthesis enzymes F and H, FabF and FabH) in *Listeria monocytogenes* and *Staphylococcus aureus*. These results were confirmed by a heterologous (*Escherichia coli*) and a homologous (*Listeria monocytogenes*) overexpression and subsequent labeling experiments of the targets. Both enzymes are essential members of the KAS-II fatty acid biosynthesis pathway. It can be found in most bacteria in a highly conserved form and consists of a series of discrete proteins, each of which catalyzes an individual biosynthetic reaction. The KAS-II pathway is vital for both survival and growth of the bacterium and is only found in prokaryotes. These features qualify the enzymatic route as an ideal antibiotic target.^[2]

Both FabF and H contain a nucleophilic active-site cysteine residue, which is able to attack the probes electrophilic ring system. The formation of this covalent bond strips the enzymes of its function.^[3,4,5] The nucleophilicity of the active site cysteine in FabF and H is enhanced by two alternate mechanisms, leading to distinct reactivities of both enzymes. These disparities in the active site reactivities are represented by the different labeling specificities of the single probes. The oxirane probes specifically labeled FabF, whereas thiirane probes were able to react with FabH and FabF. This shows how a change the composition of a ring structure, can be used to tune the reactivity of a tricyclic molecule to increase the range of enzymatic targets of the compound.

Subsequent measurements of minimal inhibitory concentrations of all probes in *Listeria monocytogenes* and *Staphylococcus aureus* revealed strong antibiotic activities of single thiirane probes (e.g. **13**: 75 μ M). Oxirane probes however did not show these effects. As a double inhibition of FabF and H results in germicidal properties, the antibiotic effect featured by the thiirane probes was proposed to be connected to this mechanism.^[6,7]

If inhibition of both enzymes was related to the antibiotic activity observed, a homologous overexpression of each target was assumed to have an alleviating effect on the outcome of the minimal inhibitory concentration assay. This, however, was not the case. The FabF and FabH dual-inhibition of the thiiranes could provide an explanation for this finding. As both FabF and H are involved in the same pathway, the enzyme less expressed might be the limiting

factor of the whole biosynthetic pathway. Therefore, the overexpression of one single enzyme should have no effect on the overall turnover of the pathway. The homologous coexpression of the two enzymes will give a final answer to this interesting question and would provide an interesting topic for a future research project.

To validate the active site specificity of the probes, the active-site cysteines of FabF and H were mutated to alanines. This mutation was thought to strip the enzymes of their catalytic activity and therefore the ability to bind the probes. As expected, the labeling intensity of the mutated FabH decrease significantly. The labeling of FabF, however, remained unchanged. This led to a first conclusion that FabF labeling was not dependant on a functional active site. On the other hand the pre-incubation of FabF wild-type enzyme with an excess of the FabF-specific inhibitor cerulenin resulted in decreased labeling intensity. The same effect could be observed when the enzyme was unfolded by heat denaturation or by alkylating the cysteines of FabF by preincubation with Iodacetamide. This puzzling result led to the conclusion, that the reaction of the oxirane and thirane probes with FabF does not depend on the active site known from literature, but on another nucleophilic cysteine residue in FabF. The identification and analysis of this alternative nucleophilic site will be subject to further mutation-studies in the future.

2 Zusammenfassung

Durch die rasche Resistenzentwicklung pathogener Keime innerhalb der letzten 50 Jahre stellen Infektionskrankheiten heutzutage wieder ein ernstzunehmendes Problem für das Gesundheitssystem dar. Als Folge schrumpft die Anzahl wirksamer Medikamente im Kampf gegen diese Erreger. Mittlerweile sterben in den USA jährlich mehr Menschen an den Folgen dieser bakteriellen Infektionen als an HIV.^[1] Der Einsatz einer geringen Bandbreite an unterschiedlichen Medikamenten, die wiederum nur auf eine begrenzte Anzahl bakterieller Prozesse abzielen, begünstigen die rapide Anpassung der Bakterien an eben jene Substanzen. Daher ist in den letzten Jahren die Suche nach neuartigen Leitstrukturen, sowie die Erschließung von bislang unerforschten biochemischen Abläufen in Bakterien in den Fokus der Forschung zurückgekehrt. Eine Technologie hat sich dabei als besonders leistungsfähig für die Erforschung neuer Antibiotika herausgestellt. Im aktivitätsbasierenden Protein-profiling (ABPP) werden kleine reaktive Moleküle eingesetzt, um als Sonden spezifisch mit den aktiven Zentren verschiedener Zielenzyme zu reagieren (siehe Abbildung 2.0.0.4).

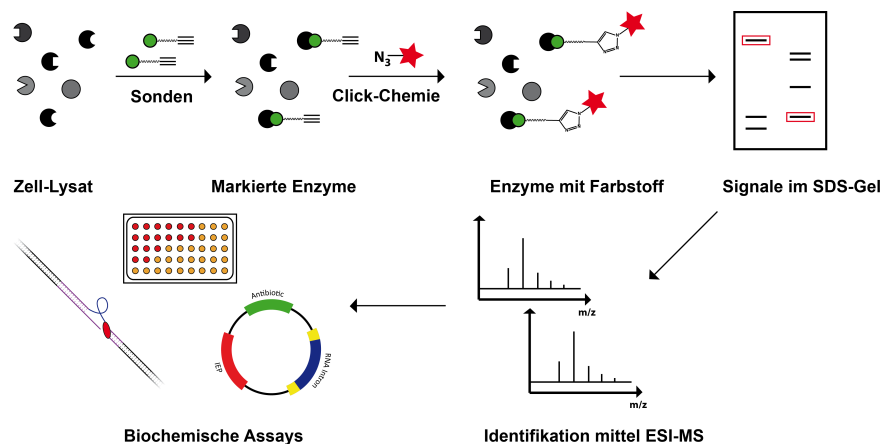


Abbildung 2.0.0.4: Schematischer Ablauf eines ABPP-Experiments

Anschließend kann ein Fluoreszenzmarker an die sondenmarkierten Proteine gekoppelt werden, welcher die Visualisierung jener Proteine in einem in-Gel-Fluoreszenzscan ermöglicht. Diese markierten Enzyme können anschließend über Massenspektrometrie identifiziert werden. Werden lebensnotwendige oder pathogenitätsassoziierte Enzyme als Targets ermittelt, können geeignete biochemische Assays dazu dienen, das pharmakologische Potential (z.B. antibiotische Aktivität, Toxizität etc.) der jeweiligen Verbindung zu erkunden.

Die Zielsetzung der hier vorgestellten Doktorarbeit war eine vergleichende Untersuchung der proteomischen Aktivität einer Reihe von Dreiringstrukturen. Hierfür wurde zunächst eine kleine Bibliothek substituierter homo- (Cyclopropane) sowie heterocyclischer Dreiringe (Aziridine, Oxirane, Thiirane) synthetisiert (siehe Abbildung 2.0.0.5).

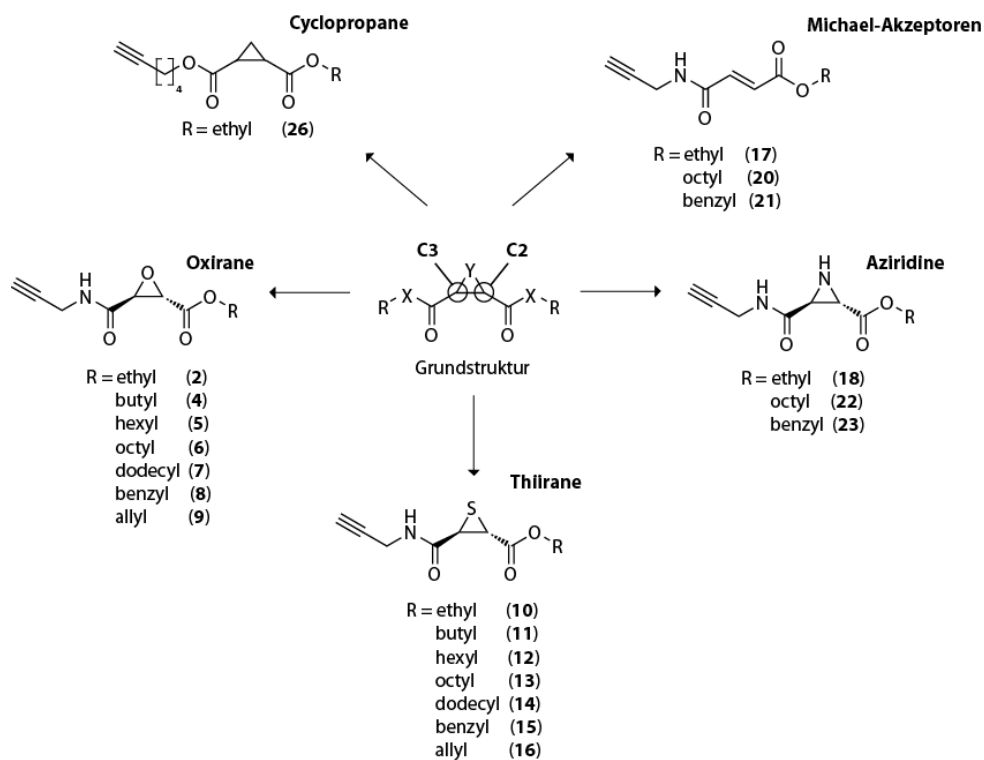


Abbildung 2.0.0.5: Übersicht über die Sondenbibliothek

Um den Einfluss der atomare Zusammensetzung des Ringes auf die proteomische Reaktivität der Sonden untersuchen zu können, galt es das Grundgerüst aller Sonden weitgehend identisch zu gestalten. Zusätzlich wurde die Bandbreite an enzymatischen Zielen zu erhöht, indem die Sonden an einer Position des Ringes (C2) mit einer Reihe von Modifikationen versehen wurden. Durch die Verknüpfung der Grundstruktur mit kurzen (Ethyl) oder langkettigen Alkylresten (Octyl), oder aber mit aromatischen Seitenketten (Benzyl) erhöht sich die Chance auf eine Interaktion der einzelnen Sonden mit den verschiedenartigen aktiven Zentren der unterschiedlichen Enzyme.

Indem Bakterien die Sonden in ihr Cytosol aufnehmen, können die einzelnen Sonden mit ihren enzymatischen Zielen in der lebenden Zelle reagieren. Die so markierten Enzyme können nach Lyse der Bakterien über Gelelektrophorese aufgetrennt und über einen Fluoreszenzscan sichtbar gemacht werden. Wie erwartet zeigten die Sonden in Abhängigkeit von der Zusammensetzung sowie des Substitutionsmusters des Ringes, Unterschiede sowohl in ihrer Reaktivität, als auch in ihrer Selektivität gegenüber einzelnen Enzymen (siehe Abbildung 2.0.0.6).

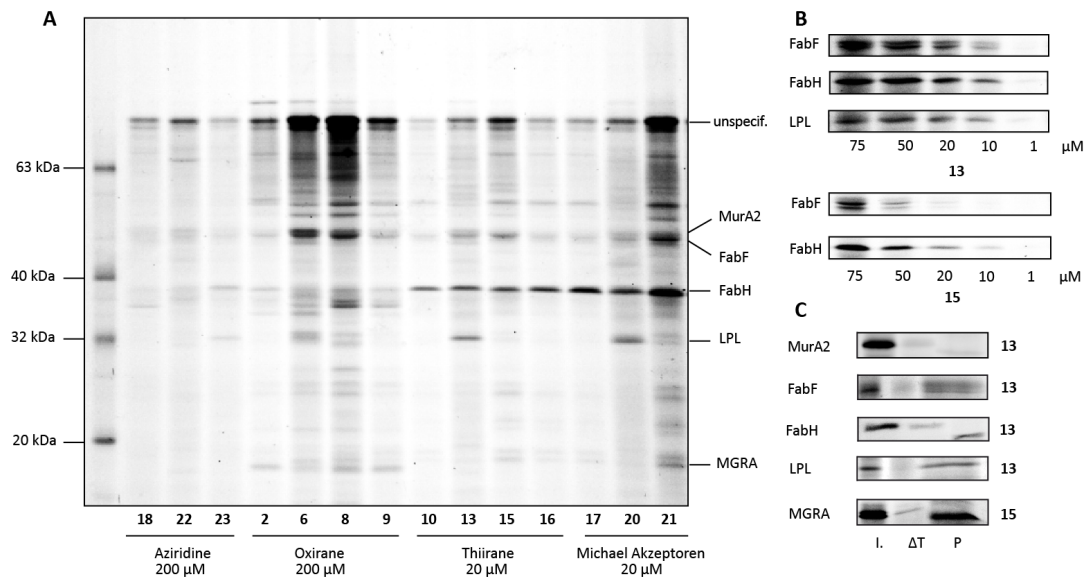


Abbildung 2.0.0.6: In situ Markierung von *S. aureus* Mu50 bei optimalen Sondenkonzentrationen (A) ermittelt über by dose-down Experimente (B). Validierung der massenspektrometrischen Ergebnisse mittels einer Markierung der rekombinanten Proteine (C)

Thiiran- und Oxiran-basierte Sonden zeigten die intensivsten Signale und zeichneten sich durch spezifische Markierungsereignisse bei Konzentrationen bis zu 10 μM aus. Die Analyse der markierten Enzyme mittels HPLC-MS führte unter anderem zu der Identifizierung zweier Proteine (FabF und H), welche lebenswichtig für eine Reihe von Bakterien sind (z.B. *Listeria monocytogenes* und *Staphylococcus aureus*). Die Identität beider Enzyme konnte mittels homologer und heterologer Überexpression bestätigt werden.

Die zwei Enzyme sind ein zentraler Bestandteil des KAS-II Systems, welches für die bakterielle Fettsäurebiosynthese verantwortlich ist. Dieser Prozess ist sowohl für das Wachstum als auch für das Überleben vieler Bakterien unerlässlich. Das KAS-II System liegt in einem Großteil aller Bakterien konserviert vor und besitzt keine homologe Entsprechung in Eukaryoten, weshalb es als ideales Ziel für Antibiotika gilt. Sowohl FabF als auch FabH besitzen ein nukleophiles Cystein in ihrem aktiven Zentrum, das einen Angriff auf den elektrophilen Grundkörper der Sonden ermöglicht.^[3,4,5] Dennoch unterscheiden sich die Reaktivitäten der beiden aktiven Zentren deutlich, da die Aktivierung der Cysteine auf zwei unterschiedlichen Mechanismen beruht. Diese Unterschiede in der Aktivität spiegeln sich in den Markierungsspezifitäten der einzelnen Sonden wider. So reagieren Oxiran-basierte Sonden ausschließlich mit FabF, während Thiiransonden sowohl FabF als auch FabH markieren. Dies zeigt, wie durch eine Änderung der Zusammensetzung des Dreiringes die Reaktivität eines Moleküls optimiert werden kann, um neue enzymatische Ziele erschließen zu können.

Die Untersuchung der minimalen inhibitorischen Konzentration der Sonden ergab eine antibiotische Aktivität der Thiirane bis zu 75 μM (Sonde **13**) in den pathogenen Stämmen *Listeria monocytogenes* EGD-e and *Staphylococcus aureus* Mu50. Die Oxiran-Sonden zeigten hingegen keinerlei antibiotische Wirkung. Da laut Literatur die duale Inhibition der beiden Fettsäuresynthasen das Wachstum sowie die Überlebensfähigkeit von Bakterien stark einschränkt, wird die antibakterielle Wirkung der Thiirane auf diesen dualen Inhibitionsmechanismus zurückgeführt.^[6,7]

Um diese Hypothese zu beweisen, wurde im Weiteren der Effekt der getrennten homologen Überexpression von FabF und H in *Listeria monocytogenes* EGD-e auf die minimale inhibitorische Konzentration der Thiirane untersucht. Erwartet wurde eine Zunahme der Konzentration, da ein Überschuss

an Enzym zu einer vermehrten Absorption des antibiotisch wirksamen Moleküls führen sollte. Dieser Effekt konnte so jedoch nicht beobachtet werden. Eine mögliche Erklärung bietet der duale Inhibitionsmechanismus der Thiirane. Da beide Enzyme an der Fettsäurebiosynthese beteiligt sind, limitiert das geringer exprimierte Enzym den Durchsatz des Gesamtprozesses. Daher ist es wahrscheinlich, dass die Überexpression des zweiten Enzyms keinen entscheidenden Einfluss den Gesamtdurchsatz hat. Einen eindeutigen Nachweis wird die homologe Coexpression beider Enzyme liefern, die zum gegenwärtigen Zeitpunkt vorgenommen wird.

Um die Spezifität der Sondenmarkierung zu belegen, wurden die nucleophilen Cysteine in den aktiven Zentren beider Moleküle durch Punktmutationen gegen katalytisch inaktive Alanine ausgetauscht. Erwartungsgemäß konnte das modifizierte FabH nicht mehr von den Thiiransonden markiert werden. FabF hingegen zeigte überraschenderweise keinen erkennbaren Unterschied in der Intensität der Markierung, was auf eine unspezifische Reaktion der Sonden hinweist. Jedoch führte sowohl die Präinkubation mit einem Überschuss des FabF-spezifischen Inhibitors Cerulenin, als auch eine Hitzedenaturierung des Enzyms zu einer Reduktion der Signalintensität. Diese Ergebnisse deuten auf eine Reaktion der Sonde mit Aminosäuren außerhalb des literaturbekannten aktiven Zentrums hin. Die Untersuchung dieses Mechanismus wäre ein lohnenswertes Thema für zukünftige Forschungsarbeiten.

3 Introduction

3.1 The return of an old foe

From the discovery of penicillin in 1928 by Alexander Fleming to its introduction to the public in 1944, it took 16 years of intensive international pharmacological development to prove its antibacterial potency and to find a way for mass production.^[8,9] At this time, over 94 % of *Staphylococcus aureus* isolates were susceptible to the new miracle drug. The war against infectious diseases seemed to have ended with a triumphant victory. However only 6 years later, half of the isolated bacteria were immune, another ten years later many hospitals reported outbreaks of methicillin-resistant *S. aureus* (MRSA). Today only 10 % of *S. aureus* strains are Penicillin susceptible^[10,11] and MRSA are estimated to make up 40 % of hospital-acquired infections in the U.S. and Europe, posing again a serious and rising threat to public health (see Figure 3.1.0.7).

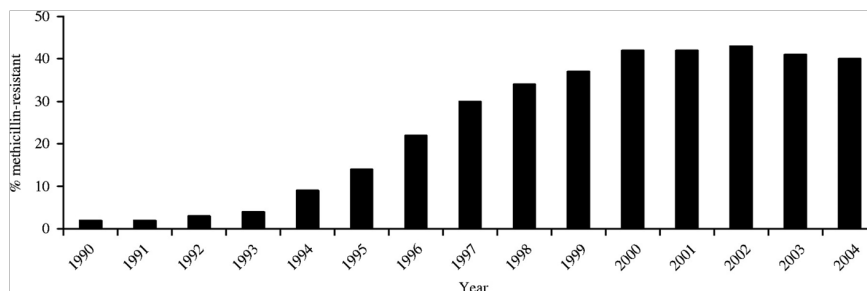


Figure 3.1.0.7: *Proportion of isolates of methicillin-resistant S. aureus from blood culture in England and Wales.*^[12]

A study conducted in the U.S. in 2005 concluded that MRSA were responsible for an estimate of 94,000 life-threatening infections and 18,650 deaths in the same year – more than were caused by HIV in the same period.^[1] Additionally, infections are no longer limited to people with weakened immune systems: about 15 % of invasive infections occurred in people with no

known health care risk.^[1] The first reports from the European Antimicrobial Resistance Surveillance System (EARSS) in 2001 indicated that bloodstream infections with MRSA were an alarmingly widespread problem, with the resistant bacteria accounting for >25 % of *S. aureus* population in the majority of European countries (see Figure 3.1.0.8).

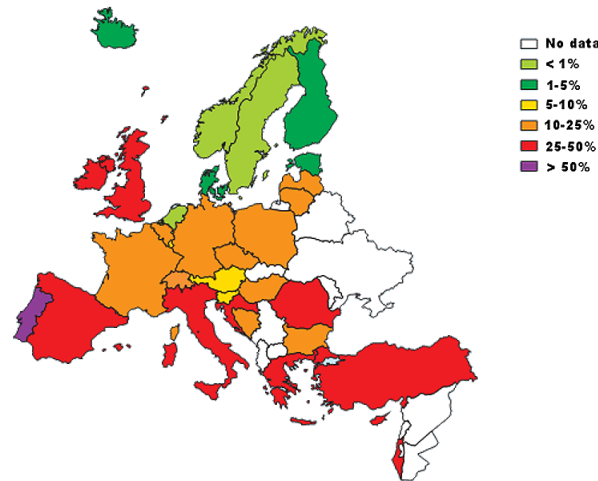


Figure 3.1.0.8: *Proportion of invasive MRSA isolates resistant to oxacillin in 2008*^[13]

Several attempts to reduce the numbers of MRSA infections seemed to initially have little effect, with the rates of methicillin resistance among invasive *S. aureus* remaining high in many countries over the next few years. However, in 2008 the EARSS Annual Report noted that 'For the first time more countries showed decreasing MRSA proportions instead of increasing trends', but also stating that MRSA proportions are still above 25 % in one third of countries.^[12,13] Given these appalling numbers, the identification of new antimicrobial substances should be seen to be one of the priority goals of the current pharmaceutical research. Instead, with the exception of two new antibiotics, the lipopeptidic Daptomycin and the 1,3-oxazolidinone Linezolid, there have been no new classes of clinically relevant antibiotics discovered in over 20 years. The deployment of any novel antibiotic has been followed by the evolution of clinically significant resistance to that same substance in as little as 3 to 10 years (see Figure 3.1.0.9). Thus research in this field became economically unattractive, leaving the possibility of a post-antibiotic era all too real.^[14,15]

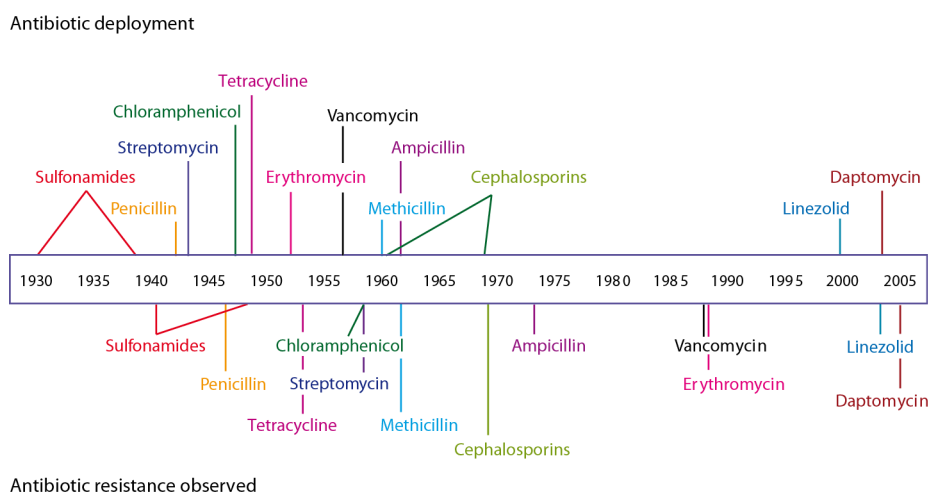


Figure 3.1.0.9: *Timeline of antibiotic deployment (above line) and the evolution of antibiotic resistance (below line).*^[14]

The rapid development of resistance is not only caused by overprescriptions^[16], shortened courses by patients^[17] and the liberal use of antibiotics in the farming industries^[18,19]. But it is also understood that the majority of currently available antibiotics target only a very limited number of the bacterias vital cellular functions such as cell wall synthesis, protein biosynthesis, DNA replication or RNA transcription.^[20,21] The largest fraction of antimicrobial agents is even restricted to the inhibition of the first two processes, e.g. β -lactams, macrolides, quinolones and aminoglycosides, which make up the majority of currently available compounds. Although these compounds were effective in the past, the selective pressure applied on just a handful of enzymes by a limited number of molecules with similar core structures led to a rapid development of resistance. Maybe the best studied examples for this process are the mutations in the so called penicillin binding proteins (PBPs), which are responsible for the biosynthesis of peptidoglycans, a central element of the bacterial cell wall. β -lactams (which include Penicillins, Cephalosporins, and Carbapenems) target the transpeptidase activity of these enzymes, thereby obstructing this cellular process which is vital for cell division. The mutation just one or two amino acids of the PBP creates enough structural changes in the protein to allow the modified enzyme PBP2a to perform the critical cell wall cross-linking reaction even in the presence of β -lactam antibiotics.^[22,23] This novel PBP2a is encoded by the *mecA* structural gene that is

part of a larger mobile genetic element called the staphylococcal chromosomal cassette *mec* (SCC*mec*), and allows for a rapid horizontal gene exchange in bacterial populations.^[24,25]

Besides changing the target structure, three additional general mechanisms of resistance are deployed by bacteria in order to survive antibiotic treatment.^[26] One is the reduction of the effective intracellular concentration of the compounds by an increased expression of efflux pumps which are able to promote the active removal of a wide variety of antibacterial substrates. Proteins like ATP-Binding Cassette (ABC) transporters^[27] the multidrug and toxic compound extrusion (MATE) family,^[28] and especially the resistance-nodulation-division (RND) superfamily play a key role in this clinically relevant resistance in bacteria.^[29,30,31,32] The second method is the overexpression of the pharmacological target to absorb large quantities of the antibiotic.^[33] E.g. by changing the composition, the linkage and the thickness of the bacterial cell wall, the recognition sequences for the antibiotic are multiplied, thereby leading to a decreased susceptibility towards the antibiotic.^[33,34] Amongst others, this mode of antibiotic resistance can be found in multiresistant bacteria (e.g. *S. aureus* Mu50), where it is closely connected to a rising Vancomycin resistance. The third, and probably the most traditional method of dealing with antibiotics is the production of enzymes that are able to metabolize antimicrobial agents. These enzymes often have a limited target specificity and focus only on the core motif, thereby rendering a whole class of antibiotics useless.^[35] The most famous examples are β -lactamases which are thought to have evolved from the PBPs, judged by their high sequence homology. Their development was likely due to the selective pressure exerted by β -lactam-producing soil organisms found in the environment and not due to human interference. The first representative was identified in *Escherichia coli* prior to the release of Penicillin for use in medical practice.^[36,37] Resistance related to these enzymes can often be circumvented by a combination therapy of specific lactamase inhibitors along with the actual antibiotic.^[38] The above mentioned mechanisms often occur in a synergistic manner, significantly increasing the resistance of the organism. By relying on the activity of the same known core structures, targeting the same pathways and ignoring the advances of bacterial evolution the arsenal of future antibiotics is dwindling. The neglected quest for new core structures and the discovery of unexplored

biochemical pathways, which could be exploited as antibacterial targets must return to the focus of the scientific community. With the publication of a list of unsettling reports of a rising threat by community acquired multiresistant pathogens in the last years, this finally seems to be the case.

3.2 Proteomics

“In the wonderland of complete (genomic) sequences, there is much that genomics cannot do, and so the future belongs to proteomics: the analysis of complete complements of proteins”^[39]. With these words Stanley Fields summarized in an article in the journal ‘Science’ the state of the biological sciences after the determination of the human genome in the year 2001. The scientific community believed to be able to understand the complex biochemistry of life by only deciphering the genetic code of different organisms. A hope soon followed by a disappointment. Classical genomic analysis soon reached their limits, as it became clear that the regulation of the translational products of the DNA, the proteins, was far more complex than imagined. By only observing mRNA levels and monitoring the downstream effects of knockout mutations it is nearly impossible to gain an insight into the elaborate web of inter-protein regulation mechanisms, as the amount of mRNA does not necessarily correspond to protein levels or their activity.^[40] The insufficiency of genomic studies to fully describe the mechanistic functioning of a cell led to the creation of the field of proteomics; the study of the proteome, the entire complement of proteins of a cell at a certain point of time under specified conditions. This discipline, in analogy to genomics, was soon called proteomics.

Classical proteomic approaches investigated the expression levels of these different enzymes under different conditions. The quantity of available enzymes under certain conditions were thought to relate to the cellular functions of these enzymes. The effects of inhibitor molecules on the organism were deduced, by comparing enzyme quantities of untreated and treated cells. This first approximation of equalizing protein expression levels with cellular function soon proved to be lacking. Since in many cases proteins are subject to downstream regulatory processes, the amount of a given protein occasio-

nally does not correlate with its biological activity or its related physiological function. This is particularly important for degradative enzymes, such as proteases. Because unregulated proteases can pose a threat to the function of a cell, the activity of proteases is therefore tightly regulated through a series of post-translational processes like phosphorylation, acetylation or glycosylation. These modifications may serve as address labels for intracellular transport, up- or downregulate activity or tag them for immediate recycling. Therefore classical proteomic methods did not allow direct conclusions regarding protein function or the mechanism of action of inhibitor molecules. To overcome this limitation, a new chemical proteomics approach, called activity-based protein profiling (ABPP), was established by the research groups of Cravatt^[41,42] and Bogoy^[43,44] about ten years ago.

3.3 Activity-based protein profiling

3.3.1 General

ABPP relies on the design of small molecule probes to investigate enzyme families in complex proteomes and to provide the basis for a functional investigation of individual enzymes. ABPP probes utilize a range of chemical scaffolds based on protein-reactive natural products or other general electrophilic motifs. By covalently reacting with the active site of a functional enzyme the probes bind to their target enzyme, allowing the attachment of a tag to visualize labeled enzymes. With this technique it is possible to identify enzymes and study their activity, function, and regulation *in vitro* as well as *in situ*. These features can for example be used in the development of new antibiotic lead structures. The classical procedure for the discovery of bioactive compounds is a tedious process and relies in many cases on coincidence (e.g. high-throughput screens). In the end it is all too often outrun by the rapid development of bacterial resistances in the ensuing years. A streamlined approach to identify novel antibiotic targets and the intracellular interaction

partners of new lead compounds could possibly help to shorten the timeline of the development of new antibacterial compounds. The identification of proteomic binding partners of a novel antibiotic lead-structure can then be used as a starting point for the structure-based optimization, thereby creating a rationale for synthetic chemists.

3.3.2 Basic design of an ABPP probe

The so called probes used in ABPP are small organic molecules, generally consisting of one optional and three essential elements. The protein reactive group, which covalently binds to the active sites of individual enzymes with a high affinity. A tag which either enables the addition (e.g. alkyne-tag) of a reporter group or serves as a reporter function itself. And finally a spacer linking the foresaid elements (see Figure 3.3.2.1).

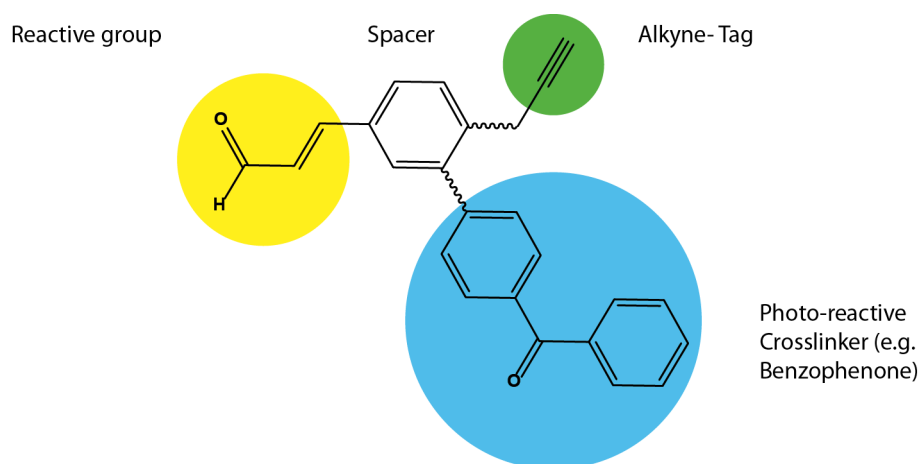


Figure 3.3.2.1: *Schematic structure of a Michael acceptor-based ABPP probe*

A reporter group can either be attached during synthesis (classical ABPP) or after binding to the target enzyme (tag-free ABPP), with the latter being more favorable. As the reporter tag in the classical ABPP either consists of a fluorescent dye or a biotin, the steric hindrance reduces the cell-permeability of the probes and may disable binding to the target enzyme. The fourth and

optional element consists of a photoreactive crosslinker like Benzophenone or a Diazirin. As mentioned above a covalent bond to the target enzyme is must for the method to work. Reversible inhibitors like zinc chelating hydroxamate probes, can be attached to the active site by a photoinduced radical reaction of the benzophenone with the binding pocket as soon as they are bound to their target enzyme.^[45,46] The Benzophenone group offers several advantages over other photocrosslinkers. One being a high specificity towards C-H bonds, even in the presence of solvent water and other bulk nucleophiles, the other being a relatively high photostability which further increases specificity. In contrast to other photoreactive groups, which are activated in an irreversible, photodissociative mode, BP probes may almost only relax electronically. Thereby they maintain their binding and photoactivatable properties and allows them to undergo many excitation-relaxation cycles until a favorable geometry for covalent modification is achieved. These properties combined allow the production of highly efficient covalent modifications of macromolecules, frequently with remarkable site specificity.^[47]

3.3.3 Tag free-ABPP

By employing a spacer with a terminal alkyne, different tags can be attached after the labeling using a bioorthogonal Cu^{I} -catalyzed azide-alkyne cycloaddition (Click-Chemistry, CC). As shown in Figure 3.3.3.1 the first step is the activation of the alkyne by an insertion of Cu^{I} .

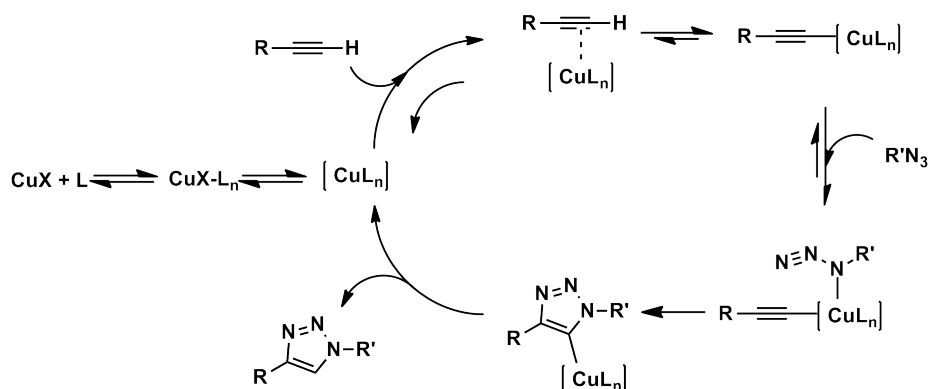


Figure 3.3.3.1: Mechanism of the Cu^{I} -catalyzed Azide-Alkyne Cycloaddition^[48]

Cu^{I} catalysis however has two problems: the sensitivity of the reactive Cu^{I} towards oxygen and the tendency of alkynyl copper species to form catalytically inactive polynuclear copper acetylides. The first problem can be circumvented by the *in situ* reduction of Cu^{II} by reducing agents like Ascorbate or tris(2-carboxyethyl)phosphine (TCEP). To prevent the oligomerization of the copper acetylides and to stabilize the active Cu^{I} , triazol ligands like tris-(5-benzyl-1H-triazol-4-yl)-methanamine (TBTA) can be deployed. This tetradentate ligand stabilizes active dinuclear Cu^{I} complexes by shielding the copper with its tripodal structure, while leaving enough space for the azide to enter the reaction sphere. Additionally, the strong electron donating properties of the central nitrogen increase the reactivity of the catalytic complex.^[48]

The second step in the reaction is the activation of the azide by coordination to the Cu^{I} -complex and the attack of a nucleophilic nitrogen of the azide moiety on the Cu^{I} -coordinated triple bond. Thereby, a 1,4-disubstituted triazol is created. As the copper only binds to the less substituted side of the alkyne, the reaction proceeds under a high regioselectivity, which is not the case under uncatalyzed Huisgen conditions.^[48,41]

3.3.4 Course of a tag free-ABPP experiment

The general course of an ABPP experiment consists of a number of consecutive steps. The first step is the application of the probes to a proteome where they covalently bind to the free active site of their target enzyme, providing an alkyne handle on the labeled enzymes. The second step, detection of the labeled enzymes, can follow different strategies. In recent years, several gel-free methods have been developed that meet different demands, such as higher sensitivity or simultaneous determination of the binding position of a probe in an enzyme. Among these, tandem orthogonal proteolysis (TOP),^[49] antibody-based methods,^[50,51] and the two-dimensional LC-MS/MS protein identification technology (MudPIT)^[52] should be mentioned. One of the most mature and frequently used analytical methods for ABPP is in-gel fluorescence scanning (IGFS). Though limited regarding detection limits and resolution of the gel electrophoresis (SDS-PAGE), IGFS offers a high throughput of samples, combined with easy handling and reasonable sensitivity. It was therefore used throughout the present work.

The alkyne handle of the labeled enzymes can be connected via click-chemistry to a tag, either for visualization (carboxy-tetramethyl-rhodamine, TAMRA) or for identification purposes by mass spec (biotin). The biotinylated enzymes are selectively enriched on Avidin beads to ensure adequate amounts and to further reduce background in the mass-spec measurement. In the following step, the labeled proteomes are separated by SDS-PAGE followed by analysis via fluorescence detection. The bands are subsequently cut out from the gel, subjected to tryptic digest and are analyzed by liquid chromatography/mass spectrometry (LC-MS, see Figure 3.3.4.1).^[45]

In inactive enzymes, the catalytic centers are either blocked or not assembled in the right conformation and therefore not accessible to small molecules. These enzymes are not bound by the probes, and thus cannot be visualized. This presents an important distinction to classical 'amount-based' proteomic techniques. By comparing the labeling patterns of probes in different proteomes, conclusions about the role of the different enzymes can be drawn. For example comparing the labeling profiles in pathogenic and non pathogenic bacteria, related enzymes can be discovered. These enzymes can then be investigated more thoroughly and can later serve as therapeutic and diagnostic targets.

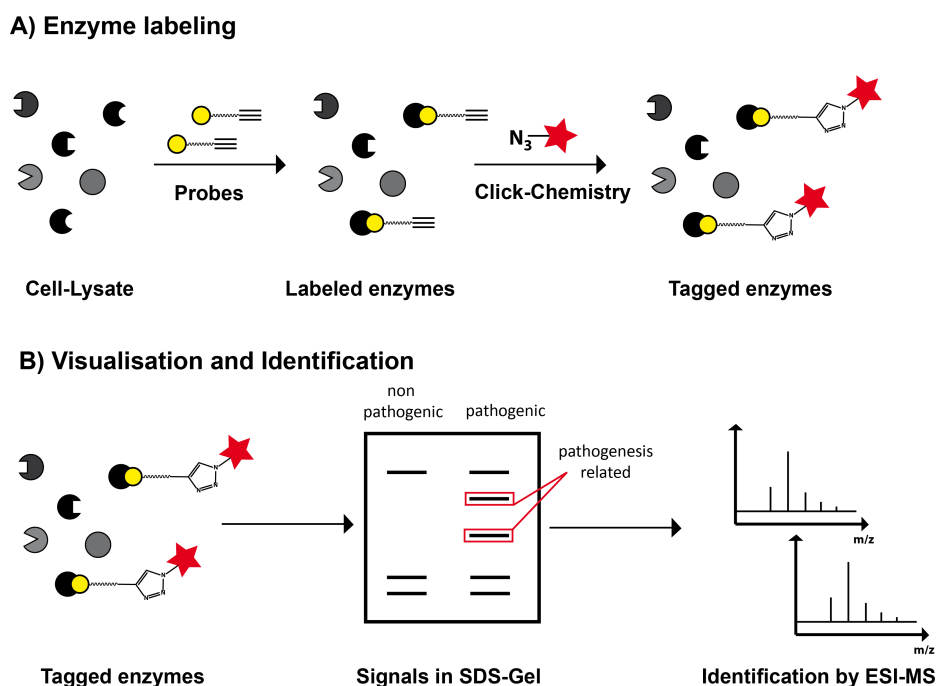


Figure 3.3.4.1: *Schematic overview of an ABPP experiment*

In ABPP two different main strategies are distinguished. The undirected and the directed approach. The undirected approach scans for interaction partners of a specific reactive moiety within a proteome, e.g. lactones^[53,54], epoxides^[55], Michael acceptors^[56,57,58] or phenylsulfonates^[59,51]. This strategy can be employed to identify targets of a reactive probe or to determine the mechanism of action of a drug. Using this method, a series of discoveries was reported during the last years which were related to the activity and function of uncharacterized pathogenesis-associated enzymes and central regulators of virulence.^[54,60]

When the proteomic targets of a probe are already known, the second and directed approach can be applied to investigate the reactivity profiles of different inhibitors and to analyze off target effects of drugs. For interesting proteomic targets, a variety of probes can be specifically designed, using structure based synthesis. One prominent example are fluorophosphonate probes, which specifically target serine proteases^[50,61,49] or the antibioticly active β -lactams^[62,63]. The results of the labeling experiments can then be used for further structural optimization of the probe, for example by attaching dif-

ferent decorations to the probe. Thereby the binding specificity of the probe can be increased and reactivity can be finely tuned to match the individual requirements of the target. We could show that by varying the decoration of cinnamic acid ABPP probes, the binding constants to the main enzymatic target can be changed by the factor 50.^[57]

3.3.5 Identification of proteins by mass-spectrometry (MS)

The proteins isolated by the IGFS method are proteolytically digested in gel and the resulting peptides are washed out of the gel. The purified peptides are then applied to a high resolution liquid chromatography mass-spectrometer (HR-LC-MS). This analytical device consists of two components, a liquid chromatography (LC) unit and a mass analyser (MS), that allow the separation and a subsequent identification of samples. The first part, the LC comprises a stationary phase (standard: hydrophilic materials like silica or alumina, reversed phase: silica coated with hydrophobic residues, e.g. C18) in a column to which the samples are applied. A mobile phase of varying composition is flushed through the stationary phase dragging the samples through the column. The strength of the interactions of the samples with the stationary phase determine the speed by which the samples pass the column. This allows a separation based on the hydrophobicity of the different samples. In the present work a reversed chromatography was employed, which used a hydrophobic stationary phase and a water/acetonitrile gradient. By slowly increasing the percentage of acetonitrile in the mobile phase, more unipolar peptides are washed from the stationary phase. As the retention times of the single peptides differ they can be injected separately into the second part of the LC-MS, a high resolution electron spray ionization (ESI) mass spectrometer (see Figure 3.3.5.1). The solvent containing the peptides passes a positively charged needle (Anode), thereby increasing the charge in the liquid. The nozzle of the spectrometer on the other hand is negatively charged (Cathode) which leads to the formation of an electric field between the needle and the nozzle.

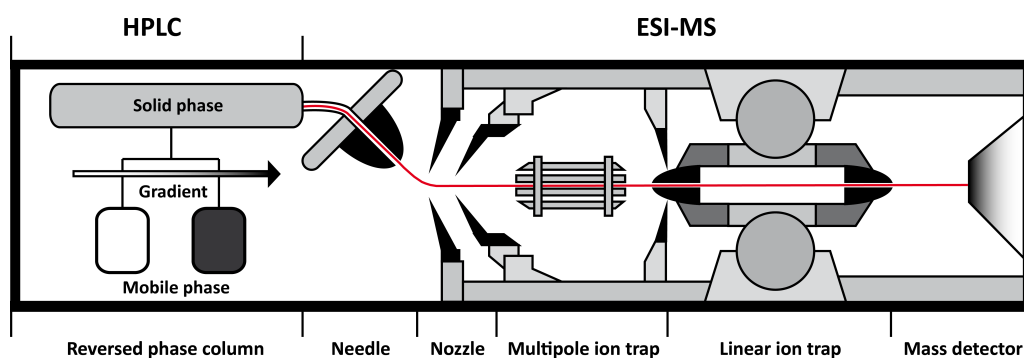


Figure 3.3.5.1: *Schematic overview of LC-ESI-MS*

The solvent containing the peptides passes a positively charged needle (Anode), thereby increasing the charge in the liquid. The nozzle of the spectrometer on the other hand is negatively charged (Cathode) which leads to the formation of an electric field between the needle and the nozzle. As seen in Figure 3.3.5.2, the solvent leaves the needle as a fine nebula (Analyte spray), each drop carrying a certain charge and is accelerated towards the nozzle.

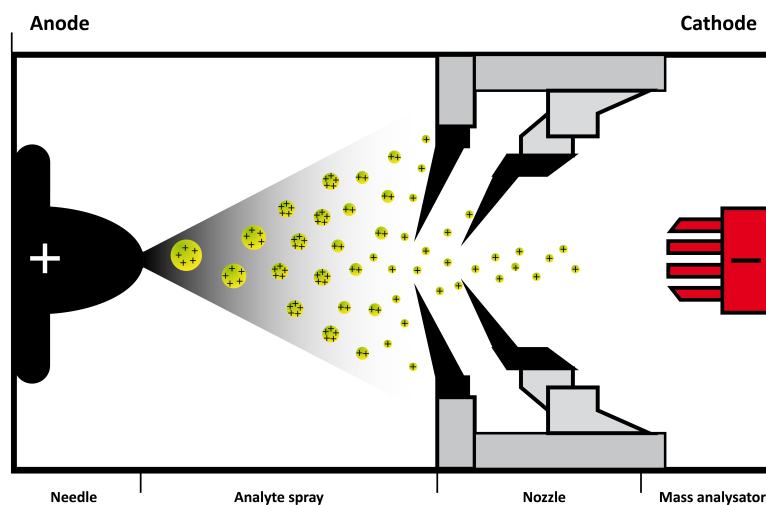


Figure 3.3.5.2: *Mechanism of ESI*

As more and more solvent evaporates from every drop, the charge to size ratio increases on the way to the mass analyser. Upon reaching a certain size (the so called Rayleigh-limit) the droplets become unstable. At this point,

they deform and emit charged jets in a process known as Coulomb-fission, losing a small percentage of its mass (0.03-2.3 %) along with a relatively large percentage of their charge (15.3-41.1 %).^[64,65] The resulting, highly charged ions enter the nozzle and can be detected by a mass analyzer like sector field^[66], time of flight (TOF)^[67], Orbitrap^[68] or Fourier transform ion cyclotron resonance^[69,70].

The mass data derived from LC-MS measurements of a protein digest, can then be compared to databases which contain virtual proteomes derived from an *in silico* translation of the sequenced genome. Specialized algorithms like SEQUEST^[71] or MASCOT^[72] are able to virtually execute a digest on a database proteome. This results in a theoretical mass spectrum which allows the identification of proteins by comparing experimental data to the computer derived model. Results are given with an error value, illustrating the bias of the measurement.

3.4 Natural products in ABPP

Although natural products represent the majority (approximately 60 %) of all approved pharmacologically active substances, many of their target locations and modes of action still remain unknown.^[73,74,75] Natural products normally display a finely attuned reactivity for their natural molecular targets. They bind specifically and selectively to a limited number of molecular structures, such as proteins, nucleic acids, or complexes thereof. The interaction of natural products with their target proteins can range from relatively weak protein-ligand interactions to very stable covalent modifications. Some of the structures show a specific affinity for a particular enzyme or enzyme class; however, others react with protein targets throughout different enzyme families. Over the course of millions of years, natural products were optimized for their specific effects by evolution, and thus their reactive or high-affinity central elements (see Figure 3.4.0.3) represent privileged structures.

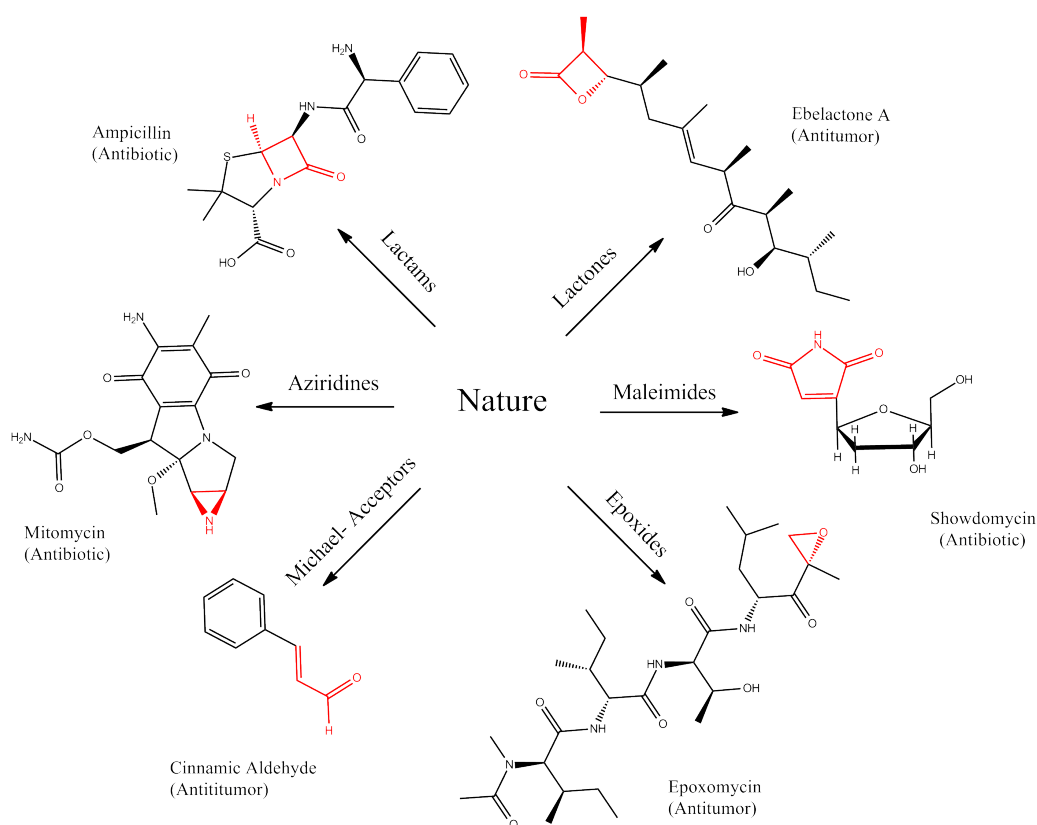


Figure 3.4.0.3: *Reactive groups in natural products*

Some natural products contain highly reactive groups, which at first glance appear to be barely compatible with the many possible reaction partners present in a living organism. However, the reactivity of these compounds can be appropriately adjusted through modification so that they inhibit fewer enzymes and thereby achieve a more specific effect in the target organism.^[76] The finely tuned reactivity of these compounds presents a very promising basis for their systematic investigation and modulation through the synthesis of derivatives. These tailored changes enable a customization of their reactivity and can make them accessible to entirely new target proteins.

The binding preferences of natural products is as versatile as their application spectrum, thus giving their deployment as pharmacological agents a particular relevance.^[52,73,74,75] Examples of their designated use span from basic lead structures in the design of biologically active agents, to the identification of enzymatic targets of known compounds, as well as their use as molecular tools. To quickly grasp the biological activity of a natural product it can be synthetically modified with an alkyne handle (see 3.3.2) to rapidly assemble a natural product based ABPP-probe. Based on the proteome reactivity of this probe, the mechanism of action along with potential off-target effects can be effectively investigated. This allows a first assessment of the pharmacological potential of a natural product, increasing the effectiveness of clinical studies by giving scientist the possibility to focus on the most promising lead structures.

3.5 Scope of this work

As mentioned above, protein-reactive natural products are a viable source for the development of novel ABPP probes for the investigation of pathogen related and vital enzymes in bacteria. Several natural compounds which show antibiotic or cytotoxic properties comprise three-membered rings as their core motif, rendering the scaffold interesting for the pharmacological research (see Figure 3.4.0.3). Only a few examples, like the papain protease inhibitor E-64 isolated from *Aspergillus japonicus*, have been looked at in detail to this day. Most compounds which have been reported to show biological activity, their mechanism of action remains elusive. The investigation of these mechanisms

would give a deeper insight into the biochemical pathways involved and may lead to the development of new drugs. The scope of this thesis was to provide a comparative study of the biological activities of different three membered carbo- and heterocycles by using them as probes in ABPP. To accomplish this task, the probe library had to meet several requirements:

- The layout of the molecules had to be based on a single structural element. Ideally the only difference should be the chemical composition of the ring, to allow for a comparative proteomic analysis of the different heterocycles.
- All types of three membered rings that can be found in natural products should be investigated including cyclopropanes (C-C-C), aziridines (C-N-C), epoxides (C-O-C) and thiiranes (C-S-C).
- The probes had to be biologically active.
- The possibility of the attachment of an alkyne tag, as well as a second decoration, in order to create a diverse ABPP-probe library for every cycle. This way, a large number of enzymes with structurally diverse active sites should be covered.
- In order to react with the proteome under physiological conditions the probes had to be water soluble.

All requirements were met in the basic 2,3-carboxy-substituted design of the epoxide based inhibitor E-64. Two modifiable positions were available at the two electron-withdrawing substituents, which were expected to increase reactivity as well as solubility by their high polarity (see Figure 3.5.0.4).

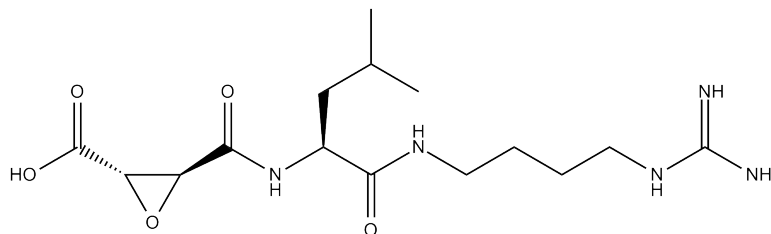


Figure 3.5.0.4: *Reactive groups in natural products*

The first step in this project was the synthesis of a small compound library. The probes were then intended to be comparatively studied in regard to their proteome reactivity, antibiotic and cytotoxic properties, and (if successful) to their inhibitory mechanisms based on the composition of the ring.

4 Results

4.1 Synthesis

4.1.1 Cyclopropanes

4.1.1.1 General

The synthetic routes to cyclopropanes can be divided into two groups. The first and the most prominent way is the introduction of a formal carbenoid into a carbon-carbon double bond, the second is a base catalyzed condensation-reaction.

In 1959, Simmons and Smith discovered that cyclopropanes could be obtained in high yields by the cheletropic reaction of olefins with diiodomethane in the presence of activated zinc.^[77] The reactive species in the synthesis is 'RZnCH₂I' which can be seen as a carbenoid transfer agent. Because the methylene unit is delivered to both carbon atoms of the alkene simultaneously, the configuration of the double bond is preserved in the product and the reaction is stereospecific(see Figure 4.1.1.1).^[78]

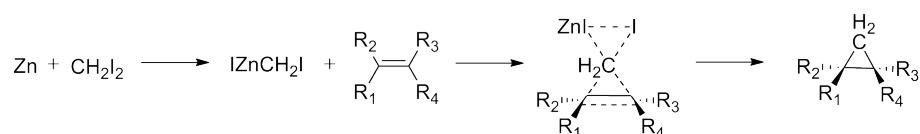


Figure 4.1.1.1: *Mechanism of the Simmons-Smith-reaction*

The reaction is subject to steric repulsions with bulky side chains, and thus usually takes place on the less hindered face.^[79] On the other hand, by coordination of the zinc with directing groups like hydroxy functions, the

cyclopropanation will take place *cis* to the hydroxyl group, even if this is sterically not favorable.^[80]

A variant of the Simmons-Smith reaction uses diazomethane under palladium(II) catalysis to convert terminal, 1,1-disubstituted or 1,2-disubstituted olefins into cyclopropanes.^[81,82] In general this method proceeds with a low diastereoselectivity and is very limited regarding suitable educts. Higher diastereoselectivity can be reached by adding sulfonium ylides to α, β -unsaturated carbonyls or carboxyls. The reaction mechanism for this so called Johnson-Corey-Chaykovsky reaction consists of a nucleophilic 1,4-addition of the 'soft' ylide to the 'soft' Michael acceptor system. As the sulfonium cation is a good leaving group, it gets expelled from the molecule leading to the formation of the cyclopropane ring (see Figure 4.1.1.2).^[83]

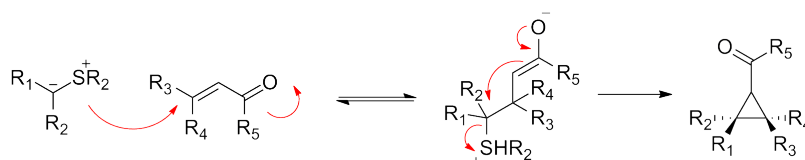


Figure 4.1.1.2: *Mechanism of the formation of a cyclopropane by a Corey-Chaykovsky reaction*

The second method for the synthesis of cyclopropanes is a base-catalyzed condensation of α -haloesters with α, β -unsaturated carboxylic esters, which leads to 1,2-cyclopropane-dicarboxylic acid-diester. By deprotonation of the acidic α -proton of the haloester by a strong base (e.g. sodium hydride), a strong nucleophile is generated, which can then attack on the Michael acceptor in a 1,4-type addition reaction (see Figure 4.1.1.3). The resulting carbanion can then form the cyclopropane ring by a nucleophilic attack on the halogen carbon. In contrast to the procedures mentioned above, this method can provide the activated racemic cyclopropanes with a high diastereoselectivity.^[84]

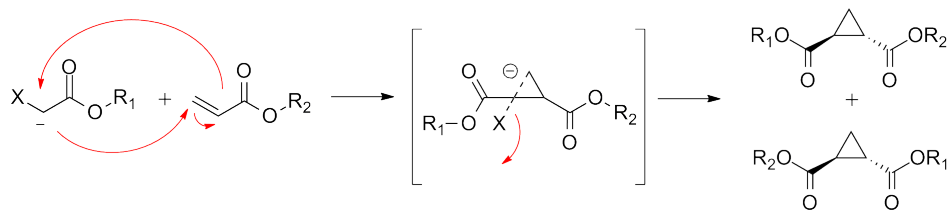


Figure 4.1.1.3: *Mechanism of the haloester condensation reaction leading to cyclopropanes*

4.1.1.2 Synthetic strategy

In this work, α -chloroacetate was deprotonated using sodium hydride and reacted with ethyl acrylate. The following reaction gave the racemic *trans*-cyclopropane in low yields (see Figure 4.1.1.4). Selective saponification of one ester was achieved in good yields by reaction with aqueous sodium hydroxide.

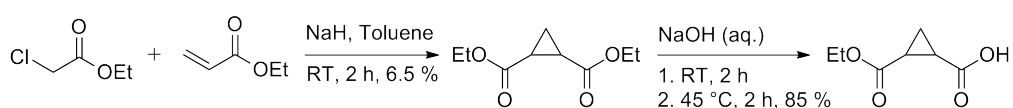


Figure 4.1.1.4: *First part of the synthetic route to the cyclopropane probe*

The amidation to the cyclopropane ABPP-probe was accomplished by activation of the free acid to the mixed anhydride followed by reaction with propargylamine (see Figure 4.1.1.5).

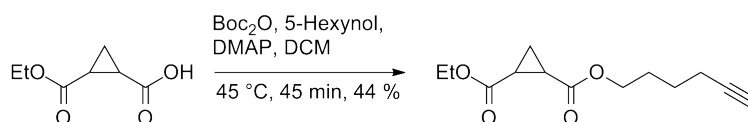


Figure 4.1.1.5: *Second part of the synthetic route to the cyclopropane probe*

4.1.2 Oxiranes

4.1.2.1 General

Oxiranes (epoxides, ethylene oxides) are a well characterized class of functional groups which can be obtained by a variety of synthetic approaches. Their chemical properties are largely determined by the epoxy cycle which forms an almost regular triangle with bond angles of about 60°. This ring strain lends a significant potential energy on the carbon-oxygen bond which corresponds to the bond energy of 105 kJ/mol.^[85] An opening of the ring through a nucleophilic attack on the epoxy cycle results in the release of this energy and is therefore highly favored. Substituents on the C2 and C3 positions can further influence the stability of the ring. Electron-withdrawing groups (EWGs) like esters or nitriles increase the reactivity by amplifying the partial positive charge on the cyclic carbon atoms and by decreasing the electron density of the ring structure. This makes the ring more prone to the reaction with electron rich nucleophiles.^[86] As the majority of successful, bioactive epoxide compounds contain EWGs as decorations (e.g. the antibioticly active cerulenin isolated from *Cephalosporium caerulens*, see Figure 4.1.2.1) on the carbon atoms 2 and 3 we chose this particular design for our epoxide probes.

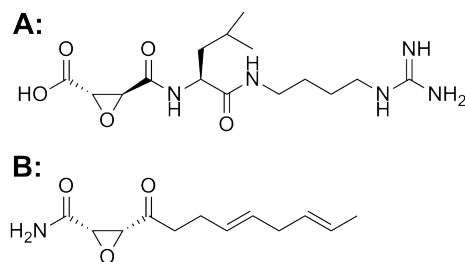


Figure 4.1.2.1: Oxirane containing natural products E64 (A) and cerulenin (B)

The installation of the oxirane ring proved to be the key challenge in the synthesis of the oxirane probes. Two different main routes have been developed over time. The first method introduces the epoxide by oxidation of a donor substituted alkene, the second relies on the intramolecular attack of

an alcohol on a vincinal bromide. The most prominent example of the first route is the Prilezhaev reaction, which employs peracids to form a 'butterfly' transition state which ultimately leads to a *syn*-epoxide in a rather low enantioselectivity (see Figure 4.1.2.2).^[87,88]

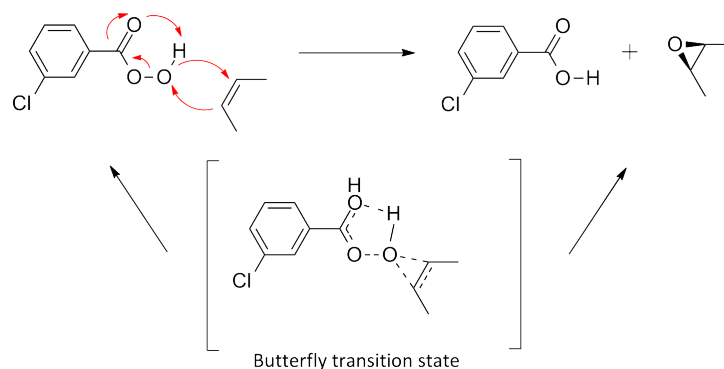


Figure 4.1.2.2: Mechanism of the Prilezhaev reaction

A more advanced method that offers a higher enantioselectivity is the Sharpless epoxidation^[89]. It comprises the use of tert-Butyl hydroperoxide, and a chiral catalyst which is assembled *in situ* from $\text{Ti}(\text{OiPr})_4$ and Diethyl-tartrate (see Figure 4.1.2.3). However, for this reaction to work, an allylic alcohol is required as the educt – a grave limitation for synthetic chemists.

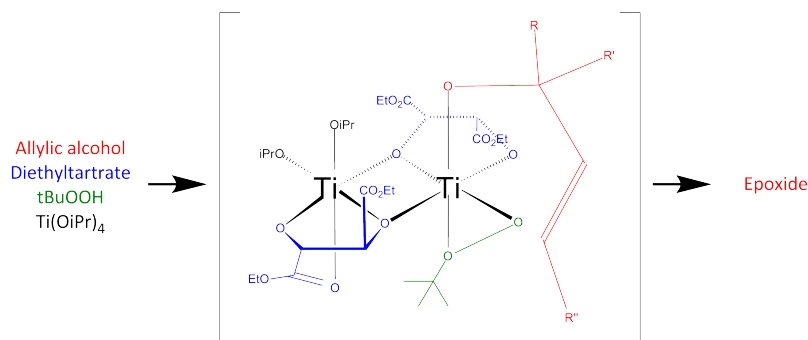


Figure 4.1.2.3: Catalytically active Sharpless complex

The application of unfunctionalized (*Z*)-olefins as substrates for epoxidation reactions was made possible some years later by the invention of optically active Salene-manganese(III) complex catalysts (see Figure 4.1.2.4) in combination with NaOCl (Jacobsen Katsuki^[90]) or peroxides like H_2O_2 ^[91].

When using deploying (E)-olefins as starting materials, the yields decrease dramatically.

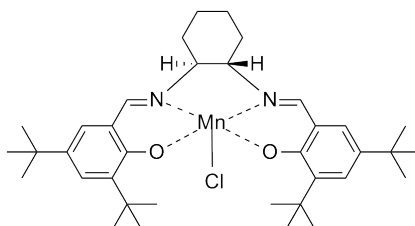


Figure 4.1.2.4: *Manganese-Salene complex of the Jacobsen Katsuki reaction*

This problem was tackled by the Shi-epoxidation^[92], which uses a fructose-derived organocatalyst along with oxone (Potassium peroxymonosulfate) as the primary oxidant. As depicted in Figure 4.1.2.5, oxone and the catalyst form a highly reactive chiral dioxirane *in situ* which then inserts an oxygen atom into the double bond.

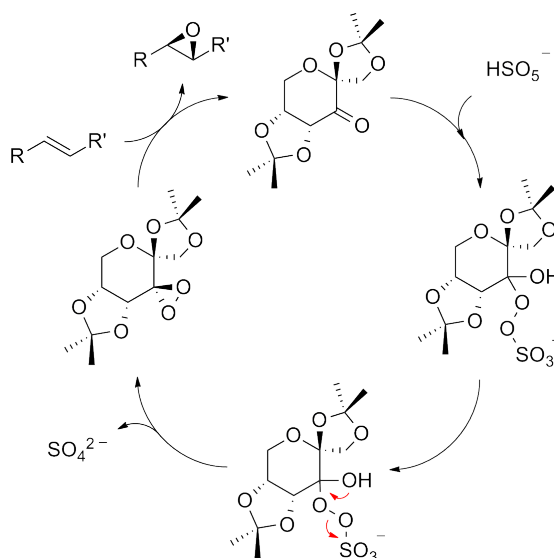


Figure 4.1.2.5: *Mechanism of an epoxidation catalyzed by a Shi-Ketone prepared from D-Fructose*

Although powerful, all the methods mentioned above fail when using acceptor-substituted alkenes as substrate, as they all rely on the attack of an electron-rich double bond on a partially positive oxygen of the oxidizing compound

(e.g. MCPBA). If the double bond is poor in electron density, this attack is strongly disfavored.

The second general method for epoxydation circumvents this problem by using bromohydrins as an educt, which can be readily synthesized from bishydroxy compounds. The formation of the epoxide ring is achieved by applying basic conditions to the bromohydrin. Thereby the hydroxy function is deprotonated and acts as a nucleophile which then undergoes an intramolecular S_N2 reaction with the vicinal bromide under inversion of the stereocenter. The reaction works well with acceptor-substituted educts as a partial positive charge at the carbon carrying the bromide accelerates the S_N2 reaction (see Figure 4.1.2.6).

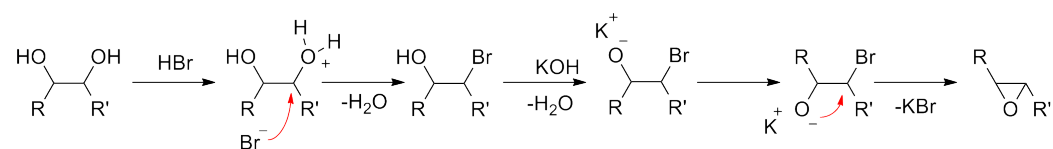


Figure 4.1.2.6: *Mechanism of epoxide synthesis via bromohydrins*

4.1.2.2 Synthetic strategy

The design for our oxirane-based probes had to meet several prerequisites: an active epoxide ring to ensure proteome reactivity and two functional groups that could be easily and orthogonally modified with a variety of decorations (e.g. an alkyne handle for the click-chemistry) to create a probe library. The synthesis had to be simple and should offer a high stereoselectivity. The basic design of the well known cysteine-protease inhibitor E64 (see Figure 4.1.2.7) fulfills all these key requirements, as it possesses two carboxylic groups which allow a modification by esterification or amidation and can additionally act as EWGs to activate the epoxide. In case of the *trans*-diastereomers the compounds have a rotational axis. This greatly simplifies the stereochemical challenges of the synthetic route, as the modification of either carbonyl function leads to the same diastereomer.

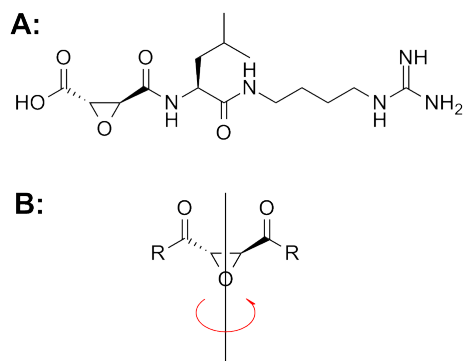


Figure 4.1.2.7: *Natural product E64 (A) and its core element with the rotational axis(B)*

Several epoxidation strategies to produce this core structure were tested, but none of them succeeded (see Figure 4.1.2.8).

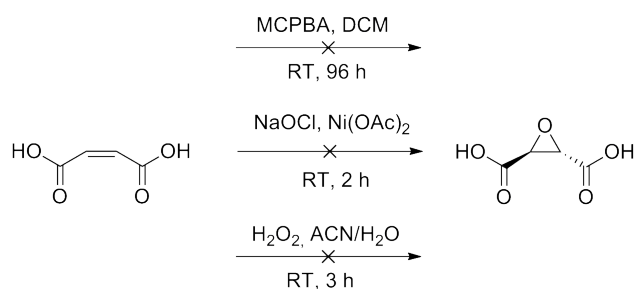
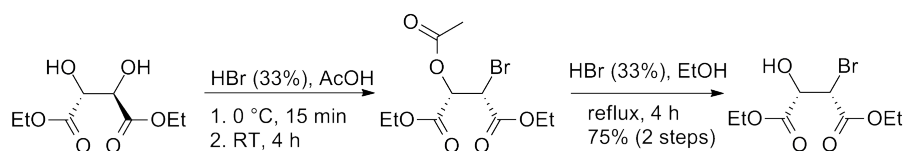
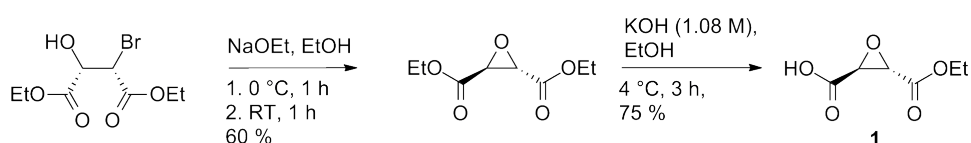


Figure 4.1.2.8: *Synthetic approaches to oxiranes shown not to work*

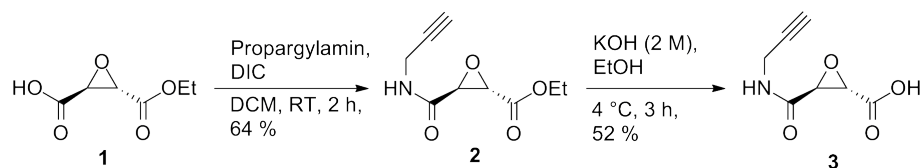
Only the synthesis pioneered by Mori^[93] employing the bromohydrin method, proved to be applicable in this case. Based on diethyltartrate, a cheap and chiral starting material which is readily available, the synthesis of the corresponding bromohydrin can be achieved in two steps with very good yields (see Figure 4.1.2.9).^[94] By picking either L- or D-tartrate as starting material, it is possible to select the enantiomeric configuration of the final product, as every step of the reaction proceeds under stereospecific conditions. In this work we used the L-enantiomer due to its easier availability.

Figure 4.1.2.9: *Synthesis of the bromohydrin*

The bromohydrin can then be converted to the epoxide by an intramolecular ring closure under basic conditions in good yields. Selective saponification of a single ester moiety was accomplished by the slow application of diluted KOH in EtOH (see Figure 4.1.2.10).

Figure 4.1.2.10: *Synthesis of compound 1*

The alkyne tag was coupled to the free acid by using propargylamine along with standard peptide coupling reagents. The resulting amide bond is resilient against conditions of the basic ester hydrolysis, so that the second ester can be cleaved selectively (see Figure 4.1.2.11).

Figure 4.1.2.11: *Synthesis of compounds 2 and 3*

The free acid could then be derivatized to a broad spectrum of esters using Boc-anhydride as an activation reagent (see Figure 4.1.2.12). To maximize enzyme coverage, the compound library varies in their C2 decoration by small (ethyl-, allyl-) and long (octyl-) aliphatic residues as well as by an aroma-

tic residue (benzyl-) which enhances the chance of binding into structurally diverse enzyme active sites.

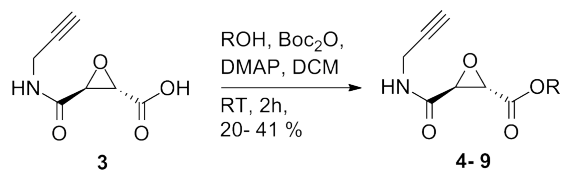


Figure 4.1.2.12: *Synthesis of the oxirane library 4 to 9*

4.1.3 Thiiranes

4.1.3.1 General

Thiiranes (episulfides, propylene sulfides) are three membered rings containing a sulfur atom as their heteroatom and have been discovered almost 100 years ago by Staudinger and Pfenninger.^[95] The limited stability of thiiranes in relation to their oxirane counterparts has resulted in a limited number of synthetic routes and even less information regarding their biological activity.^[96] The chemistry of thiiranes is in many ways very similar to their oxirane counterparts which, in contrast to the episulfides have been studied thoroughly. The key differences between both compound classes can be derived from the structural and physical properties of the tricycle. The strain energy of ethylene sulfide amounts to 18.6 kcal/mole, about 28 kcal/mol for ethylene oxide, 27 kcal/mol for ethylenimine, and 27.5 kcal/mol for cyclopropane.^[97,98] These values are correlated to a narrowing of the C-X-C binding angles (X being the heteroatom or C in case of cyclopropane) from 60 ° (cyclopropane, oxirane and aziridine) to 48 ° in the case of the thiiranes (see Figure 4.1.3.1).^[99,100,101]

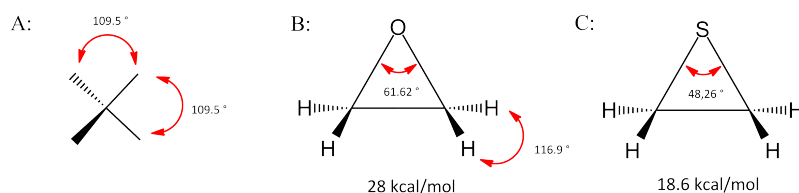


Figure 4.1.3.1: *Bond angles and ring strain energies in methane (A), ethylene oxide (B) and ethylene sulfide (C)*

However the reactivity of the thiiranes regarding a ring opening is higher than those of the other homo- and heterocyclic analogues. The lower ring strain of the thiiranes is overruled by the lower bond energy of C-S vs. C-C, C-O or C-N bonds.^[102]

To this day only a handful of pharmaceutically active thiiranes are known, and are applied in completely different areas like the treatment of breast cancer

(Epithiostannol^[103]), the inhibition of cholesterol synthesis^[104], or in lowering blood glucose levels by irreversible inhibition of mitochondrial fatty acid derivatization.^[105,106] Substituted propylene sulfides have been reported to be active against tuberculosis^[107] and some furanoid epithiosugars demonstrate immunostimulatory effects (see Figure 4.1.3.2).^[108]

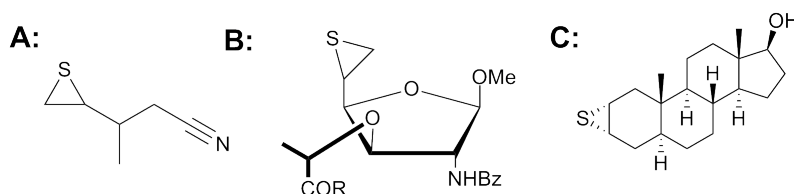


Figure 4.1.3.2: *Examples of bioactive thiiranes: Inhibitor of fatty acid derivatization (A), immunostimulatory epithiosugar (B) and breast cancer drug Epithiostannol (C)*

For the synthesis of thiiranes, two main strategies are known, both of which use olefins as the basic substrate. The first, direct approach relies on the oxidation of olefins with either sulfur transferring reagents like sulfurmonochloride or sulfur itself.^[109] The second, indirect strategy is based on the oxidation of the olefins prior to the formation of the thiirane. One example is based on the transformation of the olefin to a thiol with a vincinal leaving group. These groups can e.g. be acetates^[110,111], tosylates^[112] or halogens^[113,114] to name just a few. By an intramolecular S_N2 attack of the thiol on the leaving group, the thiirane ring is closed (see Figure 4.1.3.3).

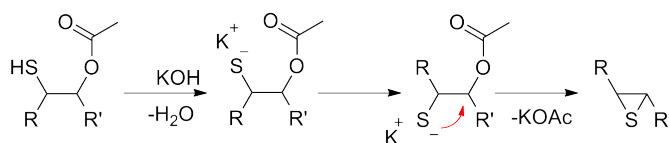


Figure 4.1.3.3: *Mechanism of thiirane synthesis via intramolecular S_n2 reaction*

The most important general method for the synthesis of thiiranes appears

to be the conversion of an olefin into the corresponding oxirane, followed by a sulfur-oxygen exchange of the ring. Two of the most prominent sulfur exchange reagents are thiocyanate salts^[115,116] and thiourea^[117,118] which are both suggested to induce a nucleophilic ring opening followed by an intramolecular ring closure under a Walden inversion on both stereocenters (see Figure 4.1.3.4).^[116]

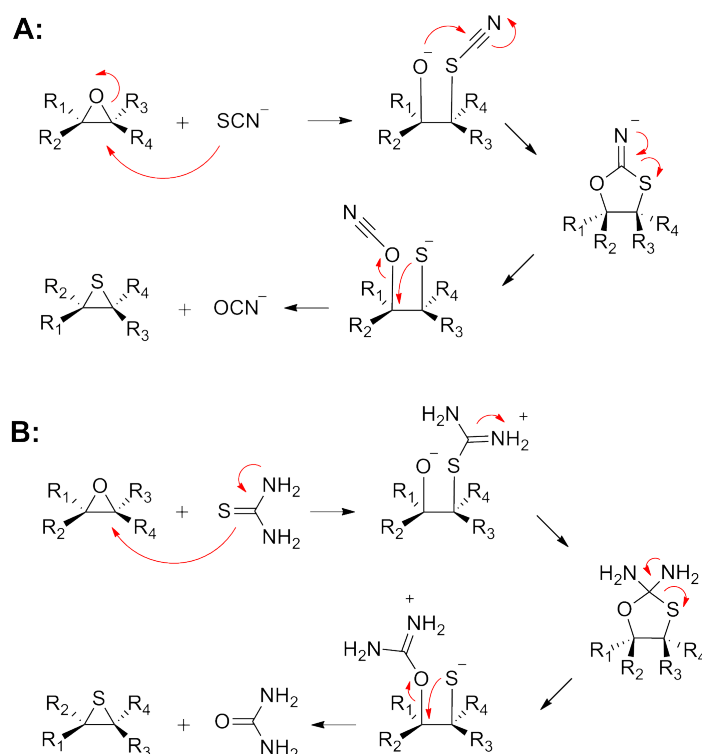


Figure 4.1.3.4: Mechanism of thirane synthesis with thiocyanate (A) and thiourea (B)

4.1.3.2 Synthetic strategy

A major aspect of our research was the comparison of the bioactivity between different threecyclic compounds based on the composition of the ring. In order to avoid a *de novo*-synthesis of the thiranes, we chose to use the oxygen-sulfur exchange reaction to form our library, thus shortening the synthetic route by

several steps. The transformation reaction of the oxirane probes with both KSCN and thiourea was tried under several conditions, but only returned the starting materials (see Figure 4.1.3.5). The electron withdrawing groups may prevent the formation of the thiirane ring, as the reactions are described to work with donor-substituted epoxides.

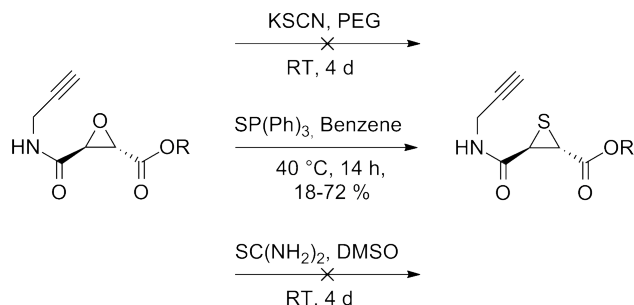


Figure 4.1.3.5: *Oxirane-thiirane conversion*

Nevertheless a third method first published by Finkenbine^[119], using triphenylphosphine sulfide as the sulfur transfer agent was applied successfully. The general mechanism of the reaction is analogous to the mechanism of thiocyanate/thiourea with an oxirane (see Figure 4.1.3.6).

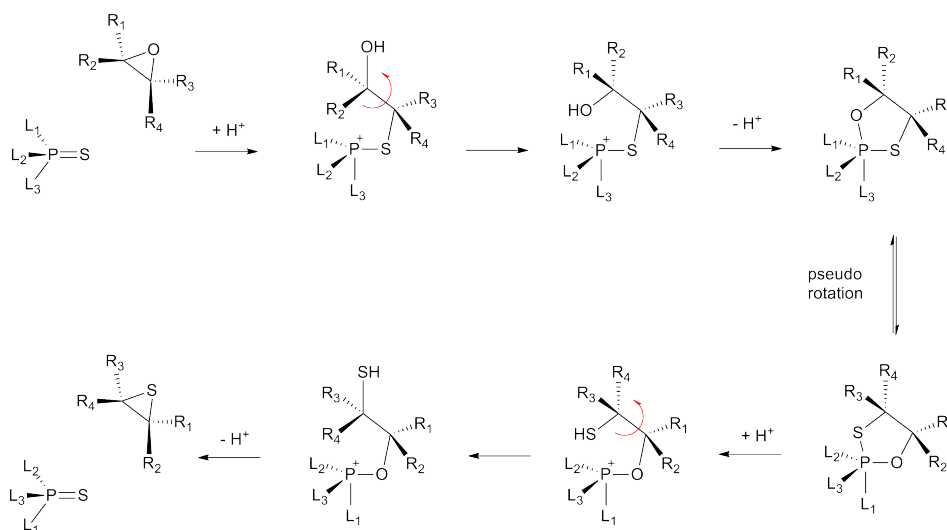


Figure 4.1.3.6: *Mechanism of thiirane synthesis with triphenylphosphine sulfide*

The driving force behind the reaction with triphenyl-phosphine-sulfide is the formation of the P=O bond in the resulting phosphine oxide, which is energetically much more favorable compared to its P=S analogue (P-O single bond: 595 kJ/mole, P-S single bond: 285 kJ/mole).^[120,121,119] The formation of such an thermodynamically stable product explains why this reaction allows the use of inactivated substrates in comparison to thiocyanate/thiourea.

4.1.4 Aziridines

4.1.4.1 General

Aziridines (ethylene imines, azacyclo-propanes) are the smallest saturated nitrogen heterocycles, and are often used as reactive intermediates in either natural product synthesis or medicinal chemistry. Just like their heterocyclic relatives, they are subject to ring-opening reactions by a wide variety of nucleophiles (amines, alcohols and thiols) as a consequence of their strained cyclic structure. Their reactivity makes them not only versatile synthetic intermediates, but they are also found as reactive warheads in the structures of various natural products.^[100] The aziridine's basicity, its rigidity and its potential reactivity contribute to specific molecular interactions with biomolecules of all kind. In most cases, however, their distinctive biological activities are caused by their strong DNA-alkylating properties as seen in the antitumor agent Azinomycin A^[122] or the antibiotics Ficellomycin^[123,124] and Mitomycin^[125] (see Figure 4.1.4.1).

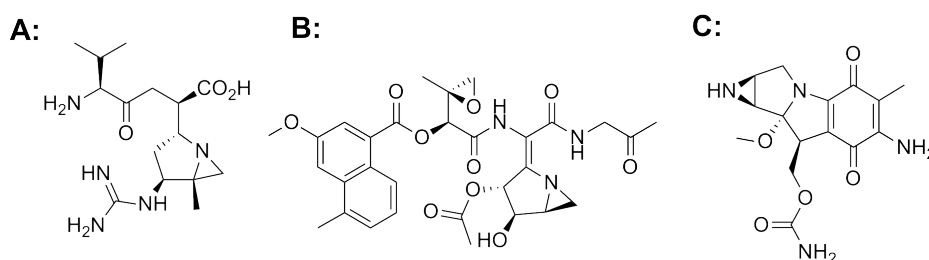


Figure 4.1.4.1: *Examples of bioactive natural products containing aziridine moieties: antibiotic Ficellomycin (A), antitumor agent Azinomycin A (B) and antibiotic Mitomycin (C)*

Due to these interesting properties, several strategies for the facile synthesis of a range of structurally diverse aziridines have been developed. The iron-catalyzed diazoacetate decomposition in the presence of an imine^[126], as well as the aza-Darzens reaction^[127] allow the synthesis of aziridines from imine, or sulfinimine substrates (see Figure 4.1.4.2).

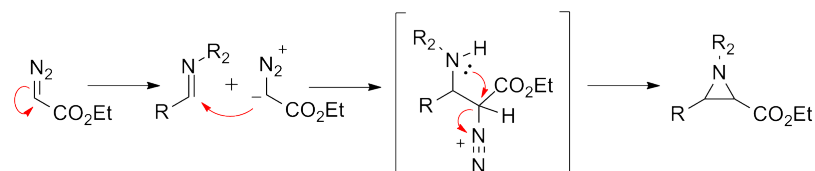


Figure 4.1.4.2: *Mechanism of a aza-Darzens type aziridine synthesis*

Other, more traditional routes utilize precursors like 1,2-azidoalcohols in a Staudinger-type reaction (see Figure 4.1.4.3)^[128,129,130], 1,2-amino alcohols in a Wenker reaction^[131] or 2-haloamines in the Gabriel Ethylenimine Method^[132] for an internal neighboring group cyclisation.^[133]

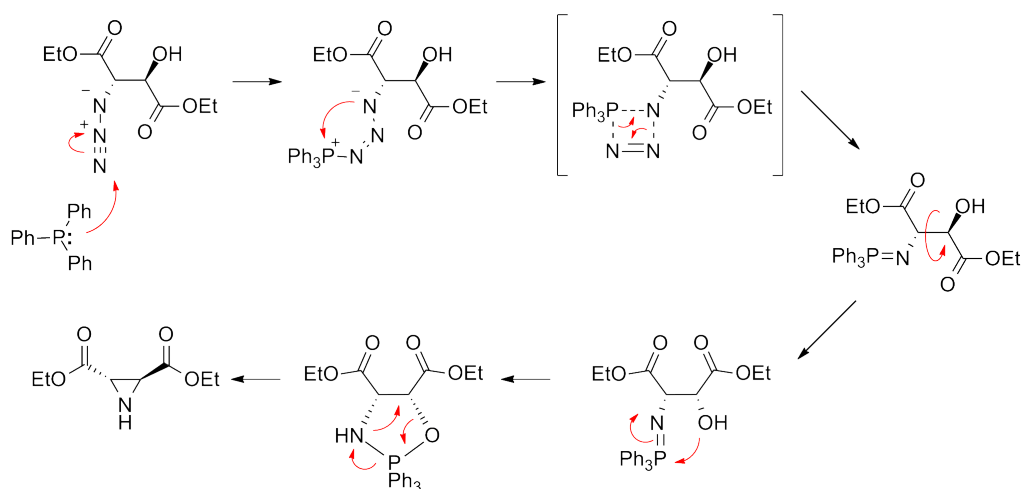


Figure 4.1.4.3: *Mechanism of a Staudinger type aziridine synthesis*

A complementary alternative to the above mentioned methods is the utilization of direct nitrene addition to alkenes, a reaction closely related to

the peracid epoxidation of olefins. The nitrogen source for this reaction, a nitrene or nitrenoid, can be generated in various ways, e.g. by a copper catalysis in combination with PhIO or PhI(OAc)₂ and sulfonamides (see Figure 4.1.4.4).^[134,135]

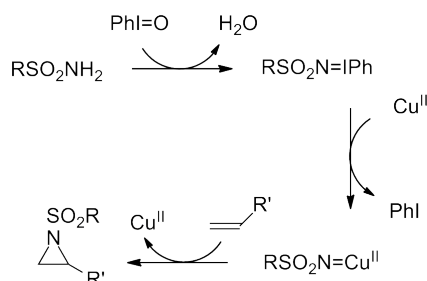


Figure 4.1.4.4: *Mechanism of a copper catalyzed nitrenoid-insertion to an olefine*

In general, the addition of nitrenoids to an alkene is stereochemically not well controlled, as mixtures of *cis*- and *trans*-aziridines are readily being formed. This is due to the rapid interconversion of the singlet and triplet nitrene states which determine the stereochemistry of the addition.^[136]

A rather neglected, yet convenient and versatile method uses the 1,4-type addition of alkylated sulfilimines on α,β -unsaturated carbonyls to give the corresponding racemic aziridines in good yields (see Figure 4.1.4.5).^[137,138]

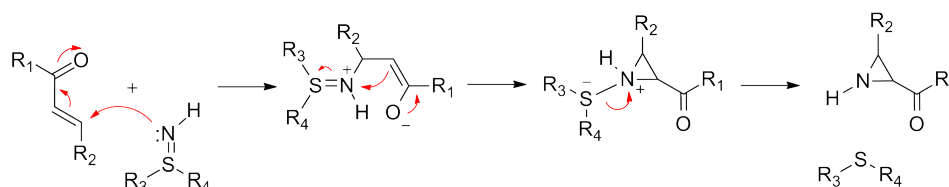
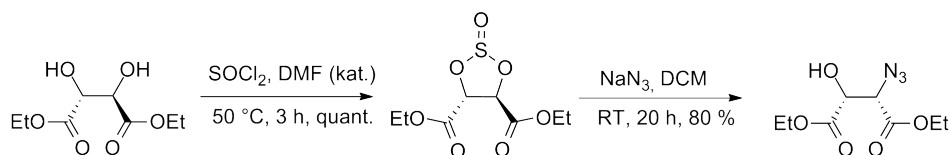


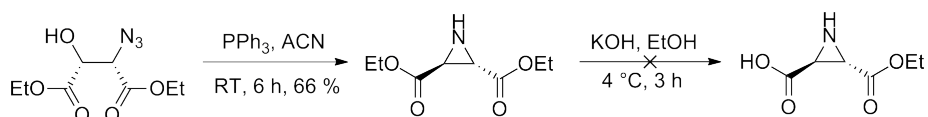
Figure 4.1.4.5: *Mechanism of the Michael type addition of a sulfilimine to an olefine*

4.1.4.2 Synthetic strategy

For the synthesis of aziridine analogues of the oxirane and thiirane probes (see 4.1.2 and 4.1.3) we first chose to employ 1,2-azidoalcohols in a Staudinger-type reaction (see Figure 4.1.4.3). This decision was based on the fact that the synthesis of the azidoalcohol precursor followed the style of the synthesis of our oxirane probes and would proceed under stereospecificity.^[139] The first step, the activation of the diol by reaction with SOCl_2 and catalytic amounts of DMF, led to the product in quantitative yield. Reaction with sodium azide in DCM at RT gave the azidoalcohol under inversion of one stereocenter in excellent yields (Figure 4.1.4.6).

Figure 4.1.4.6: *Synthesis of the aziridine precursor*

The Staudinger-type cyclisation reaction in ACN at RT gave the aziridine in good yields. The following deprotection of one ester by standard methods however resulted in the complete decomposition of the aziridine. Experiments to deprotect the azidoalcohol before the cyclisation-reaction resulted in decomposition as well. Experiments with alkyne esters or amides as starting points for the synthesis of the azidoalcohols were not successful either (Figure 4.1.4.7).

Figure 4.1.4.7: *Synthesis of the aziridine*

Due to these problems, we switched our strategy to the 1,4-attack of *S,S*-diphenyl-sulfilimine to an α,β -unsaturated carbonyl. The synthesis of the Michael acceptor precursor started from the monoethylester of fumaric acid. The amidation of the free acid by propargylamine with the standard peptide

coupling reagent DIC in DCM gave the amide **17** in good yields. Deprotection of the ethylester with KOH in EtOH resulted in the free acid **19** (Figure 4.1.4.8).

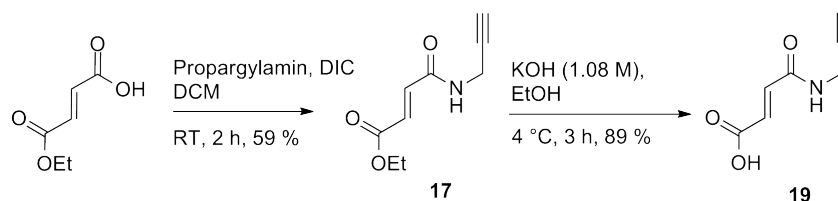


Figure 4.1.4.8: *Synthesis of the Michael acceptor (17) and deprotection to the free acid (19)*

Esterification with n-octanol or benzylalcohol by activation of **19** with Boc-anhydride gave compounds **20** and **21** in acceptable yields (Figure 4.1.4.9).

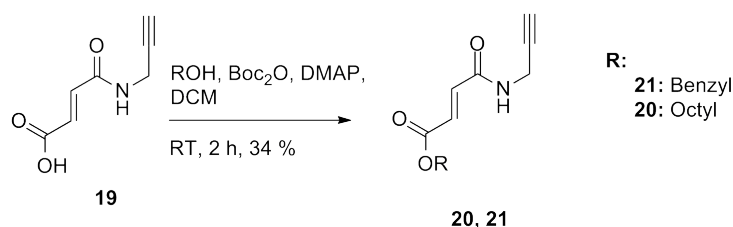


Figure 4.1.4.9: *Synthesis of the Michael acceptor probe 20 and free acid 21*

The cyclisation reaction with the sulfilimine in the fashion of a Michael-type addition at 110 °C in toluene gave the aziridine probes **18**, **22** and **23** in rather low but yet acceptable yields (Figure 4.1.4.10).

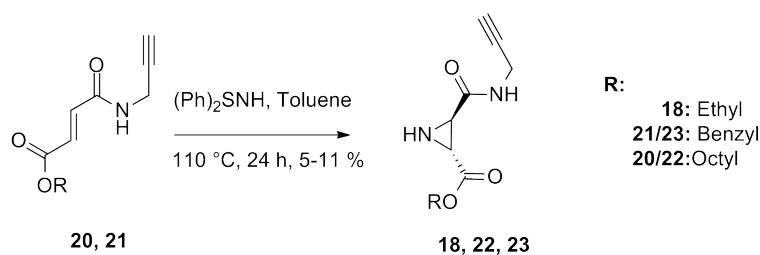


Figure 4.1.4.10: *Conversion of the Michael acceptor probes to the aziridine probes 18, 22 and 23*

4.2 Summary

In summary a library of three membered ring ABPP probes (see Figure 4.2.0.11) could be synthesized following procedures described in the literature. Cyclopropane as well as aziridine probes could be obtained as racemic mixtures, whereas oxirane as well as thiirane probes were synthesized enantioselectively. To maximize enzyme coverage, the compound library varies in their C2 decoration by small (ethyl-, allyl-) and long (octyl-) aliphatic residues as well as by an aromatic residue (benzyl-) which enhances the chance of the ABPP probe to bind into structurally diverse enzyme active sites.

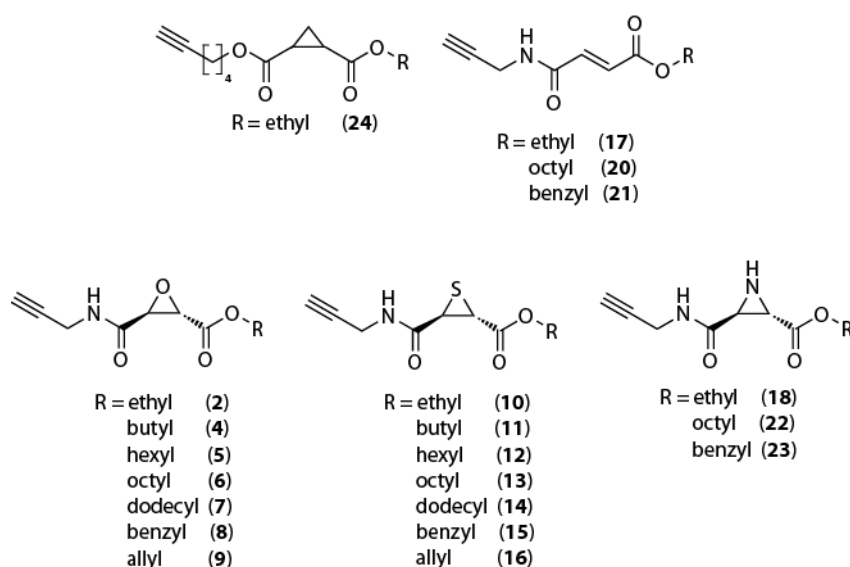


Figure 4.2.0.11: *Library of synthesized probes*

4.3 Stability

Strained molecules like three-membered rings are likely to undergo thermal and photochemical reactions, often leading to their decomposition. The reactivities of the different compound classes, as well as the associated mechanisms vary widely. A range examples of thermal dissociations of substituted oxiranes^[140,141,142], aziridines^[143,144,145] and cyclopropanes^[146,147,148] are known,

all depending on high temperatures and prolonged reaction times. This can be related to the high stability of the C-X bond (C-O: 1.436 , C-N: 1.488) which lies in the same area of the C-C bond in the molecules (C-C: 1.472-1.480).^[142] However, several cases are known in the literature where thiiranes decompose even under mild temperatures down to 0 °C.^[149,150] They either react under cleavage of the carbon-sulfur bond, which often leads to rearrangement products, isomeric or polymeric materials, or extrusion of sulfur which results in the formation of alkenes. Several mechanisms have been postulated to account for all observed products. A careful examination of the kinetics of the thermal decomposition of 2,2-dichloro-3-(9-fluorenyl)ethene episulfide by Warren *et al.*^[151] led to the proposal of two different routes depending on the concentration of the reactant (see Figure 4.3.0.12.

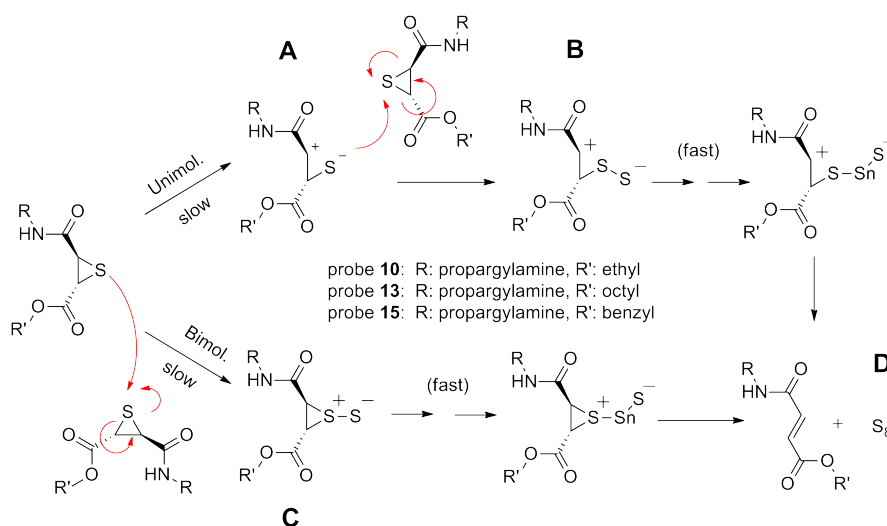


Figure 4.3.0.12: Thermal conversion of the thiirane probes to the corresponding Michael acceptor probes

At low concentrations, the thermal ionization of the C-S bond is likely to occur as the first and rate-determining step. Such an intermediate has also been proposed for the reactions between 9-diazoxanthene and coumarin-2-thione. The fastest step in this route would therefore involve subsequent attack by the sulfur anion species (A) on a second thiirane molecule, resulting in intermediate B. This species would acquire sulfur atoms sequentially until stable sulfur rings (S₆ and S₈) are formed along with the Michael acceptor

(D). When the concentration of thiirane is increased, the second term in the rate equation becomes more important, leading to a bimolecular mechanism. The rate-determining step of this pathway is the reaction of two episulfide molecules by abstraction of the sulfur atom from another, giving intermediate C. The fast step is the subsequent elongation of the sulfur chain until S_8 is formed and extruded from the molecule, giving the Michael acceptor D.^[151,96]

Warren *et al.* could also show that the reaction rates depended strongly on the solvent, increasing the reaction rate by a factor of 218 when employing DMF instead of toluene.^[152]

Since stability under physiological conditions was one of the key requirements for an ABPP probe, we investigated the reactions of the different heterocyclic probes in different solvents at room temperature, prior to the labeling experiments. The experiments were executed by creating 100 mM solution of the different heterocyclic probes in the respective solvent and monitor the potential changes by 1H NMR Spectroscopy. One sample of the thermal conversion of probe **10** is shown in Figure 4.3.0.13.

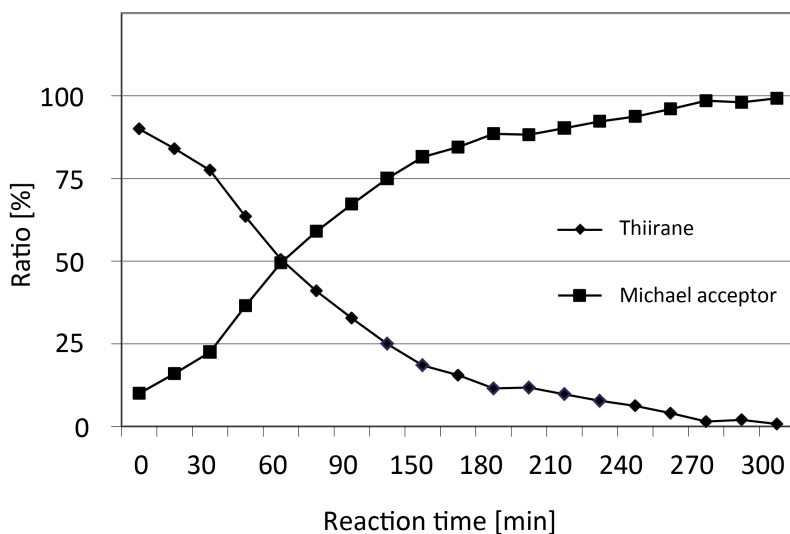


Figure 4.3.0.13: Thermal conversion of the thiirane probe **10** to the corresponding Michael acceptor probe at RT

As shown in Table 4.3.0.1, both aziridine as well as oxirane probes proved a high stability in all experiments by showing no change in their $^1\text{H-NMR}$ signals for over two weeks. The thiirane probes however were only stable in CDCl_3 and Acetone. In DMSO, a rapid conversion at RT could be observed.

Table 4.3.0.1: *Half life of probes in different solvents (Aceton/D₂O, 1:1 (v/v))*

probe	in DMSO	in CHCl_3	in Aceton/D ₂ O
18	>2 weeks	>2 weeks	>2 weeks
2	>2 weeks	>2 weeks	>2 weeks
10	60 min	>2 weeks	>2 weeks
13	245 min	>2 weeks	>2 weeks
15	73 min	>2 weeks	>2 weeks

During the conversion, the C2 and C3 Proton signals at 3.55-3.8 ppm, which are characteristic to the thiiranes, decreased in intensity. In the same rate two signals in the aliphatic range appeared. Taking into account the mechanisms of the conversion mentioned above, these two signals belonged to the olefinic protons of the developing Michael acceptor, which could be confirmed by ESI-MS. These two doublets showed coupling constants of ~ 16 Hz, an evidence that the reaction gave specifically a *trans*-olefin. In general the thermally induced desulfurizations, have been classified as non-stereospecific. In the case of our probes the reaction proceeds under tight stereochemical control, and could be used in the stereoselective synthesis of Michael acceptors despite the disadvantage of a laborious synthesis for the educt.

The most important result however was the proof of prolonged stability of the thiirane probes in water at room temperature, which was essential for the application as an ABPP probe in aqueous proteomes. Nevertheless the instability in DMSO however forbade the use of this standard solvent for the production of probe stocks. Instead we employed acetone for longer storage, or used freshly (max. 5 min before usage) prepared DMSO stocks if acetone was not applicable.

4.4 Proteomics

To investigate the proteomic reactivity of our probe library, we first incubated the probes with proteomes obtained by sonication of bacterial cells (*in vitro*-experiment, see 5.2.4.2.6). The bacterial strains used, are known to be model organisms for related pathogens, which were unavailable at that time. Before use, the proteomes were split into a cytosolic and a membrane fraction by centrifugation. After incubation with the probe library the fluorescent tag was attached by click-chemistry, samples were separated by SDS-PAGE, and analyzed with a fluorescent scanner (see Figure 4.4.0.14). First results proved the cyclopropane probe to be too unreactive to show labeling events in any of the used proteomes. The strong band appearing is related to an unspecific reaction with an abundant unidentified protein.

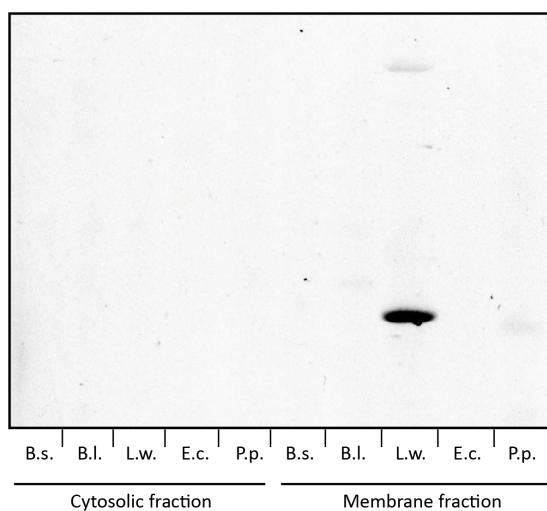


Figure 4.4.0.14: *Analytical in vitro-ABPP experiment with the cyclopropane probe (26) at 100 μ M in the cytosolic proteomes of Bacillus subtilis (B.s.), Bacillus licheniformis (B.l.), Listeria welshimeri (L.w.), Escherichia coli (E.c.) and Pseudomonas putida (P.p.)*

The labeling experiments of the heterocyclic probes however gave distinct and specific signals at varying intensities, depending on the used core motif (see Figure 4.4.0.15). Conclusions on the enzymatic targets of small molecule probes drawn from *in vitro* experiments however are of only limited value.

The lysis of bacterial cells releases the whole set of bacterial enzymes and puts an end to the fine tuned regulation of protein reactivity. Oxygen sensitive proteins which require the reductive environment of an intact cell, like many metal- or cysteine-dependent enzymes, may not function properly in lysates and can therefore not be detected by an activity-based probe.

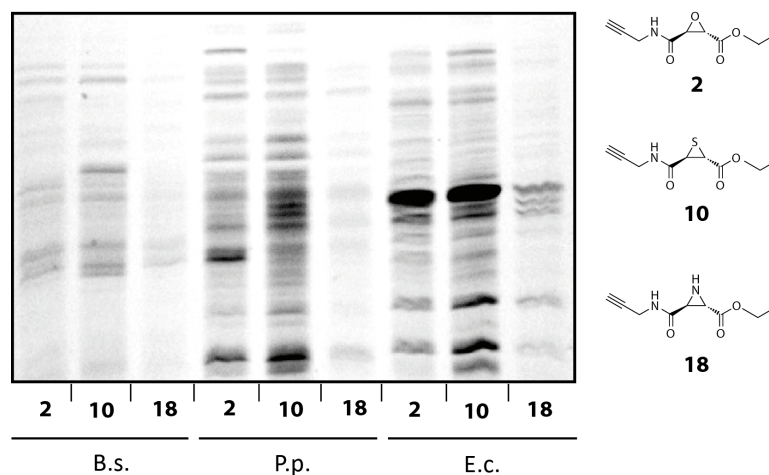


Figure 4.4.0.15: Analytical in vitro-ABPP experiment with heterocyclic probes **2**, **10** and **18** at $50 \mu\text{M}$ in the cytosolic proteomes of *B. subtilis* (*B.s.*), *P. putida* (*P.p.*) and *E. coli* (*E.c.*)

This can be circumvented by lysis of the bacteria under inert gas conditions or by using reduction agents like DTT. In addition to oxidation of the proteins, proteases cut down a significant amount of active enzymes before they can be targeted by the probes. This could be prevented by the addition of protease inhibitors like phenylmethyl-sulfonyl fluoride (PSMF). These inhibitors however render possible proteolytic target enzymes inactive as well so they can not be visualized. A strong disadvantage while scanning for novel enzymatic targets.

Results of higher significance can therefore be obtained by incubation of the probe with intact cells (see 5.2.4.2.7). After labeling under these *in vivo*-like conditions, the cells are lysed, the fluorescent marker is attached by click-chemistry, the samples are separated by SDS-PAGE and analyzed by a fluorescence scan. In these *in situ*-proteome studies, the probes face similar barriers as they would do under physiological conditions. Cell wall permeability, metabolic stability and target specificity are just a few of the important qualities of a probe, which contribute to the labeling under these circum-

stances. To identify possible vital or virulence related enzymes of pathogenic bacteria, only virulent strains were used in the following experiments. Probes labeling pathogenesis associated targets may serve later on as inhibitors for the regulation of the labeled virulence factors. By preventing the discharge of these factors into the host organism the pathogenic bacteria can be 'disarmed' and may be consumed by the immune system.^[53] If enzymes are labeled, which are essential for the survival of the bacterium, antibiotic properties of the probe are very likely. Additionally they could act as tools which may lead to mechanistic insights in the mode of action of these compounds. Prior to *in situ*-labeling, optimal probe concentrations for each compound class were determined by dose down experiments. Taking into account the lacking reactivity of the cyclopropane probes, *in situ*-labeling experiments were executed with the heterocyclic probes only. As expected the differences of the chemical properties (ring strain, stability of C-X bond) had a major influence on the reactivity of the different probes. As pictured in Figure 4.4.0.16 oxirane probe (**6**) showed an optimal signal to noise ratio at concentrations around 200 μM , whereas the more reactive thiirane probe (**13**) gave the best results at concentrations of 75-20 μM .

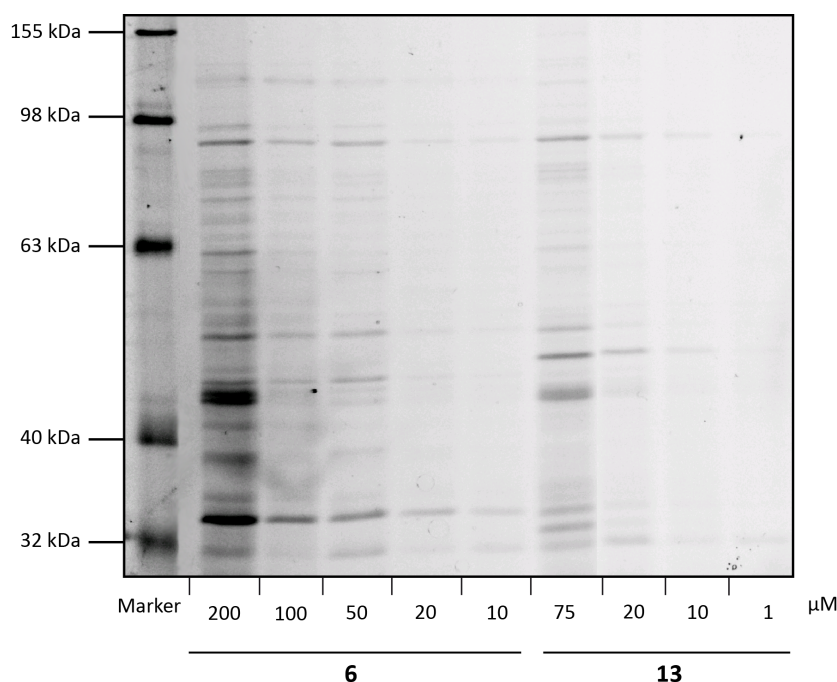


Figure 4.4.0.16: *In situ*-dose down experiment of oxirane probe **6** and thiirane probe **13** in *Listeria monocytogenes*

To compare the influence both the heterocyclic scaffold as well as the decorations on the proteomic reactivity, a labeling experiment of each organism with the whole compound library was placed on a single SDS-Gel. In the fluorescence scan, most of the heterocyclic probes showed distinct signals, with a variety of enzymatic targets depending on both their core motif as well as the decorations. Examples for these results can be seen in Figure 4.4.0.17 which depicts the fluorescent scan of an *in situ* profiling experiment in *S. aureus* Mu50. The aziridine probes only show weak signals even at concentrations around 200 μM , whereas the oxirane probes give significant labeling events at the same concentration. Thiirane and Michael acceptor probes were able to label their enzymatic targets at 20 μM , underlining their high proteome reactivity. The decoration have a major impact on target specificity, with long aliphatic chains (octyl) or aromatic residues (benzyl) are more favorable for target binding as can be seen with the signal at ~ 55 kDa.

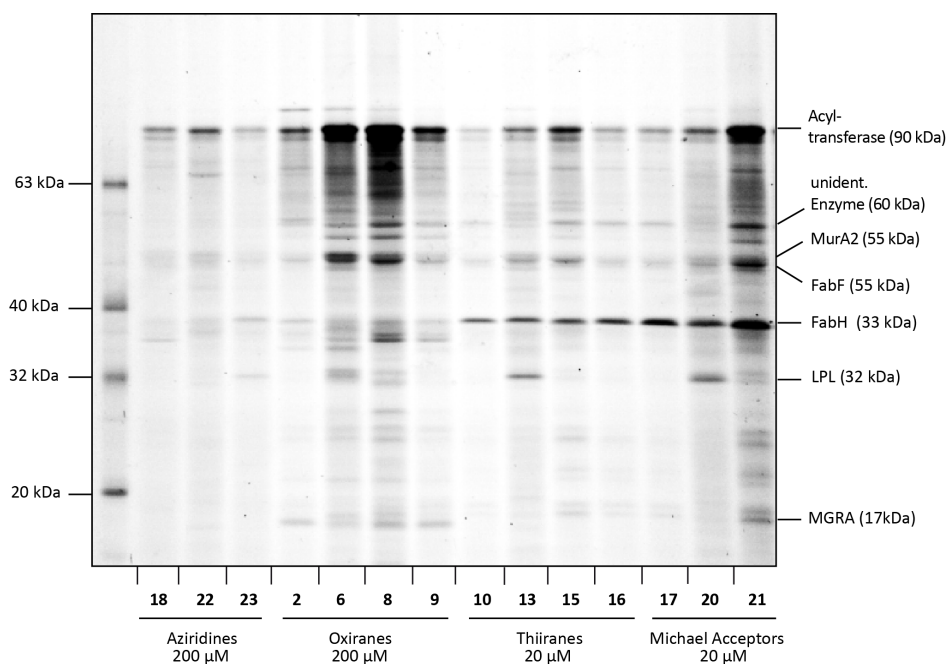


Figure 4.4.0.17: *In situ-experiment of all heterocyclic and Michael acceptor probes in S. aureus Mu50*

After cutting out the band from the gel, tryptically digesting the embedded enzymes the resulting peptides were extracted from the gel slices (see 5.2.4.2.8). These peptide mixtures could then be applied to an HPLC-MS

(see 3.3.5). The results were compared to databases which contain virtual proteomes derived from an *in silico* translation of the genome of the respective bacterium. The genomes were obtained by using NCBI databases (*S. aureus* Mu50^[153], *L. monocytogenes*^[154]).

A variety of peptide fragment fingerprinting software are available today to identify proteins from complex peptide mixtures. Two of the most popular programs are MASCOT and SEQUEST. Both programs virtually execute a digest on a database proteome. This results in a theoretical mass spectrum which allows the identification of proteins by comparing experimental data to the computer derived model. MASCOT uses an unpublished algorithm^[72] which calculates the probability for a match between an observed peak with its *in silico* counterpart to be random.^[155] Smaller values represent a higher confidence in the validity of the hit. Compared to SEQUEST, MASCOT leads to less identified peptides, however those being identified having a superior confidence.^[156]

SEQUEST, which was employed in the present work, uses a specialized and patented scoring algorithm which is based on a cross-correlating approach.^[71,157] The scoring function of SEQUEST is a two step procedure. At first a preliminary score (S_p) is calculated based on the length of a continuous y/b-ion sequence identified from the experimental spectrum. By this first step a collection of 500 candidate sequences is selected to which more resource-intensive computational methods can be applied.^[156] Additional statistical values like number of matched peptides between the theoretical spectrum and the experimental data (Peptides) or the peptide probability (P) help with protein identification. The P-value represents the number of ions that given the data, SEQUEST would have been able to find at least one peptide with as many matching ions in a search on a database of random sequences.

Several other quality factors are calculated by which the statistical significance of the results can be rated. One being the score of the number of fragment ions that are common to two different peptides with the same precursor mass and the cross-correlation score for all candidate peptides (XCORR, values >2.5 are considered 'good'^[158]). Another being the so called final score (S_f , values above 0.7 are considered 'good'^[158]) which is supposed to reflect the statistical strength of the SEQUEST hit. All proteins identified in the present work met each of the quality standards mentioned above (see Table 4.4.0.2

and Table 5.2.4.3).

The band at ~ 55 kDA in our gel (see Figure 4.4.0.17) could be enriched on Avidin beads and identified by LC-ESI-MS (see 5.2.4.2.8) as FabF. Additionally to FabF which showed up with the oxirane probes, a band at ~ 38 kDA could be found with all thirane and Michael acceptor probes. This enzyme was identified as FabH which appears to be selectively labeled by these two core motifs.

Both Fab-enzymes are part of the fatty acid biosynthesis in bacteria the so called KAS-II system, which is vital for both survival and growth of bacteria and has no direct homologies in eukaryotes. This pathway can be found in most bacteria in a highly conserved form and consists of a series of discrete proteins, each of which catalyzes an individual reaction of the biosynthesis. At least two different KAS enzymes are necessary for the function of the type II pathway. FabH (KAS-III) is thought to be responsible for the catalysis of the first condensation reaction of malonyl-acyl carrier protein (malonyl-ACP) with acetyl-CoA, which gives the butyryl-thioester of acyl carrier protein. The butyryl ester works as a primer for the following condensation or elongation reactions. This reaction is catalyzed by FabF (KAS-II) the second enzyme in the cycle (see Figure 4.4.0.18).^[2]

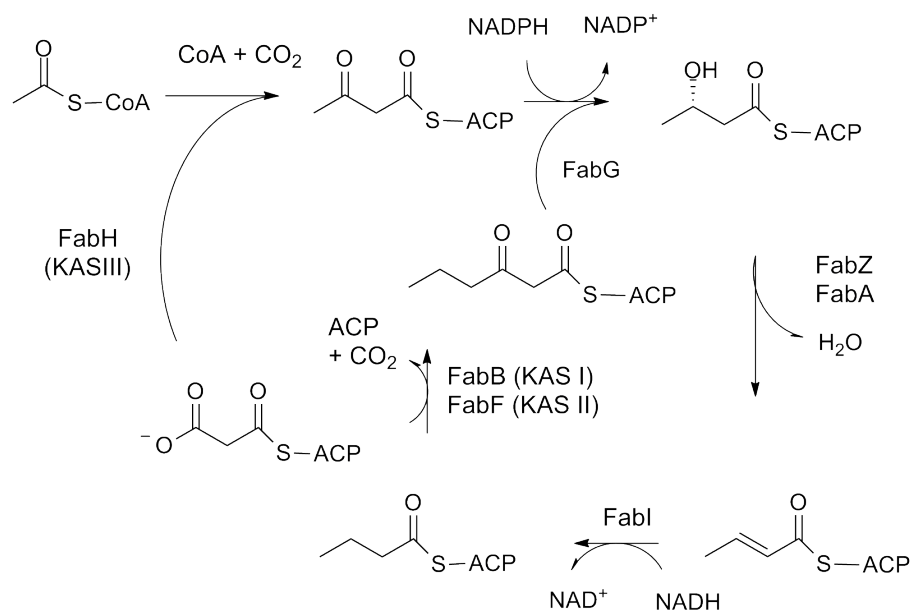


Figure 4.4.0.18: *Scheme of Kas-II pathway*

The thiirane as well as the Michael-acceptor probes decorated with octyl residues showed one of the strongest labeling signals and gave rise to an additional band at ~ 32 kDa. Mass spectrometry identified this band as a lipoate protein ligase (LPL). This enzyme exists in most prokaryotic and eukaryotic organisms and catalyzes the transfer of the cofactor lipoate to enzymes like the Pyruvate dehydrogenase.^[159] It features a nucleophilic cysteine in its active site, providing a point of attack for our probes. A similar experiment in *L. monocytogenes* showed comparable results both in reactivity as well as target profiles of the probes (see Figure 4.4.0.19).

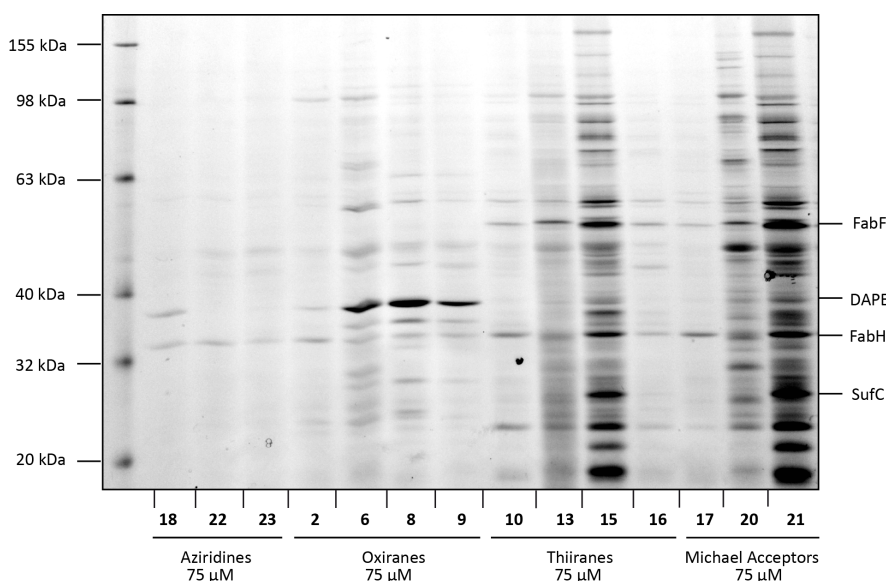


Figure 4.4.0.19: In situ-experiment of all heterocyclic and Michael acceptor probes in *L. monocytogenes*

As the oxirane probes were applied at $75 \mu\text{M}$ the overall signal strength was low, one exception being the band at ~ 40 kDa which was identified as a diaminopimelat epimerase (DAPE). This enzyme takes part in the lysine biosynthesis via the intermediate meso-diaminopimelic acid (meso-DAP), which is also a vital cell wall component in Gram-negative bacteria.^[160] The enzyme comprises a reactive cysteine in its catalytic pocket, which is supposed to attack the ring structure of our probes. Thiirane and Michael acceptor probes used at $75 \mu\text{M}$ however, showed strong labeling events as seen with the bands at ~ 55 kDa (FabF), ~ 38 kDa (FabH) and ~ 31 kDa. The latter was iden-

tified as a [Fe–S]-cluster protein (SufC) which is responsible for protoheme biosynthesis and the formation of iron-sulfur clusters under stress conditions in many bacteria.^[161,162] The common feature with enzymes mentioned above, is an active cysteine residue which SufC contains in its active site and which enables a covalent bonding with the probes. Interestingly, differences in target binding related to probe decorations were not observed in *Listeria*.

Table 4.4.0.2: List of peptides from preparative *in situ* labeling experiment in *Staphylococcus aureus* Mu50

Peptide	MH+	P(pro)	S _f	XCorr	Cov.	MW	Peptides	Cont.
MurA2 (Accession code: P65456)	-	1,29E-08	4,76	50,29	-	45046,5	5 (5 0 0 0 0)	0
2036	R.TLNGEVNIHGAK.N	1,51E-07	0,93	2,93	0,74	519,0	16/22	-
2591	R.GYTDIVLHLK.A	4,52E-07	0,96	3,57	0,60	1086,5	16/18	-
2805	K.LEGLPQISDVK.T	1,93E-02	0,92	3,44	0,46	590,1	15/20	-
2912	R.INNNAPYQFVDIK.T	2,55E-04	0,97	3,38	0,76	1119,5	20/24	-
3202	K.NSAVAIPATLLAQGHVK.L	1,29E-08	0,98	5,39	0,79	1164,2	26/34	-
FabH (Accession code: P68795)	-	2,22E-16	7,41	80,33	-	33857,9	8 (8 0 0 0 0)	0
1691-1697	K.ITDLTDR.S	2,76E-04	0,9	2,38	0,46	491,4	11/12	-
1987-1989	K.GFGAYAPEK.I	1,87E-05	0,85	2,53	0,63	451,6	11/16	-
2069	R.GHSYEM*GSDGTGGK.H	4,20E-09	0,97	3,41	0,89	1162,3	19/28	-
2329-2332	R.HWADDDQDTSDLAYEASVK.A	2,22E-16	0,99	6,54	0,97	261,1	27/36	-
2404-2406	R.GHSYEMGSDGTGGK.H	1,50E-07	0,98	4,24	0,64	2480,8	23/28	-
2506	K.QYVQSGDYHNILVVGADK.L	1,37E-05	0,79	2,46	0,48	476,9	17/34	-
2920	K.YGNTSAAIPLSIDQELK.N	1,45E-05	0,95	4,41	0,74	488,2	19/34	-
3012	K.ANLTSDIDILFIPHQANIR.I	3,78E-09	0,98	5,48	0,86	979,4	24/36	-
LPL (Accession code: Q99TW1)	-	1,64E-06	2,30	30,18	-	31861,3	3 (3 0 0 0 0)	0
1565-1567	K.MKEAFVEK.A	1,40E-04	0,66	2,11	0,44	382,5	9/14	-
1767	K.EIDDKVK.E	7,14E-03	0,68	2,76	0,24	275,4	10/14	-
2707	R.VISQGLLEGFK.N	1,64E-06	0,95	3,65	0,76	544,3	15/20	-
mgrA (Accession code: Q99VT5)	-	3,14E-08	5,62	60,23	-	17078,9	6 (6 0 0 0 0)	n.a.
1966-1968	K.VIHAFDETKK.-	6,58E-06	0,95	3,04	0,70	807,4	16/20	-
2026	K.VIHAFDETK.E	2,50E-07	0,88	2,63	0,49	703,8	12/16	-
2028	K.SETIRPELSNASDK.V	9,06E-06	0,96	3,28	0,66	1339,9	19/26	-
2110	R.M*EQVDLIK.R.E	4,34E-03	0,91	2,79	0,42	552,0	14/16	-
2671	R.EVFHLTDK.S	2,88E-05	0,94	2,78	0,76	361,6	14/16	-
3600	K.VASASSLSQDEVK.E	3,14E-08	0,98	4,59	0,74	1526,7	20/24	-

Table 4.4.0.3: List of peptides from preparative *in situ* labeling experiment in *Listeria monocytogenes*

Peptide	MH ⁺	P(pro)	S _f	XCorr	Cov.	MW	Peptides	Cont.
FabF (Accession code: Q71XG4)	-	9,74E-10	7,51	80,25	-	44252,2	8 (8 0 0 0 0)	0
1452 K.M*AIDDAGLTPDK.V	1262,59778	4,90E-07	0,84	2,98	0,67	150,7	13/22	-
1516 R.GDADAM*ITGGAEAPITK.M	1633,77826	1,79E-07	0,98	4,94	0,85	1634,7	21/32	-
1539 K.M*SLAGFTANK.A	1055,52349	5,67E-05	0,95	3,21	0,71	771,7	15/18	-
1862 R.LNPDDFPVK.I	1044,53601	5,54E-08	0,87	2,34	0,66	552,6	11/16	-
1866-1868 K.IAAELKDFDVEK.Y	1377,72607	6,20E-05	0,97	3,76	0,61	1566,4	17/22	-
2005 R.DNIAPTTHLK.N	1234,71545	3,26E-05	0,96	3,62	0,74	875,0	15/20	-
2496-2499 R.VVVVTGIGAVTPIGNDAETSWENAK.K	2428,23535	9,74E-10	0,97	4,75	0,71	1144,6	27/46	-
3026-3028 R.DGFIGEGAGIVLEEYEHAK.A	2260,14966	4,35E-07	0,98	4,65	0,78	1489,0	24/40	-
FabH (Accession code: Q71XG3)	-	3,26E-07	6,34	80,25	-	33949,5	8 (8 0 0 0 0)	0
1733 K.YLNLDENKK.I	1136,59460	3,97E-05	0,95	3,05	0,46	1167,1	14/16	-
2046-2048 K.ITNWDDDR.T	919,42682	2,01E-05	0,95	2,66	0,86	615,9	11/12	-
2118 -.LNLPEEK.-	842,46179	1,34E-02	0,27	1,83	0,09	311,2	8/12	-
2126 R.LNLPEEK.L	842,46179	3,92E-03	0,36	1,83	0,01	406,9	9/12	-
2175 K.NIVVVGADK.L	914,53058	3,51E-05	0,94	2,63	0,73	551,9	14/16	-
2609 K.IMDTSEWIR.T	1265,58301	1,15E-05	0,95	2,75	0,84	780,8	15/18	-
3060 R.AGLEKEKEDLLIPHQANIR.I	2145,16626	7,87E-06	0,94	4,47	0,61	944,6	35/108	-
3685-3690 K.YGNTSSSIALALVDAVEEGR.I	2139,05640	3,26E-07	0,98	4,92	0,79	1327,0	22/40	-
DAPE (Accession code: Q71Y02)	-	8,81E-07	3,59	40,19	-	36187,4	4 (4 0 0 0 0)	0
1292 K.SSEVGPQGMR.V	1176,57223	1,98E-04	0,97	3,26	0,74	1226,6	19/20	-
1321 -.M*ETHFTK.V	1022,50203	3,71E-04	0,94	2,75	0,51	829,6	13/14	-
1807 R.LSDDAIYVR.T	1051,54187	8,81E-07	0,71	2,31	0,64	225,4	9/16	-
2009 K.HSLGGADGILYVTK.S	1430,76379	2,12E-05	0,97	3,85	0,90	879,3	21/26	-
Sufc (Accession code: Q71X13)	-	2,22E-08	3,84	40,21	-	29135,7	4 (4 0 0 0 0)	n.a.
1643 K.STLSSAIMGHPK.Y	1228,63538	2,22E-08	0,97	3,37	0,86	1530,1	19/22	-
1752 K.IQLHVEIEGK.E	1280,68445	1,34E-03	0,97	4,08	0,61	1436,8	17/20	-
2793-2795 R.REEGDEIPVMQFIR.K	1718,85303	1,61E-03	0,97	4,15	0,74	962,5	19/26	-
3495 K.LAILDEIDSLDIDALK.V	1813,97937	1,38E-02	0,93	2,87	0,94	527,9	16/32	-

4.5 Assays

4.5.1 Minimal inhibitory concentration

The identified target by mass spec raised the question of a possible antibiotic effects of thiiranes and Michael acceptor probes due to their ability to be dual inhibitors of FabF/H. We therefore tested our library in a minimal inhibitory concentration assay (MIC, see 5.2.1.2.2). The antibiotically active FabF inhibitor cerulenin was used as an internal standard for the experiment. To find the lowest concentration of an antibiotic by which the growth of a bacterial culture will be inhibited, bacteria are incubated with a series of probe dilutions. The results can be read out by the optical density of the culture after 16-48 h. In accordance with the preliminary results of the *in situ*-labeling and mass spec experiments (see 4.4), thiirane and Michael acceptor probes showed strong antibiotic effects in gram positive bacteria down to 75 μM exceeding the values of the structurally similar antibiotic cerulenin (see Table 4.5.1.1).

Table 4.5.1.1: List of MIC

Compound	L.m.	Mu50
2	>500 μM	>500 μM
4	>500 μM	>500 μM
5	>500 μM	>500 μM
6	>500 μM	>500 μM
7	>500 μM	>500 μM
8	>500 μM	>500 μM
9	>500 μM	>500 μM
10	500 μM	500 μM
11	150 μM	150 μM
12	100 μM	100 μM
13	75 μM	75 μM
14	500 μM	500 μM
15	500 μM	500 μM
16	100 μM	200 μM
17	>500 μM	500 μM

20	200 μM	100 μM
21	150 μM	200 μM
18	>500 μM	>500 μM
22	>500 μM	>500 μM
23	>500 μM	>500 μM
cerulenin	150 μM	200 μM

Next to the core scaffold, the decorations on the probes proved to have a major influence on the antibiotic potency of the compounds. Long aliphatic side chains and aromatic residues seem to maximize enzyme binding, in agreement with the corresponding intensity profiles in the labeling experiments. Oxirane and aziridine compounds however showed less or no antibiotic effects up to 500 μM . Obviously the exclusive inhibition of FabF by the oxiranes is insufficient to inhibit the fatty acid biosynthesis, a result already known from knockout studies.^[7]

4.5.2 Toxicity to eucaryotic cells

Compounds that may find application as antimicrobial agents not only have to be active against their bacterial targets, but should also be well tolerated by eucaryotic cells. To investigate the potential cytotoxic side effects of our compounds, we used a Methylthiazol-tetrazoliumbromid (MTT) Assay. This assay determines the metabolic activity of cells in relation to the concentration of the inhibitor. The result can be read out by spectroscopic methods (see 5.2.2.2.3).^[163] The natural reducing agents NADH and NADPH, which are produced during metabolism of most eucaryotic cells, reduce the yellow MTT-dye to purple formazan. The turnover can be measured by the change of absorption between 500 and 600 nm with a photometer (see Figure 4.5.2.1).^[164,165] An increase or decrease in cell numbers or metabolic ac-

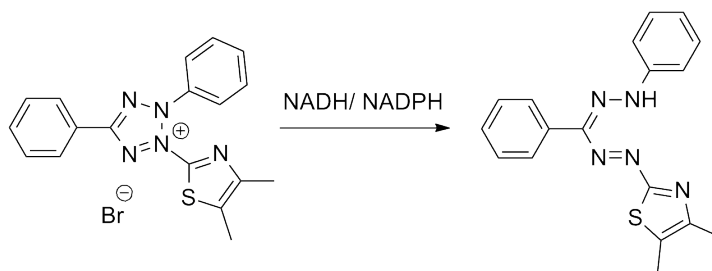


Figure 4.5.2.1: *Conversion of MTT to the corresponding formazan*

tivity result in a concomitant change in the amount of formazan formed, indicating the degree of cytotoxicity caused by the test material. Two different cell lines were used in this assay to analyze the effect of our compounds on different types of tissue (see 5.2.2.2.1). As seen in Figure 4.5.2.2 all tested compounds showed toxic effects to the eucaryotic cells in their range of antibiotic activity (75-200 μM). This result however is not surprising as the structurally related antibiotic cerulenin displays cytotoxicity at concentrations down to 5 μM .^[166] These toxic effects are due to the little specificity of cerulenin for the bacteria-exclusive KAS pathway. The eucaryotic FAS pathway, which is responsible for eucaryotic fatty acid biosynthesis is a target too. The same mechanism presumably applies for the thiirane and Michael acceptor probes as well.

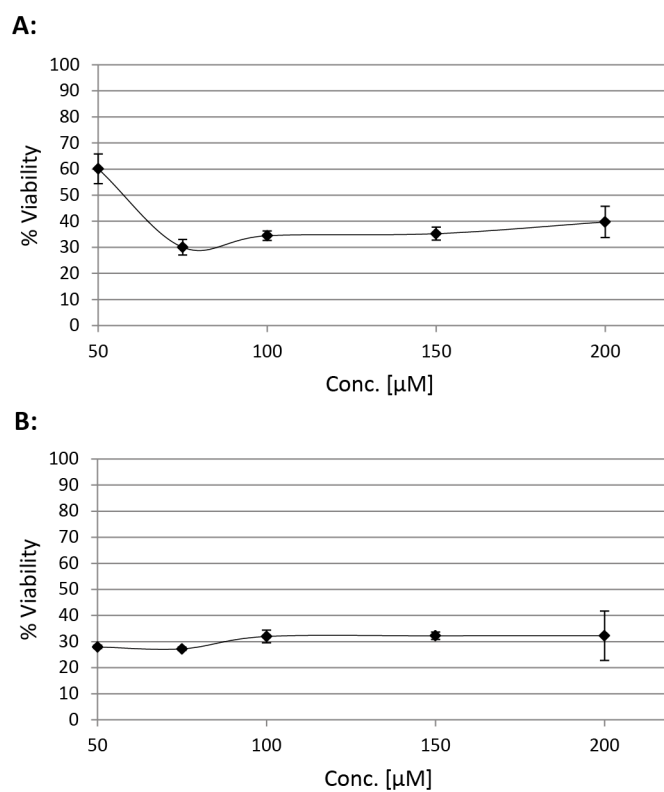


Figure 4.5.2.2: Cell viability measured by a MTT-assay in triplicates at different concentrations of probe **13** (A) and **15** (B)

4.6 Target verification by recombinant overexpression

4.6.1 General

The methods of protein identification by mass spectrometry have improved during the last years regarding sensitivity and reliability. But to this day this technique is associated with an inherent error which can be related to bias and noise of the analytic method. These errors can lead to irreproducible results, even when running replicate samples. These extraneous variabilities in mass experiments raise the need for verification of the obtained results. By combining the results of different algorithms like SEQUEST, MASCOT, PeptideProphet or Sonar it is possible to increase the quality of data. Additional statistical analyses that indicate the measure of identification certainty, or allow a determination of the false- positive rate, can be applied for large scale experiments.^[167] The method uses a decoy-database which preserves the general composition of the target database while minimizing the number of peptide sequences in shared between the target and decoy. The decoy-database can be created either by reversing^[168,169] the target protein sequences or by stochastic means, such as Markov chain modeling.^[155] By attaching the decoy- to the target-database creates a composite database against MS/MS spectra are scanned. Assuming no correct peptides are found simultaneously in the target and the decoy portions, one can estimate the total number of false positives that meet specific selection criteria.^[170] While this is an excellent validation method for MS/MS searches of large data sets, it is not useful for a search of a small number of spectra, because the number of matches is too small to give an accurate estimate.^[171,172] The MS-analysis of single gel bands, which was used in the present work is one example for a database proving too small for this procedure to give relevant results.

The method of choice to validate the MS results is the recombinant overexpression of bacterial protein targets either by the bacterial host itself (homologous) or by organisms like *Escherichia coli* (heterologous) which are specially designed for this purpose. For the efficient transformation of DNA into bacterial cells a range of plasmid shuttles is commercially available. The majority

of these so called vectors consists of at least 5 parts, which are: a regulatory promotor which can be induced to start protein overexpression, a ribosome binding site to start the initiation of the translation, a multiple cloning site for the introduction of DNA encoding the target protein, a stop codon and a selective marker, which in most cases is an antibiotic resistance. Additionally many vectors contain the DNA sequence coding for a short amino acid sequence. These so called tags can be used for the protein purification after lysis of the cell, or help to solubilize the product. After the insertion of the target DNA into the appropriate vector, the plasmid is then transformed into the host cell. Selection of the successfully transformed bacteria can be achieved based on their newly acquired antibiotic resistance from the vector. Usually single clones can be picked and cultured in the presence of a selection marker. By reaching a certain optical density (which corresponds to the cell density), the inducing agent is added. After a while cells can be harvested and lysed to obtain the desired protein. If the product contains one of the many available vector encoded purification tags, the enzyme can be purified by different affinity chromatography methods, like the Strep-Tactin or Ni(II)-affinity columns. The Strep-tag II, which was used in the present work is a synthetic peptide consisting of eight amino acids (Trp-Ser-His-Pro-Gln-Phe-Glu-Lys) with a femtomolar binding constant for Strep-Tactin. It can be eluted under mild conditions and gives the desired protein in high purity. When using Ni(II)-affinity columns a so called His-tag is attached to the protein of interest. The tag consists of six histidine residues three pairs of which each form an octahedral complex with one Ni(II)-NTA. The binding constant is low enough to provide a very efficient binding to the column material. Elution of the desired protein is achieved by washing with imidazole, thereby disrupting the metal-protein complex.

4.6.2 Heterologous overexpression in *E. coli*

The heterologous overexpression of proteins in *E. coli* is arguably the best studied bacterial system known, with a variety of commercially available strains, which have been optimized regarding time- and cost-efficiency. These strains can be deficient in restriction enzymes, overexpress chaperones which help the

folding process of the desired protein or produce larger quantities of plasmids, to name just a few examples. One of these streamlined systems using *E. coli* is the Gateway system by Invitrogen (see 5.2.3.3.4). This system relies on a set of recombination sequences, the attachment-sites (ATT) and two enzyme mixes (BP and LR Clonase) that enable a fast and efficient transfer of DNA-fragments into and between plasmids. This system was used for the overexpression of FabF and H, LPL, MGRA (all from *S. aureus* Mu50) as well as DAPE and sufC from *L. monocytogenes* EGD-e (see 5.2.3.3.4).

The first step was the selective amplification of the single genes by PCR using special primers containing ATT-sequences. After purification of the DNA by Agarose gel electrophoresis the PCR products were cloned into the vector pDONR201 (see 5.2.3.3.4). By transformation of the vector into chemically competent Top10 cells (Invitrogen) the vector was amplified by the cells (see 5.2.3.3.7). The cells were harvested, the plasmids extracted and the sequence identity was confirmed by sequencing. Cloning into the expression vector pDEST007 was achieved by using the LR-Clonase Mix II (see 5.2.3.3.4). This vector contains a StrepII tag which can be used for later purification. After transformation of the resulting vectors in chemically competent BL21 (see 5.2.3.3.7) , the overexpression could be induced by addition of Anhydrotetracyclin (see 5.2.3.3.10). After lysis of the cells, the whole cell proteome was labeled by the respective probe (see 5.2.4.2.7), ran on a SDS-Gel and analyzed by a fluorescence scan. To prove selective binding of the probes, an additional heat control was prepared (see 5.2.4.2.5). If the probe-target interaction is related to the catalytic activity of the enzyme, the heat denaturation of the active site should prevent any selective interaction with the probe, resulting in a lacking fluorescent signal in the gel.

As seen in Figure 4.6.2.1 all enzyme targets of *S. aureus* Mu50 could be verified, based on their fluorescent signals. A comparison between the non induced control (n.I.) and the induced sample (I.) shows the success of the overexpression.

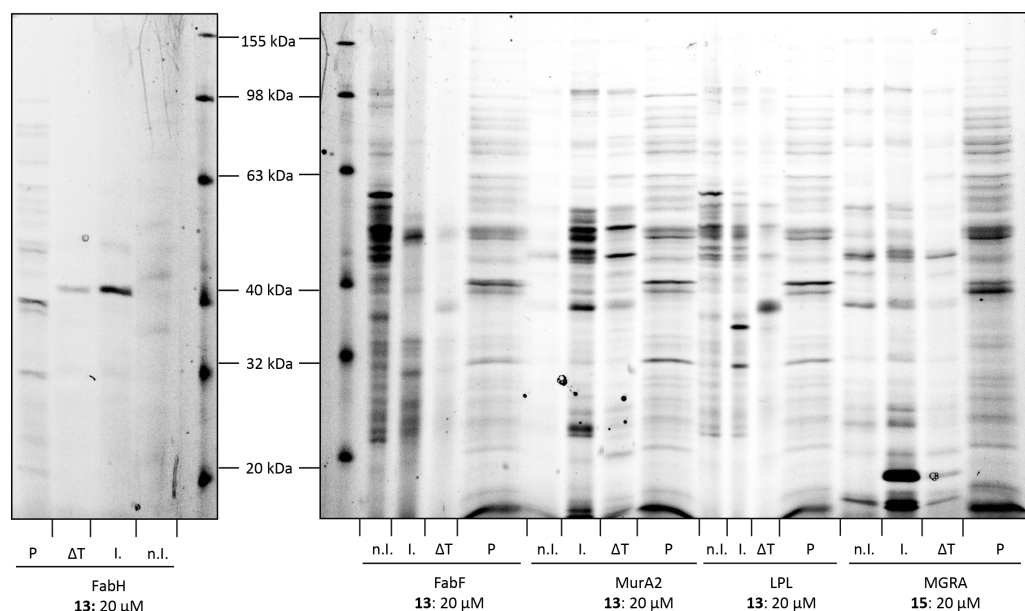


Figure 4.6.2.1: *Confirmation of the enzyme targets from S. aureus Mu50: non induced control (n.I.), induced (I), heat control (ΔT) and comparison with S. aureus Mu50 proteome (P)*

However the appearance of two bands instead of one, in all but one case (FabH) was unexpected. The answer to this problem could be found by looking at the design of the vector plasmids. All shuttles but the FabH plasmids contain two starting codons for the transcription machinery (ATG). The first starting codon is part of the vector, and is placed at the N-terminal end upstream of the Strep II tag and the following gene of the desired protein. The second ATG was inserted by the PCR product itself. Hence both fluorescent signals represent the same enzyme, one time bearing the tag the other representing the wild type enzyme. When compared to the *in situ* labeling of *S. aureus* Mu50 (labeled P) the lower of the two overexpressed signals corresponded well to its wild type counterpart. The severe reduction in labeling intensity of the heat controls verified the selective reaction of the probe with

the active sites of its targets. To validate targets identified from *L. monocytogenes*, namely the Diaminopimelat epimerase (DAPE) and the [Fe–S]-cluster protein sufC were labeled with probe **6** (OxyOc) and analyzed by SDS-PAGE followed by an in gel fluorescent scan (see Figure 4.6.2.2).

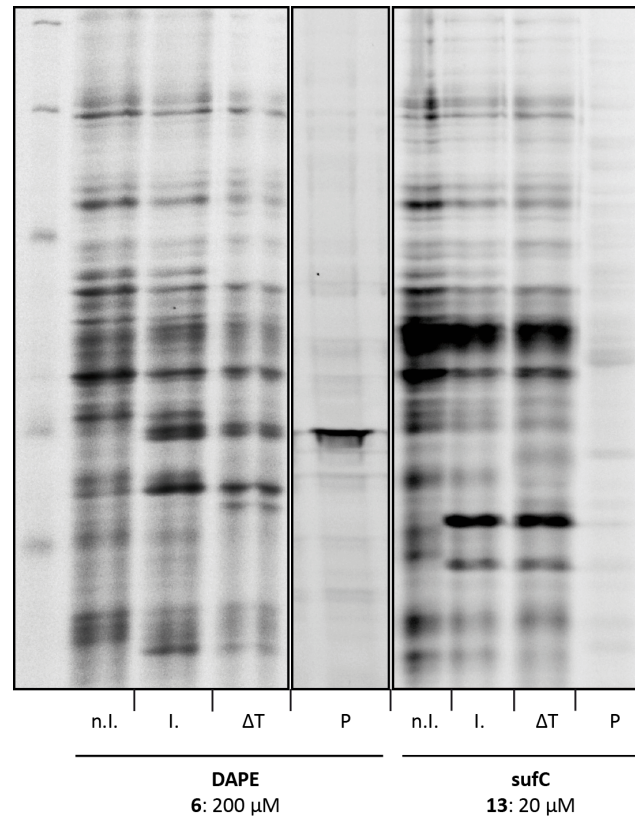


Figure 4.6.2.2: *Confirmation of the enzyme targets from *L. monocytogenes* by labeling with probe **6** at 100 μ M: non induced control (n.I.), induced (I), heat control (ΔT) and comparison with *L. monocytogenes* proteome (P)*

The overexpression of both enzymes was confirmed by comparing the non induced with the induced samples. In the induced samples strong bands appeared on the same height as the signals in the proteomic labeling experiment of the pathogen, verifying the identity of the overexpressed enzymes. The heat control however showed a reduction in signal intensity only with the epimerase. The [Fe–S]-cluster protein was still labeled, which leads to conclusion that the probe-protein interaction does not depend on a correctly folded active site of this protein.

4.7 Mechanism of action

4.7.1 Fatty acid biosynthesis

The protein targets of the thiirane probes validated by recombinant overexpression in *E. coli* raised the question, which of the enzymes were related to the antibiotic activities of the compound library (see 4.5.1). The structural resemblance of the antimicrobial FabF inhibitor Cerulenin and our probe library, indicated that FabF could be a promising candidate. FabH and F recurred in the MS analysis of the proteomic labeling of our probes in three different bacteria (*S. aureus*, *L. monocytogenes* and *P. putida*).

The crystal structure of both enzymes shows a nucleophilic cysteine (Cys) in the catalytic pocket which is activated through deprotonation by a neighboring histidine (His, see Figure 4.7.1.1). In case of FabF a second histidine enhances this catalytic diad, in case of FabH an asparagine enables the protein to form a catalytic cysteine triad.^[173,5] In both enzymes the activated cysteine should be able to attack the three membered ring of the probes by a nucleophilic ring opening reaction, crating a covalent bond to the probe.

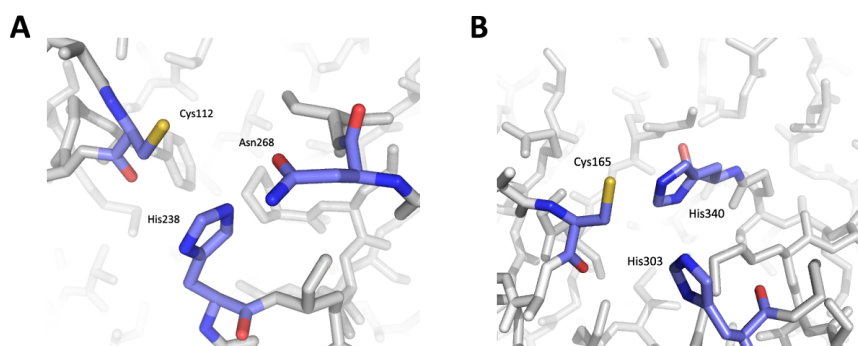


Figure 4.7.1.1: Active sites of *FabH* (A) and *FabF* (B) from *S. aureus*^[173,5]

The *in vivo* roles of both enzymes have been investigated thoroughly by knockout mutants in several organisms.^[174,7] In some bacteria *FabF* mutants are reported to be viable as backup enzymes like *FabB* (KAS-I) seem to take over the catalytic steps of *FabF*.^[7] Knockout mutants of *FabH* however main-

tain only 5-10 % of their capacity to synthesize fatty acids and are therefore not able to grow on minimal media.^[175]

Several antibiotics such as platensimycin, platensin, cerulenin or thiolactomycin are known to owe their activity to inhibition of enzymes involved in fatty acid synthetis (see Figure 4.7.1.2).^[176] Platensimycin is a structurally unique antibiotic which was isolated from *Streptomyces platensis* in 2006. It acts as a potent FabF/B inhibitor, causing its broad-spectrum gram-positive in vitro activity.^[177] The same effect can be accomplished by platensin, another natural product isolated from *Streptomyces platensis*. Its mechanism relies on a dual inhibition of FabF and H leading to a complete breakdown of fatty acid synthesis.^[6]

The broad spectrum of antibiotics targeting the FabF/H system encouraged us to investigate a possible connection between the dual labeling and the antibiotic activity of the thiirane probes.

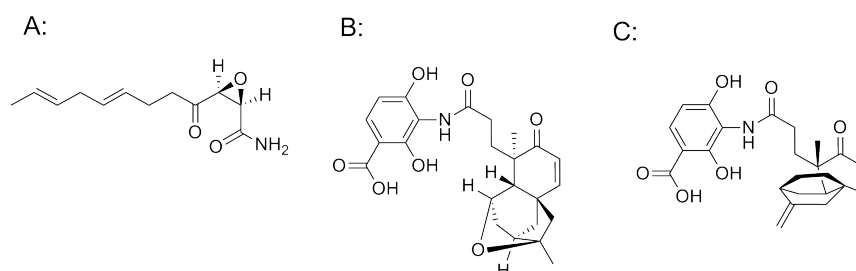


Figure 4.7.1.2: Natural products inhibiting the Kas-II pathway: Cerulenin (A), Platenimycin (B) and Platensin (C)

4.7.2 Genetic Knockout

To prove the mechanism of action of the antibiotic activity of the thiirane probes, we first decided to create FabF and H knock out mutants in *S. aureus* Mu50. By either exchanging, disrupting or deleting the gene from the chromosomal DNA, the transcription as well as the translation of the gene can be obstructed. This can be used to study the function of the gene products by comparison of the phenotypes of the wild-type and the mutant organism. The

MIC was expected to drop, as the knockout would deplete the cells of most of its functional FabF and H. If the antibiotic effect of the thiirane probes would rely on the inhibition of these enzymes, less probe molecules should be necessary to inhibit all FabF/H enzymes as less enzyme molecules are available in the cell. A decrease of the MIC values was therefore expected along with a decrease in signal intensity in ABPP experiments.

For the knockout of the FabH and the FabF gene we used the TargetTron System from Sigma Aldrich, which is based on disrupting a gene by selective reverse transcription of designed RNA into the target DNA (see 5.2.3.3.9). The first step, the design of a DNA homing sequence by PCR was successfully performed. After purification, the DNA was digested with DpnI and HindIII to produce sticky ends for the ligation reaction with the vector. After linearization of the vector pNL9164 (see 5.2.3.2) with HindIII the ligation with the PCR gave the shuttle, which could be purified by Gel electrophoresis. Dr. Mäusbacher then transformed the plasmid in *E. coli* by heat shock (see 5.2.3.3.7). After isolation and purification the vector identity was confirmed by sequencing and transformed in a restriction deficient strain RN4220 of *S. aureus* by electroporation (see 5.2.3.3.7). This step is necessary to obtain the correct DNA methylation pattern for the successful transformation in wild type *S. aureus*. Yet the transformation in *S. aureus* Mu50 proved to be difficult as selection of successful clones was impossible due to an innate resistance of the bacterium against the selection marker of the plasmid. We therefore used the transformed RN4220 strain for the knockout studies, as sequence homology FabF and H in Mu50 and RN4220 is >99 %. The gene knockout was induced by the addition of CdCl₂ (see 5.2.3.3.10) and the cells were used in an *in situ* experiment (see 5.2.4.2.6) and compared to the RN4220 wild-type cells (see Figure 4.7.2.1).

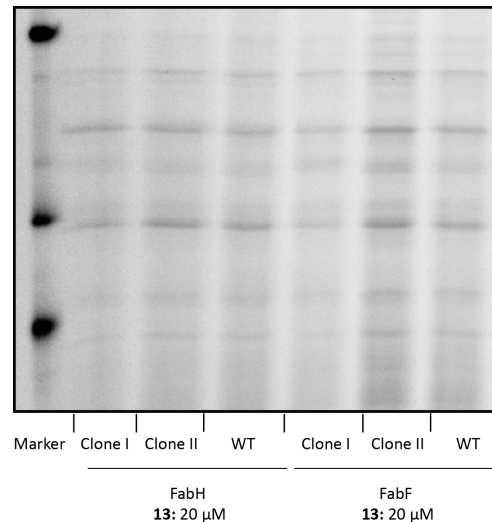


Figure 4.7.2.1: *Fluorescent scan of the overexpression on FabH and FabF in S. aureus Mu50 compared to the wild type (WT) with probe 13 at 20 μM*

The fluorescent scan of the experiment no change in labeling intensities between both strains could be detected. As the the identity of the vector isolated from the transformed RN4220 was confirmed by sequencing, obviously the induction of the enzyme knockout itself did not work. The targetron user manual points out, that some DNA designs may have a low retro-homing efficiency. The only solution for this problem is to start over, using a new design.^[178] This however was not possible due to timely restrictions.

4.7.3 Homologous overexpression

After decreasing the FabF and H concentration by genetic knockout proved to be difficult, an inverted method was tested in collaboration with Dr. Nina Mäusbacher. By increasing enzyme concentration via a homologous overexpression of the enzymes in the host organism, the cells were thought to show the reverse effect of the knockout phenotype. Increased signal intensities along with increasing MIC values of the induced cells were the anticipated result. Both *S. aureus* Mu50 as well as *L. monocytogenes* were selected for the overexpression to broaden the scope of this experiment.

The cloning procedure for the homologous overexpression of FabF/H in

Mu50 followed standard protocols. We here used the vector pRB473XylR (see 5.2.3.2) which was first digested with BamHI and EcoRI (conditions according to suppliers manual) to generate a linearized plasmid with sticky ends. The linearized vector was then purified by gel electrophoresis. After colony PCR of FabF/H of *S. aureus* Mu50 (see 5.2.3.3.2) the inserts were digested with BamHI and EcoRI (conditions according to suppliers manual) and ligated into the linearized vector by using T4 ligase (see 5.2.3.3.6). The ligation reaction was transformed in chemically competent Top10 cells, followed by a plasmid extraction. The identity of the vector was confirmed by sequencing. To obtain a certain methylation pattern on the plasmidic DNA, which is necessary for successful transformation into *S. aureus* Mu50, the vector was first placed into the restriction deficient strain *S. aureus* RN4220 (see 5.2.3.3.7). After plasmid extraction, the vector was successfully transformed into electrocompetent cells (see 5.2.3.3.7) *S. aureus* Mu50. The following cultures had to be prepared in glucose free LB medium, as glucose has an antagonistic effect on the promotor of the pRB473XylR plasmid. Several attempts to induce the overexpression with Xylose failed even when using different concentrations and expression times. As displayed in Figure 4.7.3.1 the fluorescence scan of an *in vitro* ABPP experiment (see 5.2.4.2.6) showed no difference in labeling intensities between induced and non-induced controls. This result was confirmed by looking at the Coomassie stained gel (see 5.2.4.2.2) which revealed no differences in protein amounts either.

We therefore switched to a second vector (pHPS9) that features a constitutive promotor which is not controlled by any inducer. This allows for continual transcription of its associated gene by the host organism, however deprived us of the possibility to compare non induced and induced samples. Additionally the plasmid is unstable at 37 °C so that all experiments must be conducted at 30 °C. For the vector assembly the same protocols as for pRB473XylR were used (see above). The empty pHPS9 was digested with BamHI and EcoRI (see above) vector was ligated with the PCR products and transformed in *E. coli*. The plasmid was extracted and successfully transformed in *S. aureus* RN4220. After extraction the vector was transformed into *S. aureus* Mu50 and grown to stationary phase at 30 °C. The cells were lysed and used in an *in vitro* ABPP experiment (see 5.2.4.2.6) to show overexpression. Like with vector pRB473XylR neither in the fluorescence scan nor in the Coomassie

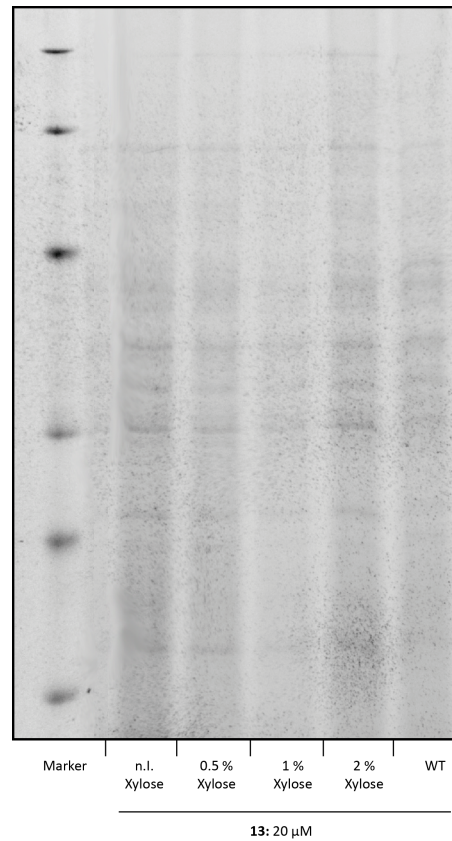


Figure 4.7.3.1: *Fluorescent scan of the overexpression on FabH in S. aureus Mu50 with different concentrations of xylose compared to a non induced control (n.I.) and the wild type (WT) with probe 13 at 20 μM*

stain an increase in signal strength could be observed. When looking at literature, surprisingly no homologous expressions in *S. aureus* Mu50 are known to this day. After we encountered these difficulties we tried the overexpression of the enzymes in RN4220. However no expression could be observed either (data not shown). This fact and the results of both our experiments led to the general finding, that the usage of *S. aureus* with the described vectors may not be possible due to unknown reasons. These issues should to be analyzed in further detail, to allow the homologous overexpression of different targets in *S. aureus*, which could prove to be very useful in the future. Because the above mentioned troubles with *S. aureus* we switched our focus to *L. monocytogenes*, a system for homologous overexpression which is described in literature. For the overexpression we used a protocol kindly supplied by the group of Prof. Dr. Fuchs from the department for microbiology of the TUM.

The technique relies on ligation independent cloning of PCR fragments into a vector by using specific, non-covalent interactions between long tails on both reaction partners (see 5.2.3.3.5). The first step is preparation of the FabF and H gene by PCR (see 5.2.3.3.2) which could be successfully deployed. After linearization of the vector pDG148Stu (see 5.2.3.2) by digestion with StuI (conditions according to suppliers manual), the purified PCR product was ligated into the plasmid by ligation independent cloning (see 5.2.3.3.5).^[179,180] The resulting vector was successfully transformed into chemically competent *E. coli* (see 5.2.3.3.7), extracted and verified by sequencing. After the transformation of the vector into electrocompetent *L. monocytogenes* EGD-e, the overexpression could be induced by addition of IPTG for 2 h. After lysis of the cells the proteome was used in an *in vitro* ABPP experiment (see 5.2.4.2.6) to analyze overexpression. As shown in Figure 4.7.3.2 both FabF and FabH were expressed in an active form, which could be labeled by our probes.

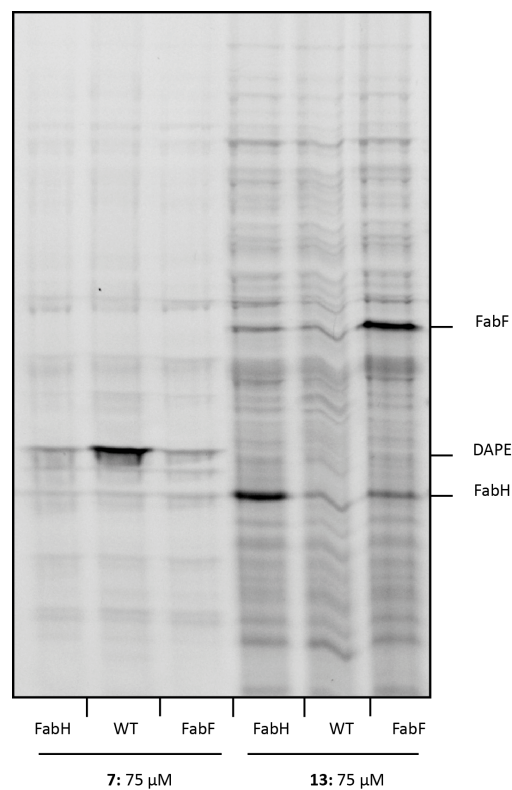


Figure 4.7.3.2: *Fluorescent scan of the overexpression of FabF and H in L. monocytogenes EGD-e compared to the wild type (WT) with probe 7 and 13 at 75 μM*

The success in this key step now allowed the investigation of the effect of the homologous overexpression on the minimum inhibitory concentration of the antibioticly active thiirane and Michael acceptor probes. 1 h before MIC experiments were conducted (addition of antibiotics) the overexpression was induced to allow for sufficient expression of the FabF/H (see 5.2.1.2.2). By using cells that were transformed with the empty vector, the wild-type strain and the non induced control as an internal standard, deviations of the MIC by overexpression were analyzed. We expected an increase of the MIC values with the overexpressing bacteria as an extended concentration of enzyme was expected to bind a higher amount of probe molecules. Surprisingly no correlated increase of the MIC could be observed; neither with the overexpression of FabF nor FabH. The MIC of probe **13** remained at 75 μ M within the controls (empty vector, non induced control), as well as the wild-type and the clones overexpressing the target enzymes. Interestingly the overexpression of FabF did not show any effect on the MIC of the internal control cerulenin either. As the antibiotic effect of cerulenin is based on a FabF inhibition an increase of the MIC was expected.

A possible explanation can be found in the dual-inhibition mechanism of the thiiranes which is supported by the labeling patterns observed in the in-gel fluorescent scans. As both FabF and H are involved in the same pathway, the less expressed enzyme of the two may be the limiting factor of the production rate of the whole biosynthetic pathway. Therefore the overexpression of a single enzyme might not have an effect on the overall turnover of the pathway. The homologous coexpression of the two enzymes will give a final answer to this interesting question and would provide an interesting topic for a future research project.

4.7.4 Point mutation

A powerful method to investigate the specificity of enzyme inhibitors and ABPP probes, is the change in binding parameters of the inhibitor with a mutated enzyme. By replacement of the active site by structurally related, but inactive amino acids (e.g. cysteine mutated to alanine) a covalent binding of the probe to the active site should be obstructed, thereby leading to reduced

labeling intensities in the fluorescence scan of the ABPP experiment. The so called point-mutation of one amino acid of an enzyme can be achieved by a technique called site-directed mutagenesis (see 5.2.3.3.8) which uses the application of specifically designed miss-match primers in a PCR-like reaction to create systematic aberrations at specific site in plasmidic DNA. These mutated plasmids can then be used for the heterologous overexpression of the mutated enzymes. We here used the pDonr vectors, created for the expression of Fab/F in *E. coli* as the template to mutate the reactive cysteine in FabF (C165) and FabH (C112) to an catalytically unreactive Alanine. After the mutation reaction (see 5.2.3.3.8) the linear vectors were transformed into *E. coli* XL1 blue cells by heat shock (see 5.2.3.3.7). The identity of the mutant was validated by sequencing the plasmid after extraction from the cells. By an LR reaction the mutated genes were placed in the pDEST007 vector (see 5.2.3.3.4) which was then transformed in *E. coli* BL21 cells by heat-shock (see 5.2.3.3.7). After the overexpression (see 5.2.3.3.10) the cells were lysed and the proteome was used in an *in vitro* ABPP experiment. The amount of protein produced could be analyzed by a Coomassie stain of the SDS-gel, using the non induced samples as a control. As shown in Figure 4.7.4.1 the overexpression of both FabF and H produced the mutated protein large quantities.

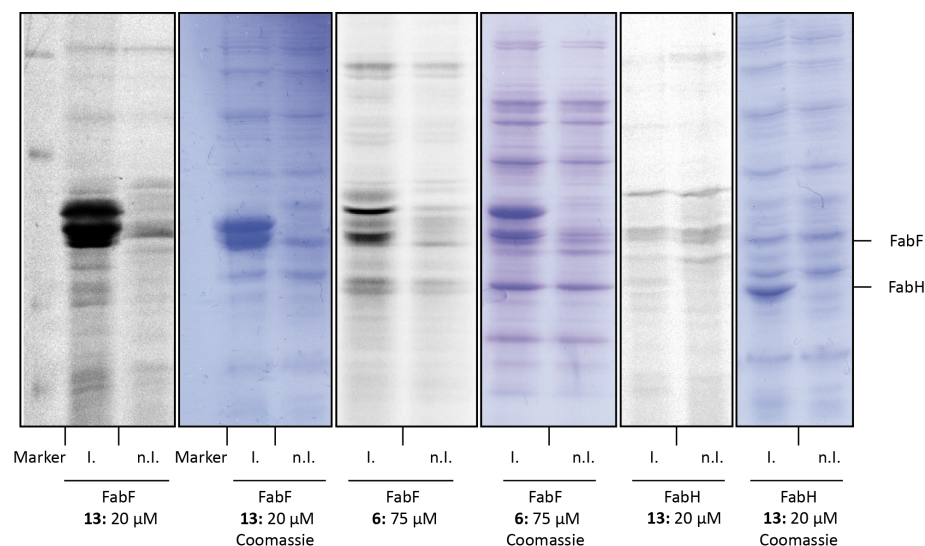


Figure 4.7.4.1: *Fluorescent scan and Coomassie stain of the overexpression of C112A-FabH and C165A-FabF compared to the non induced controls (n.I.). with probe 13 at 20 μM and probe 6 at 75 μM*

with the active site described in literature. To gain more information on the reactive site of FabF we preincubated FabF with a tenfold excess of the FabF inhibitor cerulenin. Interestingly the labeling intensity our probe was reduced greatly due to the inhibitor. This led to the conclusion that cerulenin and the probe molecules compete for the same active site, yet not for the active site described in literature. FabF features two more cysteine residues (C220 and C376) which could possibly be involved in the nucleophilic attack on cerulenin and our probe molecules. The point mutation of both residues would answer the question which of the two is responsible for probe labeling.

4.8 Summary

A small library of substituted homo-(cyclopropane) as well as heterocyclic (aziridine, oxirane, thiirane) probes was applied to living bacteria and the enzymatic targets of the different probes could be visualized by attachment of a fluorescent tag to the labeled enzymes. As expected, probes showed distinct differences in reactivity and selectivity depending on the core motif as well as their decorations. Oxirane and the thiirane probes proved to label enzymes selectively in concentrations as low as 50-10 μM . Analysis of the targets of oxirane and thiirane probes by HPLC-MS, led to the identification of two vital enzymes (FabF and FabH) in the KAS-II fatty acid biosynthesis pathway in *Listeria monocytogenes* and *Staphylococcus aureus*. This system can be found in most bacteria in a highly conserved form and consists of a series of discrete proteins, each of which catalyzes an individual reaction of the biosynthesis. Both contained a nucleophilic cysteine residue in their active sites, which were able to covalently bind to the probe by attacking the electrophilic ring structure.^[3,4,5] However the oxirane probes only labeled FabF, whereas thiirane probes were able to react with FabH and FabF. This shows how a change in the composition of a tricyclic structure can tune the reactivity of the molecule and may increase the range of enzymatic targets.

Subsequent measurements of minimal inhibitory concentrations of all probes in the above mentioned organisms, revealed a strong antibiotic activity of single thiirane probes (down to 75 μM). We could show that by replacing oxygen with sulfur drastically increases the antibiotic potential of our tricyclic

compounds. Some thiirane probes proved to be even more active than a structurally related antibiotic (cerulenin). Oxirane probes however did not show these effects. As double inhibition of FabF/H is known to kill bacteria, the antibiotic effect of the thiirane probes was thought to be connected to this mechanism.^[6]

The identity of the target enzymes could be confirmed labeling of a heterologous, as well as homologous overexpression of both targets. If inhibition of the enzymes was related to the antibiotic activity, homologous overexpression of each target was assumed to have an effect on the minimal inhibitory concentration. This however could not be shown. A possible explanation can be found in the proposed dual-inhibition mechanism of the thiiranes. As both FabF and H are involved in the same pathway, the less expressed enzyme is the limiting factor of the whole biosynthetic pathway. Therefore the overexpression of a single enzyme might not have an effect on the overall turnover of the pathway. The homologous coexpression of the two enzymes, which is currently investigated, should give a final answer to this interesting question.

The identity of the target enzymes could be confirmed by a heterologous and a homologous overexpression of both targets. If inhibition of the enzymes was related to the antibiotic activity, homologous overexpression of each target was assumed to have an effect on the minimal inhibitory concentration. This however could not be shown.

To validate the active site specificity of the probes, active site cysteines of FabF and H were mutated to catalytically inactive alanines. As expected, the labeling of the mutated FabH revealed a strong decrease in signal intensity. The labeling of FabF however remained unchanged. However the pre-incubation of FabF wild-type enzyme with an excess of the FabF inhibitor Cerulenin, the labeling decreased significantly. The same effect could be observed when the enzyme was unfolded by heat denaturation. This puzzling result lead to the conclusion, that oxirane and thiirane probes react not with the active site known from literature, but with another nucleophilic residue of FabF. The identification and analysis of this alternative active site will be subject to further investigations in the future.

5 Experimental section

5.1 Organic chemistry

5.1.1 Materials

5.1.1.1 General

All chemicals were of reagent grade or better and used without further purification. Chemicals and solvents were purchased from Sigma Aldrich or Acros Organics. For all reactions, only commercially available solvents of p. a. grade, dried over molecular sieve and stored under Argon atmosphere were used. Solvents for chromatography and workup purposes were generally of reagent grade and purified before use by distillation. In all reactions, temperatures were measured externally. All experiments were carried out under nitrogen. Column chromatography was performed on Merck silica gel (Acros Organics 0.035 -0.070 mm, mesh 60 Å). ¹H NMR spectra were recorded on a Varian Mercury 200 (200 MHz), a Varian NMR-System 600 (600 MHz) or a Varian NMR-System 300 (300 MHz) and ¹³C NMR spectra were measured with a Varian NMR-System 600 (600 MHz) and a Varian NMR-System 300 (300 MHz) and referenced to the residual proton and carbon signal of the deuterated solvent, respectively. Mass spectra were obtained by GC-MS with a Varian 3400 gas chromatograph via a 25 m CS Supreme-5 capillary column (ø 0.25 mm, layer 0.25 μm) with a gradient of 50 °C (1 min isotherm) to 300 °C (4 min isotherm), 25 °C min⁻¹ coupled with a Finnigan MAT 95 mass spectrometer in EI mode (70 eV, 250 °C source). For DEI measurements, samples were directly desorbed from platinum wire (20 – 1600 °C, 120 °C min⁻¹). ESI spectra were recorded with a Thermo Finnigan LTQ FT. HPLC analysis was accomplished with a Waters 2695 separations module, a X-Bridge BEH130

5.1.1 Materials

C18 column (4.6 x 100 mm) and a Waters 2996 PDA detector.

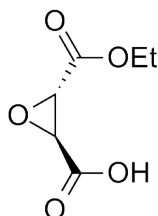
Mobile phase (HPLC grade): A = water, 0.1 % (v/v) TFA, B = acetonitril, 0.1 % (v/v) TFA. Gradient: T₀: A = 100%; T₂₅: A = 5%; T₂₉: A = 5%; T₃₇: A = 100%; T₄₀: A = 100%.

5.1.1.2 TLC Stains

Name	Application	Receipt
p-Anisaldehyd	Nucleophilic groups	350 ml cold EtOH 15 ml AcOH 3,5 ml p-Anisaldehyd 50 ml H ₂ SO ₄ add slowly over 1 h store at 0 °C
Ninhydrin	Aminoacids	1,5 g Ninhydrin 100 ml n-Butanol 3 ml AcOH
2,4-DNP	Carbonyls	12 g 2,4-Dinitrophenolhydrazin 60 ml H ₂ SO ₄ 80 ml H ₂ O 200 ml EtOH (95%)
Phosphomolybdat	General	10 g Phosphomolybdat 100 ml EtOH (95%)
Cerium Molybdate	General	12 g 2,4-Dinitrophenolhydrazin 60 ml H ₂ SO ₄ 80 ml H ₂ O 200 ml EtOH (95%)

5.1.2 Synthesis

5.1.2.1 Ethyl (2*R*,3*R*) oxirane-2,3-dicarboxylate, (1)



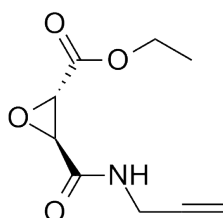
(+)-Diethyl L-tartrate (52.0 g, 252.5 mmol) was converted to diethyl (2*S*,3*R*) 2-bromo-3-hydroxy-butanedioate by the method of Mori.^[93] The bromohydrin was converted to diethyl (2*R*,3*R*) oxirane-2,3-dicarboxylate by treatment with NaOEt.⁴² The diester was converted into the monoester by addition of 1.08 M KOH in abs. EtOH, which yielded 18.2 g product (yield 45 %, over 4 steps) as a white solid.

¹H NMR (300 MHz, CDCl₃) δ = 4.34 - 4.16 (m, 2H), 3.67 (s, 2H), 1.30 (t, J =7.2 Hz, 3H);

¹³C NMR (75 MHz, CDCl₃) δ 170.62, 166.84, 62.54, 52.16, 51.65, 13.96.

ESI - MS (m/z): 178.0712 [M + NH₄⁺] calc. 178.07099, 338.1083 [2M + NH₄⁺] calc. 338.1081

5.1.2.2 Ethyl (2*R*,3*R*) 3-(*N*-propargylaminocarbonyl) oxirane-2-carboxylate (2, OxyEt)



The monoester **1** (14.00 g, 87.4 mmol, 1.00 eq) was dissolved in dry dichloromethane (DCM) (500 mL). To this solution *N,N'*-Diisopropylcarbodiimide (DIC) (19.82 g, 96.2 mmol, 1.10 eq) was added. The solution was stirred for 10 min at room temperature to form the reactive ester. Finally, propargylamine (5.06 g, 91.8 mmol, 1.05 eq) was added and stirred at ambient temperature for 15 min. While the solution turned brown, a white precipitate formed. The progress of the reaction was monitored by TLC (EtOAc/i-hexane, 1:1, R_f :0.5). After completion of the reaction the solvent was evaporated and the crude was purified by flash-chromatography (hexane/EtOAc, 2:1, R_f :0.3), which gave 11.00 g (64 %) of a slightly yellow solid.

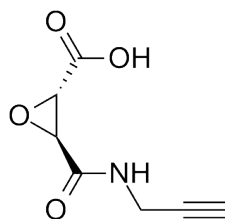
^1H NMR (300 MHz, CDCl_3) δ = 6.36 (s, 1H), 4.27 (qd, $J=7.1, 1.6$ Hz, 2H), 4.06 (ddd, $J=5.5, 2.6, 0.8$ Hz, 2H), 3.72 (d, $J=1.9$ Hz, 1H), 3.53 (d, $J=1.9$ Hz, 1H), 2.27 (t, $J=2.6$ Hz, 1H), 1.32 (t, $J=7.1$ Hz, 3H).

^{13}C NMR (75 MHz, CDCl_3) δ = 166.37, 165.69, 78.40, 72.22, 62.38, 53.78, 52.83, 28.81, 14.02.

ESI - MS (m/z): 198.0763 [$\text{M} + \text{H}^+$] calc. 198.0760, 239.1030 [$\text{M} + \text{CH}_3\text{CN} + \text{H}^+$] calc. 239.1026

$[\alpha]_{595}^{25} = -20.1$ ($c = 1.01$, CHCl_3)

5.1.2.3 (2*R*,3*R*) 3-(*N*-propargylaminocarbonyl) oxirane- 2-carboxylic acid (**3**)

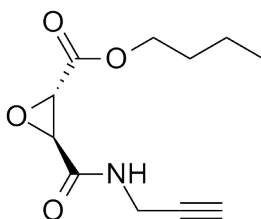


2 (11.00 g, 55.78 mmol, 1.00 eq) was dissolved in 100 mL of dry EtOH under Ar atmosphere and cooled to 0 °C. 50 mL of an ethanolic solution of KOH (3.44 g, 61.36 mmol, 1.1 eq) were added slowly while the solution thickened.

The solution was stirred for 30 min at 0 °C and 1 h at ambient temperature. The progress of the reaction was monitored by TLC (hexane/EtOAc, 1:1, R_f :0). The solvent was evaporated under reduced pressure and a yellow solid dissolved in water. The solution was washed with DCM. The pH of the solution was adjusted to ~2 by addition of 2 N HCl and three times extracted with EtOAc. The combined organic phases were dried over Na_2SO_4 , filtered and concentrated in vacuo to give 4.90 g (52 %) of a white solid which was used without further purification.

ESI - MS (m/z): 170.0451 [$M + H^+$] calc. 170.0447.

5.1.2.4 Butyl (2*R*,3*R*) 3-(*N*-propargylaminocarbonyl) oxirane-2-carboxylate (4, OxyBut)



3 (1.00 g, 5.9 mmol, 1.00 eq) was dissolved in dry Dimethyl sulfoxide (DMSO) (2.5 mL). To this solution, 4-Dimethylaminopyridine (DMAP) (72 mg, 0.6 mmol, 0.10 eq) and n-Butanol (482 mg, 6.5 mmol, 1.10 eq) were added. The solution was stirred for 10 min at room temperature until everything was dissolved. Finally, Boc_2O (1.68 g, 7.7 mmol, 1.30 eq) and Et_3N (1.19 g, 11.8 mmol, 2.00 eq) were added. Gas development could be observed while the solution turned brown. The solution was stirred for 2 h at ambient temperature. The progress of the reaction was monitored by TLC. After completion of the reaction EtOAc was added and the mixture was washed with H_2O three times. The aqueous phase was extracted with EtOAc once and the combined organic phases dried over Na_2SO_4 . The solvent was evaporated and the crude extract purified by flash-chromatography (hexane/EtOAc, 2:1) to give 406 mg

of a white solid (31 %).

TLC: R_f : 0.5 (hexane/EtOAc, 1:1).

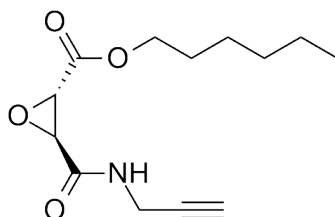
^1H NMR (250 MHz, CDCl_3) δ = 6.27 (s, 1H), 4.30 - 4.12 (m, 2H), 4.06 (ddd, $J=5.5, 2.6, 1.0$ Hz, 2H), 3.73 - 3.68 (m, 1H), 3.52 - 3.51 (m, 1H), 2.26 (t, $J=2.6$ Hz, 1H), 1.74 - 1.56 (m, 2H), 1.47 - 1.30 (m, 2H), 0.94 (t, $J=7.3$ Hz, 3H).

^{13}C NMR (63 MHz, CDCl_3) δ = 166.38, 165.64, 78.33, 72.24, 66.18, 53.77, 52.84, 30.36, 28.79, 18.94, 13.56.

ESI - MS (m/z): 226.1077 [$\text{M} + \text{H}^+$] calc. 226.1073, 267.1342 [$\text{M} + \text{CH}_3\text{CN} + \text{H}^+$] calc. 267.1339.

$[\alpha]_{595}^{25} = -27.5$ ($c = 1.01$, CHCl_3)

5.1.2.5 Hexyl (2*R*,3*R*) 3-(*N*-propargylaminocarbonyl) oxirane-2-carboxylate (5, OxyHex)



3 (1.00 g, 5.9 mmol, 1.00 eq) was dissolved in dry DMSO (2.5 mL). To this solution, DMAP (72 mg, 0.6 mmol, 0.10 eq) and n-Hexanol (664.5 mg, 6.5 mmol, 1.10 eq) were added. The solution was stirred for 10 min at room temperature until everything was dissolved. Finally, Boc_2O (1.68 g, 7.69 mmol, 1.30 eq) and Et_3N (1.19 g, 11.8 mmol, 2.00 eq) were added. Gas development could be observed while the solution turned brown. The solution was stirred for 2 h at ambient temperature. The progress of the reaction was monitored by TLC. After completion of the reaction EtOAc was added and the mixture was washed with H_2O three times. The aqueous phase was extracted with EtOAc one time and the combined organic phases dried over

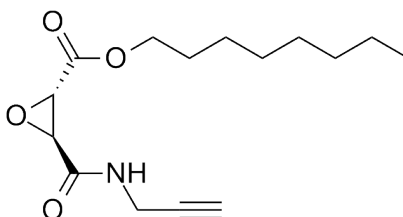
Na₂SO₄. The solvent was evaporated and the crude extract purified by flash-chromatography (hexane/EtOAc, 3:1) to give 324 mg of a white solid (23 %). TLC: R_f: 0.5 (hexane/EtOAc, 2:1).

¹H NMR (250 MHz, CDCl₃) δ = 6.25 (s, 1H), 4.30 - 4.12 (m, 2H), 4.06 (ddd, J=5.4, 2.6, 1.1 Hz, 2H), 3.72 - 3.70 (m, 1H), 3.53 - 3.50 (m, 1H), 2.26 (t, J=2.6 Hz, 1H), 1.76 - 1.60 (m, 2H), 1.45 - 1.22 (m, 6H), 0.97 - 0.82 (m, 3H).

¹³C NMR (63 MHz, CDCl₃) δ = 166.37, 165.64, 78.31, 72.26, 66.50, 53.78, 52.86, 31.29, 28.79, 28.32, 25.37, 22.45, 13.92. ESI - MS (m/z): 254.1391 [M + H⁺] calc. 254.1386, 295.1657 [M + CH₃CN + H⁺] calc. 295.1652

[α]₅₉₅²⁵ = - 45.0 (c = 1.01, CHCl₃)

5.1.2.6 Octyl (2*R*,3*R*) 3-(*N*-propargylaminocarbonyl) oxirane-2-carboxylate (**6**, OxyOc)



3 (400 mg, 2.36 mmol, 1.00 eq) was dissolved in dry DMSO (1 mL). To this solution, DMAP (29 mg, 0.24 mmol, 0.10 eq) and n-Octanol (339 mg, 2.60 mmol, 1.10 eq) were added. The solution was stirred for 10 min at room temperature until everything was dissolved. Finally, Boc₂O (671 mg, 3.07 mmol, 1.30 eq) and Et₃N (479 mg, 4.73 mmol, 2.00 eq) were added. Gas development could be observed while the solution turned brown. The solution was stirred for 2 h at ambient temperature. The progress of the reaction was monitored by TLC. After completion of the reaction EtOAc was added and the mixture was washed with H₂O three times. The aqueous phase was extracted with EtOAc once and the combined organic phases dried over

Na_2SO_4 . The solvent was evaporated and the crude extract purified by flash-chromatography (hexane/EtOAc, 4:1) to give 275 mg of a white solid (41 %). TLC: Rf: 0.27 (hexane/EtOAc, 3:1).

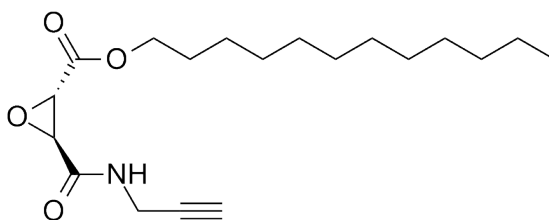
^1H NMR (300 MHz, CDCl_3) δ = 6.31 (s, 1H), 4.30 - 4.12 (m, 2H), 4.07 (ddd, $J=5.4, 2.5, 1.2$ Hz, 2H), 3.72 (d, $J=1.9$ Hz, 1H), 3.53 (d, $J=1.9$ Hz, 1H), 2.27 (t, $J=2.6$ Hz, 1H), 1.75 - 1.61 (m, 2H), 1.45 - 1.17 (m, 10H), 0.90 (t, $J=6.7$ Hz, 3H).

^{13}C NMR (75 MHz, CDCl_3) δ = 166.43, 165.68, 78.37, 72.25, 66.52, 53.79, 52.86, 31.73, 29.10, 28.81, 28.38, 25.73, 22.60, 14.05.

ESI - MS (m/z): 282.1698 [$\text{M} + \text{H}^+$] calc. 282.1699, 299.1963 [$\text{M} + \text{NH}_4^+$] calc. 299.1965, 280.1559 [$\text{M} - \text{H}^+$] calc. 280.1554

$[\alpha]_{595}^{25} = -62.1$ ($c = 1.01$, CHCl_3)

5.1.2.7 Dodecyl (2*R*,3*R*) 3-(*N*-propargylaminocarbonyl) oxirane-2-carboxylate (7, OxyDode)



3 (1.00 g, 5.9 mmol, 1.00 eq) was dissolved in dry DMSO (2.5 mL). To this solution, DMAP (72 mg, 0.6 mmol, 0.10 eq) and n-dodecanol (1.21 g, 6.5 mmol, 1.10 eq) were added. The solution was stirred for 10 min at room temperature until everything was dissolved. Finally, Boc_2O (1.68 g, 7.7 mmol, 1.30 eq) and Et_3N (1.19 g, 11.8 mmol, 2.00 eq) were added. Gas development could be observed while the solution turned brown. The solution was stirred for 2 h at ambient temperature. The progress of the reaction was monitored by TLC. After completion of the reaction EtOAc was added and the mixture was washed with H_2O three times. The aqueous phase

was extracted with EtOAc once and the combined organic phases dried over Na_2SO_4 . The solvent was evaporated and the crude extract purified by flash-chromatography (hexane/EtOAc, 10:1) to give 517 mg of a white solid (26 %). TLC: R_f : 0.5 (hexane/EtOAc, 2:1).

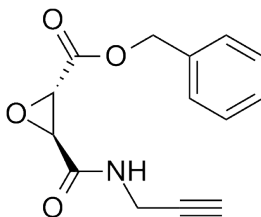
^1H NMR (250 MHz, CDCl_3) δ = 6.26 (s, 1H), 4.28 - 4.10 (m, 2H), 4.06 (ddd, J =5.4, 2.5, 0.9 Hz, 2H), 3.72 - 3.70 (m, 1H), 3.53 - 3.50 (m, 1H), 2.26 (t, J =2.6 Hz, 1H), 1.74 - 1.56 (m, 2H), 1.43 - 1.19 (m, 18H), 0.88 (t, J =6.6 Hz, 3H).

^{13}C NMR (63 MHz, CDCl_3) δ = 166.37, 165.64, 78.32, 72.25, 66.50, 53.77, 52.86, 31.87, 29.58, 29.51, 29.43, 29.30, 29.13, 28.79, 28.37, 25.71, 22.65, 14.07.

ESI - MS (m/z): 338.2330 [$\text{M} + \text{H}^+$] calc. 338.2325.

$[\alpha]_{595}^{25} = -38.2$ ($c = 1.01$, CHCl_3)

5.1.2.8 Benzyl (2*R*,3*R*) 3-(*N*-propargylaminocarbonyl) oxirane-2-carboxylate (**8**, OxyBenz)



3 (400 mg, 2.36 mmol, 1.00 eq) was dissolved in dry DMSO (1 mL). To this solution, DMAP (29 mg, 0.24 mmol, 0.10 eq) and benzyl alcohol (282 mg, 2.60 mmol, 1.10 eq) were added. The solution was stirred for 10 min at room temperature until everything was dissolved. Finally, Boc_2O (671 mg, 3.07 mmol, 1.30 eq) and Et_3N (479 mg, 4.73 mmol, 2.00 eq) were added. Gas development could be observed while the solution turned brown. The solution was stirred for 2 h at ambient temperature. The progress of the reaction was monitored by TLC. After completion of the reaction EtOAc was added and the mixture was washed with H_2O three times. The aqueous phase

was extracted with EtOAc once and the combined organic phases dried over Na_2SO_4 . The solvent was evaporated and the crude extract purified by flash-chromatography (hexane/EtOAc, 3:1) to give 120 mg of a white solid (19.6 %).

TLC: R_f : 0.3 (hexane/EtOAc, 2:1)

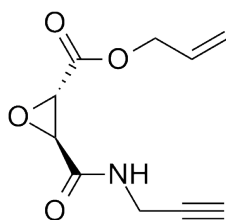
^1H NMR (300 MHz, CDCl_3) δ = 7.41 - 7.35 (m, 5H), 6.28 (s, 1H), 5.24 (q, $J=12.1$ Hz, 2H), 4.06 (ddd, $J=5.4, 2.5, 1.8$ Hz, 2H), 3.75 (d, $J=1.9$ Hz, 1H), 3.57 (d, $J=1.9$ Hz, 1H), 2.27 (t, $J=2.6$ Hz, 1H).

^{13}C NMR (75 MHz, CDCl_3) δ = 166.23, 165.52, 134.44, 128.85, 128.74, 128.63, 78.32, 72.29, 68.03, 53.84, 52.82, 28.82.

ESI - MS (m/z): 260.0916 [$\text{M} + \text{H}^+$] calc. 260.0917, 277.1181 [$\text{M} + \text{NH}_4^+$] calc. 277.1183, 258.0781 [$\text{M} - \text{H}^+$] calc. 258.0772

$[\alpha]_{595}^{25} = -48.2$ ($c = 1.01$, CHCl_3)

5.1.2.9 Allyl (2*R*,3*R*) 3-(*N*-propargylaminocarbonyl) oxirane-2-carboxylate (9, OxyAll)



3 (400 mg, 2.36 mmol, 1.00 eq) was dissolved in dry DMSO (1 mL). To this solution, DMAP (29 mg, 0.24 mmol, 0.10 eq) and allyl alcohol (151 mg, 2.60 mmol, 1.10 eq) were added. The solution was stirred for 10 min at room temperature until everything was dissolved. Finally, Boc_2O (671 mg, 3.07 mmol, 1.30 eq) and Et_3N (479 mg, 4.73 mmol, 2.00 eq) were added. Gas development could be observed while the solution turned brown. The solution was stirred for 2 h at ambient temperature. The progress of the reaction was monitored by TLC. After completion of the reaction EtOAc was added and the mixture was washed with H_2O three times. The aqueous phase

was extracted with EtOAc once and the combined organic phases dried over Na_2SO_4 . The solvent was evaporated and the crude extract purified by flash-chromatography (hexane/EtOAc, 3:1) to give 111 mg of a slightly red solid (22.4 %).

TLC: R_f : 0.5 (hexane/EtOAc, 1:1)

^1H NMR (599 MHz, CDCl_3) δ = 5.37 (dd, $J=2.8, 1.4$ Hz, 1H), 5.34 (dd, $J=2.8, 1.5$ Hz, 1H), 5.31 (dd, $J=1.1$ Hz, 1H), 5.29 (dd, $J=1.1$ Hz, 1H), 4.72 - 4.64 (m, 2H), 4.09 - 4.00 (m, 2H), 3.72 (d, $J=1.9$ Hz, 1H), 3.53 (d, $J=1.9$ Hz, 1H), 2.25 (t, $J=2.6$ Hz, 1H).

^{13}C NMR (151 MHz, CDCl_3) δ = 166.01, 165.50, 130.74, 119.84, 78.27, 72.30, 66.79, 53.80, 52.76, 28.80.

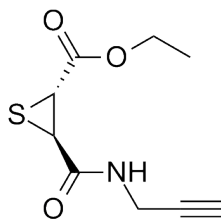
ESI - MS (m/z): 208.0619 [$\text{M} - \text{H}^+$] calc. 208.061524.

$[\alpha]_{595}^{25} = -35.0$ ($c = 1.01$, CHCl_3)

General procedure for the preparation of the thiirane probes:

All thiiranes were synthesized based on the procedure published by Korn and by Bezmenova.^[181,182]

5.1.2.10 Ethyl (2*S*,3*S*) 3-(*N*-propargylaminocarbonyl) thiirane-2-carboxylate (10, ThiEt)



27 (200 mg, 1.01 mmol, 1.00 eq) was suspended in dry Toluene (1.5 mL). To this solution, triphenylphosphine sulfide (597 mg, 2.02 mmol, 2.00 eq) and TFA (116 mg, 1.01 mmol, 1.00 eq) were added. The solution was stirred for 6 h at 50 °C. The progress of the reaction was monitored by TLC (HCCl_3 and then EtOAc/*i*-hexane, 2:1). The solvent was evaporated under reduced

pressure and the yellow solid dissolved in chloroform. The crude was directly applied onto a silica column and was purified by flash-chromatography (HCCl_3 until elution of the first spot, then EtOAc/i-hexane, 4:1) to give 84 mg of a white crystalline solid (39 %).

TLC: R_f : 0.5 (hexane/EtOAc, 2:1)

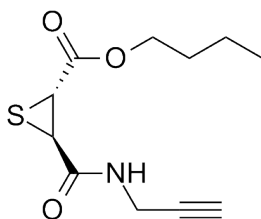
^1H NMR (250 MHz, CDCl_3) δ = 6.30 (s, 1H), 4.23 (q, $J=7.2$ Hz, 2H), 4.09 - 4.03 (m, 2H), 3.75 (d, $J=4.3$ Hz, 1H), 3.59 (d, $J=4.3$ Hz, 1H), 2.27 (t, $J=2.6$ Hz, 1H), 1.30 (t, $J=7.1$ Hz, 3H).

^{13}C NMR (63 MHz, CDCl_3) δ = 168.32, 166.13, 78.49, 72.23, 62.42, 36.47, 34.21, 29.68, 13.98.

ESI - MS (m/z): 214.0535 [$\text{M} + \text{H}^+$] calc. 214.0532, 255.0802 [$\text{M} + \text{CH}_3\text{CN} + \text{H}^+$] calc. 255.0797.

$[\alpha]_{595}^{25} = +128.4$ ($c = 1.01$, CHCl_3)

5.1.2.11 Butyl (2*S*,3*S*) 3-(*N*-propargylaminocarbonyl) thiirane-2-carboxylate (11, ThiBut)



4 (225 mg, 1.0 mmol, 1.0 eq) was suspended in dry toluene (1.0 mL). To this solution, triphenylphosphine sulfide (589 mg, 2.0 mmol, 2.0 eq) and TFA (114 mg, 1.0 mmol, 1.0 eq) were added. The solution was stirred for 6 h at. The solvent was evaporated under reduced pressure and the yellow solid dissolved in chloroform. The crude was directly applied onto a silica column and was purified by flash-chromatography (HCCl_3 until elution of the first spot, then EtOAc/i-hexane, 3:1) to give 84 mg of a white solid (18.2 %).

TLC: R_f : 0.3 (hexane/EtOAc, 2:1).

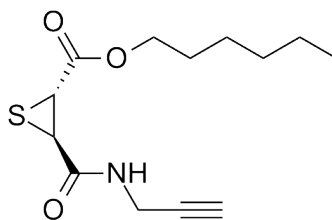
^1H NMR (250 MHz, CDCl_3) δ = 6.30 (s, 1H), 4.20 (t, $J=6.6$ Hz, 2H), 4.13 - 4.03 (m, 2H), 3.77 (d, $J=4.3$ Hz, 1H), 3.61 (d, $J=4.3$ Hz, 1H), 2.29 (t, $J=2.6$ Hz, 1H), 1.76 - 1.61 (m, 2H), 1.51 - 1.30 (m, 2H), 0.97 (t, $J=7.3$ Hz, 3H).

^{13}C NMR (63 MHz, CDCl_3) δ = 168.55, 166.81, 99.94, 77.20, 72.28, 66.30, 36.50, 34.22, 30.54, 18.97, 13.50.

ESI - MS (m/z): 242.0849 [$\text{M} + \text{H}^+$] calc. 242.0845, 283.1116 [$\text{M} + \text{CH}_3\text{CN} + \text{H}^+$] calc. 283.1111.

$[\alpha]_{595}^{25} = +100.8$ ($c = 1.01$, CHCl_3)

5.1.2.12 Hexyl (2*S*,3*S*) 3-(*N*-propargylaminocarbonyl) thiirane-2-carboxylate (12, ThiHex)



5 (253 mg, 1.0 mmol, 1.0 eq) was suspended in dry Toluene (1.0 mL). To this solution, triphenylphosphine sulfide (589 mg, 2.0 mmol, 2.00 eq) and TFA (270 mg, 2.4 mmol, 2.4 eq) were added. The solution was stirred for 6 h at 50 °C. The progress of the reaction was monitored by TLC (HCCl_3 and then EtOAc/*i*-hexane, 2:1). The solvent was evaporated under reduced pressure and the yellow solid dissolved in chloroform. The crude was directly applied onto a silica column and was purified by flash-chromatography (HCCl_3 until elution of the first spot, then EtOAc/*i*-hexane, 3:1) to give 160 mg of a white crystalline solid (59.4 %).

TLC: R_f : 0.3 (hexane/EtOAc, 2:1).

^1H NMR (250 MHz, CDCl_3) δ = 6.35 (s, 1H), 4.23 - 4.15 (m, 2H), 4.12 - 4.05

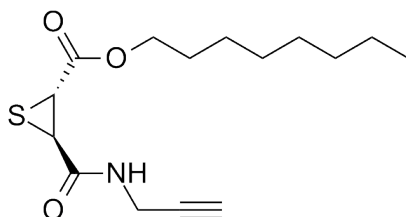
(m, 2H), 3.78 (d, $J=4.3$ Hz, 1H), 3.62 (d, $J=4.3$ Hz, 1H), 2.30 (t, $J=2.6$ Hz, 1H), 1.77 - 1.60 (m, 2H), 1.45 - 1.25 (m, 6H), 0.93 (t, $J=6.7$ Hz, 3H).

^{13}C NMR (63 MHz, CDCl_3) δ = 168.45, 166.28, 78.45, 72.29, 66.61, 36.49, 34.26, 31.34, 29.71, 28.36, 25.43, 22.48, 13.96.

ESI - MS (m/z): 270.1162 [$\text{M} + \text{H}^+$] calc. 270.1158, 311.1430 [$\text{M} + \text{CH}_3\text{CN} + \text{H}^+$] calc. 311.1424.

$[\alpha]_{595}^{25} = +93.3$ ($c = 1.01$, CHCl_3)

5.1.2.13 Octyl (2*S*,3*S*) 3-(*N*-propargylaminocarbonyl) thiirane-2-carboxylate (13, ThiOc)



6 (214 mg, 760 μmol , 1.0 eq) was suspended in dry toluene (1.0 mL). To this solution, triphenylphosphine sulfide (448 mg, 1.52 mmol, 2.0 eq) and TFA (86.72 mg, 760 μmol , 1.0 eq) were added. The solution was stirred for 6 h at 50 °C. The solvent was evaporated under reduced pressure and the yellow solid dissolved in chloroform. The crude was directly applied onto a silica column and was purified by flash-chromatography (HCCl_3 until elution of the first spot, then EtOAc/*i*-hexane, 3:1) to give 89 mg of a white crystalline solid (39,4 %).

TLC: R_f : 0.3 (hexane/EtOAc, 3:1).

^1H NMR (300 MHz, CDCl_3) δ = 6.77 (s, 1H), 4.17 (t, $J=6.7$ Hz, 2H), 4.07 (ddd, $J=5.3, 4.2, 2.6$ Hz, 2H), 3.80 (d, $J=4.2$ Hz, 1H), 3.65 (d, $J=4.2$ Hz, 1H), 2.28 (t, $J=2.6$ Hz, 1H), 1.72 - 1.60 (m, 2H), 1.40 - 1.22 (m, 10H), 0.89

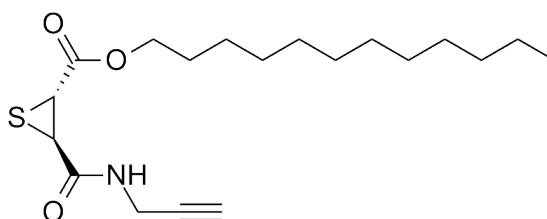
(t, $J=6.7$ Hz, 3H).

^{13}C NMR (75 MHz, CDCl_3) $\delta = 168.79, 167.09, 78.29, 72.36, 66.74, 60.70, 36.25, 34.14, 31.73, 29.88, 29.11, 28.36, 25.74, 22.60, 14.04$.

ESI - MS (m/z): 298.1468 [$\text{M} + \text{H}^+$] calc. 298.1471, 595.2852 [$2\text{M} + \text{H}^+$] calc. 595.2870.

$[\alpha]_{595}^{25} = + 111.8$ ($c = 1.01, \text{CHCl}_3$)

5.1.2.14 Dodecyl (2*S*,3*S*) 3-(*N*-propargylaminocarbonyl) thiirane-2-carboxylate (14, ThiDode)



7 (337 mg, 760 μmol , 1.00 eq) was suspended in dry Toluene (1.0 mL). To this solution, triphenylphosphine sulfide (558 mg, 2.00 mmol, 2.00 eq) and TFA (600 mg, 5.2 mmol, 6.85 eq) were added. The solution was stirred for 6 h at 50 $^{\circ}\text{C}$. The solvent was evaporated under reduced pressure and the yellow solid dissolved in chloroform. The crude was directly applied onto a silica column and was purified by Flash-Chromatography (HCCl_3 until elution of the first spot, then EtOAc/*i*-hexane, 3:1) to give 178 mg of a white crystalline solid (50.3 %).

TLC: R_f : 0.3 (hexane/EtOAc, 2:1).

^1H NMR (250 MHz, CDCl_3) $\delta = 6.29$ (s, 1H), 4.18 (t, $J=6.7$ Hz, 2H), 4.11 - 4.06 (m, 2H), 3.77 (d, $J=4.3$ Hz, 1H), 3.61 (d, $J=4.3$ Hz, 1H), 2.29 (t, $J=2.6$ Hz, 1H), 1.75 - 1.60 (m, 4H), 1.41 - 1.21 (m, 16H), 0.91 (t, $J=6.6$ Hz, 3H).

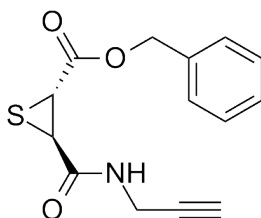
^{13}C NMR (63 MHz, CDCl_3) $\delta = 168.46, 166.27, 78.53, 72.27, 66.62, 36.50$,

34.26, 31.91, 29.70, 29.63, 29.55, 29.47, 29.34, 29.18, 28.41, 25.77, 22.68, 14.11.

ESI - MS (m/z): 354.2101 [$M + H^+$] calc. 354.2097.

$[\alpha]_{595}^{25} = + 91.8$ ($c = 1.01$, $CHCl_3$)

5.1.2.15 Benzyl (2*S*,3*S*)-3-(*N*-propargylaminocarbonyl) thiirane-2-carboxylate (**15**, ThiBenz)



8 (337 mg, 760 μ mol, 1.00 eq) was suspended in dry Toluene (1.0 mL). To this solution, triphenylphosphine sulfide (558 mg, 2.0 mmol, 2.00 eq) and TFA (600 mg, 5.2 mmol, 6.85 eq) were added. The solution was stirred for 6 h at 50 °C. The solvent was evaporated under reduced pressure and the yellow solid dissolved in chloroform. The solved crude was applied directly onto a silica column and was purified by flash-chromatography ($HCCl_3$ until elution of the first spot, then EtOAc/*i*-hexane, 4:1) to give 77 mg of a white crystalline solid (72.4 %).

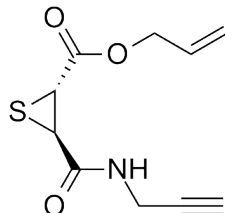
TLC: R_f : 0.5 (hexane/EtOAc, 3:1).

1H NMR (300 MHz, $CDCl_3$) δ 7.46 - 7.33 (m, 5H), 6.34 (s, 1H), 5.28 - 5.15 (m, 2H), 4.06 (dt, $J=5.4, 2.7$ Hz, 2H), 3.79 (dd, $J=4.2, 0.4$ Hz, 1H), 3.67 (dd, $J=4.2, 0.5$ Hz, 1H), 2.27 (td, $J=2.6, 0.4$ Hz, 1H).

^{13}C NMR (75 MHz, $CDCl_3$) δ 168.36, 166.10, 134.77, 128.70, 128.44, 78.51, 72.28, 68.09, 36.50, 34.11, 29.72.

ESI - MS (m/z): 293.0952 [$M + NH_4^+$] calc. 293.0954, 551.1259 [$2M + H^+$] calc. 551.1304, 274.0553 [$2M - H^+$] calc. 274.0543

$[\alpha]_{595}^{25} = + 94.6$ ($c = 1.01$, $CHCl_3$)

5.1.2.16 Allyl (2*S*,3*S*)-3-(*N*-propargylaminocarbonyl) thiirane-2-carboxylate (16, ThiAll)

9 (100 mg, 478 μmol , 1.0 eq) was suspended in dry Toluene (1.0 mL). To this solution, triphenylphosphine sulfide (281 mg, 956 μmol , 2.0 eq) and TFA (54.5 mg, 478 μmol , 1.0 eq) were added. The solution was stirred for 6 h at 50 °C. The solvent was evaporated under reduced pressure and the yellow solid dissolved in chloroform. The crude was directly applied onto a silica column and was purified by flash-chromatography (HCCl_3 until elution of the first spot, then EtOAc/i-hexane, 2:1) to give 66 mg of a white crystalline solid (61 %).

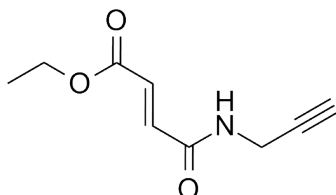
TLC: R_f : 0.45 (hexane/EtOAc, 2:1).

^1H NMR (300 MHz, CDCl_3) δ = 6.70 (s, 1H), 6.00 - 5.82 (m, 1H), 5.41 - 5.38 (m, 1H), 5.35 - 5.33 (m, 1H), 5.32 (dt, $J=2.2, 0.7$ Hz, 1H), 5.28 (dt, $J=2.2, 0.7$ Hz, 1H), 4.79 - 4.54 (m, 2H), 3.81 (d, $J=4.2$ Hz, 1H), 3.68 (d, $J=4.2$ Hz, 1H), 2.29 (t, $J=2.7$ Hz, 1H).

^{13}C NMR (75 MHz, CDCl_3) δ = 168.35, 166.87, 131.01, 119.41, 78.30, 72.40, 66.94, 36.31, 34.02, 29.88.

ESI - MS (m/z): 226.0536 [$\text{M} + \text{H}^+$] calc. 226.0532, 267.0803 [$\text{M} + \text{CH}_3\text{CN} + \text{H}^+$] calc. 267.0798.

$[\alpha]_{595}^{25} = +95.7$ ($c = 1.01$, CHCl_3)

5.1.2.17 General procedure for the preparation of the aziridine probes:**5.1.2.18 (E)-ethyl 4-oxo-4-(prop-2-yn-1-ylamino)but-2-enoate (17, MichEt)**

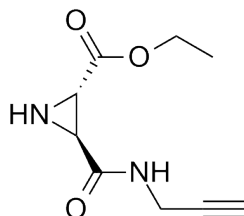
Fumaric acid monoethylester (10.0 g, 69.4 mmol, 2.00 eq) was solved in dry DCM (150 mL). To this solution, DCC (14.3 g, 69.4 mmol, 2.00 eq) and DIPEA (4.5 g, 34.7 mmol, 1.00 eq) were added. The solution was incubated for 10 min at room temperature to form the reactive ester. Finally, propargylamine (1.9 g, 55.08 mmol, 1.00 eq) was added and stirred at ambient temperature for 15 min. While the solution turned brown, a white precipitate formed. After completion of the reaction the solvent was evaporated and the crude was purified by flash-chromatography (hexane/EtOAc, 3:1), which gave 3.7 g (59 %) of a slightly yellow solid.

TLC: R_f : 0.3 (hexane/EtOAc, 2:1).

^1H NMR (250 MHz, CDCl_3) δ = 7.01 - 6.80 (m, 2H), 6.10 (s, 1H), 4.29 (q, $J=7.1$ Hz, 2H), 4.19 (dd, $J=5.3, 2.6$ Hz, 2H), 2.30 (t, $J=2.6$ Hz, 1H), 1.35 (t, $J=7.1$ Hz, 3H).

^{13}C NMR (63 MHz, CDCl_3) δ = 165.36, 163.19, 135.22, 131.31, 78.65, 72.25, 61.30, 29.61, 14.12.

ESI - MS (m/z): 182.0814 [$\text{M} + \text{H}^+$] calc. 182.0811.

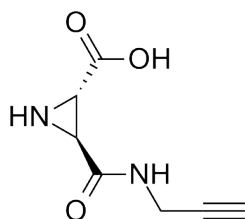
5.1.2.19 Ethyl (2*R,3*R**)-3-(*N*-propargylaminocarbonyl) aziridine-2-carboxylate (18, AziEt)**

17 (453 mg, 2.5 mmol, 1.0 eq) was suspended in toluene (10 mL). To this solution *S,S*-diphenylsulfilimine monohydrate (643 mg, 3.0 mmol, 1.2 eq) was added. The suspension was stirred for 24 h at 110 °C. The solvent was evaporated under reduced pressure and the yellow solid was purified by flash-chromatography (EtOAc/*i*-hexane, 1:1) to give 55 mg of a yellow oil (11 %). TLC: R_f : 0.3 (hexane/EtOAc, 2:1).

^1H NMR (250 MHz, DMSO) δ = 4.14 (dd, $J=14.3, 7.2$ Hz, 2H), 3.92 (dd, $J=4.9, 1.8$ Hz, 2H), 2.73 (s, 1H), 2.59 (s, 1H), 2.26 - 2.21 (m, 1H), 1.22 (t, $J=7.1$ Hz, 3H).

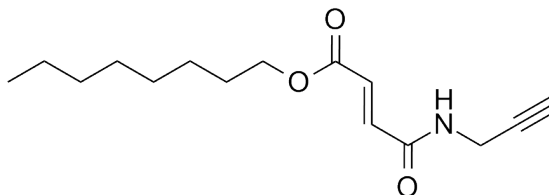
^{13}C NMR (63 MHz, CDCl_3) δ = 170.09, 167.60, 78.87, 71.81, 62.29, 37.36, 35.63, 28.84, 14.07.

ESI - MS (m/z): 197.0923 [$\text{M} + \text{H}^+$] calc. 197.0920.

5.1.2.20 (E)-4-oxo-4-(prop-2-yn-1-ylamino)but-2-enoic acid (**19**)

17 (3.70 g, 20.42 mmol, 1.0 eq) was dissolved in 30 mL of dry EtOH under Ar atmosphere and cooled to 0 °C. 50 mL of an ethanolic solution of KOH (1.26 g, 22.46 mmol, 1.1 eq) were added slowly. The solution was stirred for 30 min at 50 °C and 1 h at ambient temperature. The progress of the reaction was monitored by TLC (hexane/EtOAc, 1:1, R_f : 0). The solvent was evaporated under reduced pressure and the yellow solid dissolved in water. The solution was washed with DCM. The pH of the solution was adjusted to $\tilde{2}$ by addition of 2 N HCl and three times extracted with EtOAc. The combined organic phases were dried over Na_2SO_4 , filtered and concentrated in vacuo to give 2.8 g (89.5 %) of a yellow solid which was used without further purification.

ESI - MS (m/z): 154.0500 [$\text{M} + \text{NH}_4^+$] calc. 154.0498.

5.1.2.21 (E)-octyl 4-oxo-4-(prop-2-yn-1-ylamino)but-2-enoate (20, MichOc)

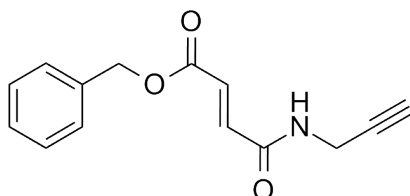
19 (1.00 g, 6.53 mmol, 1.00 eq) was dissolved in dry DMSO (2.0 mL). To this solution, DMAP (79.77 mg, 653 μ mol, 0.10 eq) and n-Octanol (850.00 mg, 6.53 mmol, 1.00 eq) were added. The solution was stirred for 10 min at room temperature until everything was dissolved. Finally, Boc_2O (1.85 g, 8.49 mmol, 1.30 eq) and Et_3N (1.32 g, 13.05 mmol, 2.00 eq) were added. Gas development could be observed while the solution turned brown. The solution was stirred for 2 h at ambient temperature. The progress of the reaction was monitored by TLC. After completion of the reaction EtOAc was added and the mixture was washed with H_2O three times. The aqueous phase was extracted with EtOAc once and the combined organic phases dried over Na_2SO_4 . The solvent was evaporated and the crude extract purified by flash-chromatography (hexane/EtOAc, 3:1) to give 584 mg of a yellow oil (34 %). TLC: R_f : 0.5 (hexane/EtOAc, 3:1).

^1H NMR (250 MHz, CDCl_3) δ = 6.92 (dd, $J=15.4$ Hz, 2H), 6.41 (s, 1H), 4.27 - 4.06 (m, 4H), 2.29 (t, $J=2.6$ Hz, 1H), 1.81 - 1.51 (m, 2H), 1.43 - 1.20 (m, 10H), 0.90 (t, $J=6.6$ Hz, 3H).

^{13}C NMR (63 MHz, CDCl_3) δ = 165.49, 163.25, 135.27, 131.21, 78.70, 72.14, 65.46, 38.09, 31.72, 29.13, 28.83, 28.49, 25.84, 22.59, 14.03.

ESI - MS (m/z): 266.1755 [$\text{M} + \text{H}^+$], calc. 266.1750.

5.1.2.22 (E)-benzyl 4-oxo-4-(prop-2-yn-1-ylamino)but-2-enoate (21, MichBenz)



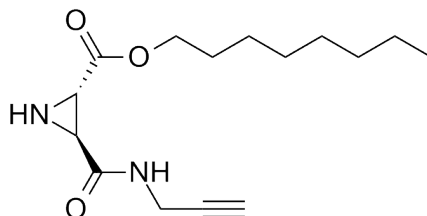
19 (1.00 g, 6.53 mmol, 1.00 eq) was dissolved in dry DMSO (2 mL). To this solution, DMAP (79.77 mg, 653 μ mol, 0.10 eq) and benzylic alcohol (850 mg, 6.53 mmol, 1.00 eq) were added. The solution was stirred for 10 min at room temperature until everything was dissolved. Finally, Boc_2O (1.85 g, 8.49 mmol, 1.30 eq) and Et_3N (1.32 g, 13.05 mmol, 2.00 eq) were added. Gas development could be observed while the solution turned brown. The solution was stirred for 2 h at ambient temperature. The progress of the reaction was monitored by TLC. After completion of the reaction EtOAc was added and the mixture was washed with H_2O three times. The aqueous phase was extracted with EtOAc once and the combined organic phases dried over Na_2SO_4 . The solvent was evaporated and the crude extract purified by flash-chromatography (hexane/EtOAc, 3:1) to give 584 mg of a yellow oil (34 %). TLC: R_f : 0.5 (hexane/EtOAc, 3:1).

^1H NMR (360 MHz, CDCl_3) δ = 7.75 (d, $J=15.4$ Hz, 1H), 7.45 - 7.30 (m, 6H), 6.77 (d, $J=15.4$ Hz, 1H), 5.25 (s, 2H), 4.49 (d, $J=2.4$ Hz, 2H), 2.20 (t, $J=2.4$ Hz, 1H).

^{13}C NMR (63 MHz, CDCl_3) δ = 167.83, 167.03, 79.10, 71.99, 66.67, 37.57, 35.79, 31.91, 29.30, 28.63, 25.95, 22.78, 14.23.

ESI - MS (m/z): 244.0972 [$\text{M} + \text{H}^+$] calc. 244.0967.

5.1.2.23 Octyl (2*R**,3*R**) 3-(*N*-propargylaminocarbonyl) aziridine-2-carboxylate (**22**, AziOc)



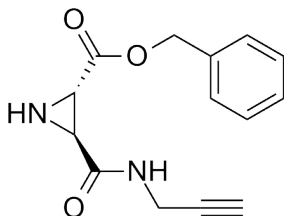
20 (584 mg, 2.20 mmol, 1.00 eq) was suspended in Toluene (10.0 mL). To this solution *S,S*-diphenylsulfilimine monohydrate (565 mg, 2.64 mmol, 1.20 eq) was added. The suspension was stirred for 24 h at 110 °C. The solvent was evaporated under reduced pressure and the yellow solid was purified by flash-chromatography (EtOAc/*i*-hexane, 3:1) to give 29 mg of a yellow oil (5 %).

TLC: R_f : 0.2 (EtOAc/ hexane, 3:1).

^1H NMR (250 MHz, CDCl_3) δ = 6.62 (s, 1H), 4.22 - 4.14 (m, 2H), 4.04 (dd, $J=5.5, 2.5$ Hz, 2H), 2.87 (d, $J=2.0$ Hz, 1H), 2.66 (d, $J=1.9$ Hz, 1H), 2.25 (t, $J=2.5$ Hz, 1H), 1.84 (s, 1H), 1.75 - 1.60 (m, 2H), 1.44 - 1.19 (m, 10H), 0.90 (t, $J=6.4$ Hz, 3H).

^{13}C NMR (63 MHz, CDCl_3) δ = 167.83, 167.03, 79.10, 71.99, 66.67, 37.57, 35.79, 31.91, 29.30, 28.63, 26.79, 25.95, 22.78, 14.23.

ESI - MS (m/z): 281.1864 [$\text{M} + \text{H}^+$] calc. 281.1859.

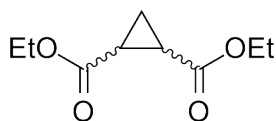
5.1.2.24 Benzyl (2*R**,3*R**)3-(*N*-propargylaminocarbonyl) aziridine-2-carboxylate (**23**, AziBenz)

21 (584 mg, 2.20 mmol, 1.0 eq) was suspended in toluene (10 mL). To this solution *S,S*-diphenylsulfilimine monohydrate (565 mg, 2.64 mmol, 1.2 eq) was added. The suspension was stirred for 24 h at 110 °C. The solvent was evaporated under reduced pressure and the yellow solid was purified by flash-chromatography (EtOAc/*i*-hexane, 3:1) to give 29 mg of a yellow oil (5 %). TLC: R_f : 0.3 (EtOAc/ hexane, 3:1).

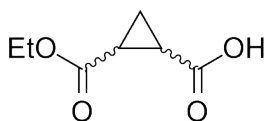
^1H NMR (250 MHz, CDCl_3) δ = 7.69 - 7.60 (m, 2H), 7.47 - 7.34 (m, 2H), 7.14 (s, 1H), 6.52 (s, 1H), 5.19 - 4.94 (m, 2H), 3.94 - 3.75 (m, 2H), 2.78 (d, $J=8.4$ Hz, 1H), 2.55 (d, $J=6.4$ Hz, 1H), 2.10 (t, $J=2.5$ Hz, 1H), 1.69 (s, 1H).

^{13}C NMR (63 MHz, CDCl_3) δ = 168.10, 167.60, 159.66, 135.59, 128.89, 128.70, 78.40, 71.97, 70.84, 38.08, 35.81, 26.41.

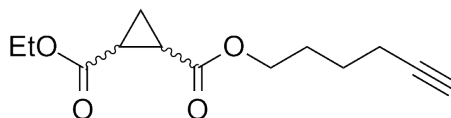
ESI - MS (m/z): 259.1082 [$\text{M} + \text{H}^+$], calc. 259.1076.

5.1.2.25 Diethyl cyclopropane-1,2-dicarboxylate (**24**)

The racemic **24** was synthesized following a procedure published by Csuk et al.^[183] which yielded the product as a transparent oil (27 %).

5.1.2.26 2-(ethoxycarbonyl)cyclopropane-carboxylic acid (**25**)

24 (372 mg, 2 mmol, 1.00 eq) was diluted in 9 mL H₂O and 1 mL of a 2 M NaOH (aq.) was added and stirred at 45 °C for 2 h. By addition of 2 M HCl the solution was brought to pH=2. The aqueous phase was extracted with Et₂O three times and the combined organic phases dried over MgSO₄. The solvent was evaporated and the crude (135 mg, 85 %) was used without further purification.

5.1.2.27 1-ethyl 2-hex-5-yn-1-yl cyclopropane-1,2-dicarboxylate (**26**, CycloEt)

25 (100 mg, 0.63 mmol, 1.00 eq) was dissolved in dry dichloromethane (DCM) (0.1 mL). To this solution, 4-Dimethylaminopyridine (DMAP) (8 mg, 0.06 mmol, 0.10 eq) and Hex-5-ynol (93 mg, 0.95 mmol, 1.50 eq) were added. The solution was stirred for 10 min at room temperature until everything was dissolved. Finally, Boc₂O (179 mg, 0.82 mmol, 1.30 eq) and Et₃N (127 mg, 1.26 mmol, 2.00 eq) were added. A development of gas could be observed while the solution turned brown. The solution was stirred for 45 min at 45 °C. The progress of the reaction was monitored by TLC. After completion

of the reaction EtOAc was added and the mixture was washed with H₂O three times. The aqueous phase was extracted with EtOAc once and the combined organic phases dried over Na₂SO₄. The solvent was evaporated and the crude extract purified by flash-chromatography (hexane/EtOAc, 5:1) to give 67 mg of a transparent oil (44%). TLC: R_f: 0.3 (hexane/EtOAc, 5:1).

¹H NMR (360 MHz, CDCl₃) δ = 4.18-4.00 (m, 4H), 2.21 (td, *J*=7.0, 2.6 Hz, 2H), 2.03 (dd, *J*=8.4, 6.7 Hz, 2H), 1.93 (t, *J*=2.6 Hz, 1H), 1.81-1.68 (m, 2H), 1.67-1.48 (m, 4H), 1.23 (t, *J*=7.1 Hz, 3H).

¹³C NMR (91 MHz, CDCl₃) δ = 169.85, 169.83, 83.82, 68.68, 64.43, 60.96, 27.59, 24.83, 21.58, 21.55, 18.02, 14.16, 11.61.

ESI - MS (*m/z*): 239,1278 [M + H⁺] calc. 239,1278, 261,1102 [M + Na⁺] calc. 261,1097.

5.2 Biochemistry

5.2.1 Microbiology

5.2.1.1 Materials

5.2.1.1.1 Bacteria

- *Escherichia coli*: K12
- *Bacillus subtilis*: 168
- *Bacillus licheniformis*: ATTC 14580
- *Pseudomonas putida*: KT 2440
- *Pseudomonas aeruginosa*: PAO1
- *Listeria welshimeri*: SLCC 5334 Serovar 6B
- *Listeria monocytogenes* EGD-e
- *Listeria monocytogenes* F2365
- *Staphylococcus aureus*: NCTC8325
- *Staphylococcus aureus*: RN4220
- *Staphylococcus aureus*: Mu50

5.2.1.1.2 Antibiotic stocks

Antibiotic	Concentration	Solvent
Carbenicillin/Ampicillin	100.0 mg/mL	ddH ₂ O, pH 7.5
Chloramphenicol	5.0 mg/mL	Ethanol abs.
Kanamycin	25.0 mg/mL	ddH ₂ O
Erytromycin	1.0 mg/mL	Ethanol abs.

Tetracyclin	12.5 mg/mL	Ethanol abs.
IPTG	238.3 mg/mL	ddH ₂ O

5.2.1.1.3 Media

Media were prepared as follows and autoclaved before use:

Media	Composition
LB Medium	10 g/L tryptically digested casein 5 g/L yeast extract 5 g/L NaCl adjust pH to 7,5
BHB Medium	37 g/L brain-heart-broth
3.5 x SMHEM	81.47 g Saccharose (952 mM) 178 mg MgCl ₂ x 6 H ₂ O (3.5 mM) 417 mg HEPES (7 mM) Ad 250 mL H ₂ O adjust pH to 7.2

5.2.1.1.4 Agar plates

Media	Composition
Agar plates	500 mL medium (e.g. LB) 7.5 g agar-agar autoclave ~ 50 °C add antibiotic cast gel
Sheep blood agar (5 %) Heipha, Dr. Müller GmbH	14 g/L caseine pepton 4.5 g/L pepton from meat 4.5 g/L yeast extract 16 g/L agar 50 mL/L mutton blood 5 g/L NaCl

5.2.1.2 Methods

5.2.1.2.1 Cryostocks

Cryostocks were prepared from the respective overnight culture. 150 μ l of sterilized Glycerin were added to 850 μ L of the respective overnight culture, mixed by inversion of the cryo-tube, frozen in liquid nitrogen and stored at -80 °C

5.2.1.2.2 Competent cells

Competent (electro- or heat competent) cells can be used for the transformation of plasmidic DNA. Chilling cells in the presence of divalent cations such as Ca^{2+} (in CaCl_2) prepares the cell membrane to become permeable to plasmid DNA.

Chemically competent

The following bacteria were prepared by this protocol:

- *Escherichia coli*: K12, OneShot TOP10, Invitrogen
- *Escherichia coli*: K12, BL21, Invitrogen
- *Escherichia coli*: K12, XL1 Blue, Agilent

All working steps were done on ice. Heat competent cells should never reach a temperature >4 °C otherwise they lose their competence. 200 mL of a sterile 50 mM CaCl_2 solution were cooled down to 4 °C. An overnight culture of the bacteria was set up. 300 mL medium were inoculated 1:100 with the overnight culture. At an OD_{600} of 0.5-0.7 the cells were split in 50 mL aliquots and stored on ice for 15 min. The cells were harvested by centrifugation at 4000 g and 4 °C for 2 min and the supernatant was discarded. 25 mL of a sterile ice cold CaCl_2 solution was added to each tube and the cells were carefully resuspended by pipetting up and down. The cells were incubated on ice for 30 min and centrifuged at 4000 g and 4 °C for 2 min. The supernatant was removed and the cells were resuspended in 1.25 mL of the ice cold CaCl_2 solution and incubated on ice for 30 min. Finally 125 μL of sterile Glycerin (end concentration 10 % v/v) were added to the cells on ice and mixed by inversion of the tube. The cells were prepared as 50 μL aliquots in sterile 1.5 mL tubes, frozen in liquid nitrogen and stored at -80 °C.

Electro competentProtocol for *Listeria monocytogenes* EGD-e:

200 mL BHB were inoculated with 2 mL of an overnight culture and incubated at 37 °C until an OD₆₀₀ of 0.5-0.7 was reached. 200 µL Penicillin G were added to break down the cell wall. The cells were incubated for 15 min at 37 °C and put on ice for 10 min. The cells were centrifuged at 4000 g and 4 °C for 10 min. All further steps were performed on ice. The supernatant was removed and the pellet was washed with 30 mL ice cold SMHEM (see 5.2.1.1.3). The pellet was then resuspended in 2 mL ice cold SMHEM, 100 µL aliquots were prepared in sterile precooled tubes, frozen in liquid nitrogen and stored at -80 °C

Protocol for *Staphylococcus aureus* RN-4220 and NCTC 8325:

200 mL BHB were inoculated with 2 mL of an overnight culture and incubated at 37 °C until an OD₆₀₀ of 0.5-0.7 was reached. The cells were centrifuged at 4000 g and RT for 7 min. The pellet was washed with sterile 200 mL ddH₂O. The cells were centrifuged at 4000 g and RT for 7 min and the pellet was washed with 40 mL of a sterile 10 % (v/v) glycerol solution. Cells were spun down and resuspended in 20 mL of a sterile 10 % (v/v) glycerol solution. The cells were incubated for 15 min at RT. After centrifugation at 4000 g and RT for 7 min the supernatant was removed and the cells were resuspended in 2 mL of a sterile 10 % (v/v) glycerol solution. 70 µL-Aliquots were prepared in sterile tubes, frozen in liquid nitrogen and stored at -80 °C.

Minimal inhibitory concentration assay

Probe-mediated growth inhibition of *L. monocytogenes*, *S. aureus* Mu50 and *P. aeruginosa* was obtained in 96 well plate-based assays. Various concentrations of oxiranes and thiiranes (1 µL dissolved in Acetone) were added to 99 µL of medium, which contained a fresh 1:1000-fold dilution of the corresponding bacterial overnight culture. The well plates were incubated at 37 °C for 14 h. The MIC value was determined by several (>3) independent

experiments (each experiment with at least triplicate runs for each concentration) and represented the lowest concentration of probe at which no growth of bacteria could be observed by the eye.

5.2.2 Cell culture

5.2.2.1 Materials

5.2.2.1.1 Buffers

Medium	Composition
HACAT	PAA DMEM (high Glucose; no Ca^{2+} ; no L-Glutamine) 10 % dialyzed FCS heat-inactivated 5 mL L-Glutamine (200 mM)
NIH3T3 Culture	PAA DMEM (high Glucose; L-Glutamine 4 mM) 10 % FCS-GOLD heat-inactivated

5.2.2.2 Methods

5.2.2.2.1 Cultivation and splitting

HACAT

HACAT (human adult high calcium low temperature keratinocytes) are skin cells that have a close similarity in functional competence to normal keratinocytes and are frequently used in cytotoxicity assays. In absence of Ca^{2+} they remain undifferentiated and keep a high rate of proliferation. The cells were cultivated in appropriate medium (see 5.2.2.1.1) at 37 °C in gassed (95 % air and 5 % CO_2) humidified incubators. Passages were done by disaggregating the cells at 80% confluency, with 0.5 mg/mL trypsin/EDTA solution (final concentration) in $\text{Ca}^{2+}/\text{Mg}^{2+}$ -free PBS for 5-10 min at 37 °C. Attached cells

were detached by a short clap of the flask. Trypsinization was stopped by addition of 10 mL fresh medium. The solution was transferred to a falcon and spun down at 800 rpm for 5 min. The supernatant was removed and the cells were resuspended in 8 mL fresh medium. 2 mL (1:4) of this solution were used to inoculate a new flask.

NIH3T3

The NIH3T3 cells is the standard fibroblast cell line obtained from embryo mouse tissue which is characterized by a high rate of proliferation. The cells were cultivated in appropriate medium (see 5.2.2.1.1) at 37 °C in gassed (95 % air and 5 % CO₂) humidified incubators. Passages were done by disaggregating the cells at no more than 80% confluency, with 0.5 mg/mL trypsin/EDTA solution (final concentration) in PBS for 5-10 min at 37 °C. Attached cells were detached by a short clap of the flask. Trypsinization was stopped by addition of 10 mL fresh medium. The solution was transferred to a falcon and spun down at 800 rpm for 5 min. The supernatant was removed and the cells were resuspended in 16 mL fresh medium. 2 mL (1:8) of this solution were used to inoculate a new flask.

5.2.2.2.2 Counting

Cells were counted after detachment from culture flasks (see 5.2.2.2.1) and resuspension in 10 mL medium. The counting chamber was prepared by wetting the edges and putting on the cover glass and applying pressure to the cover glass until "rainbow rings" show up. A 1:1 dilution (10 µL each) of Tryptophane blue and cell solution was prepared. Put 10 µL of the resulting solution were placed in the counting chamber. All 4 big squares were counted (cells on left and upper border did count, cells on the right and down border did not), averaged, multiplied by 2 (due to the 1:1 dilution) and multiplied by 10⁴. The unit of the resulting number is cells/mL.

5.2.2.2.3 MTT Assay

General

The determination of toxic effects of unknown compounds *in vitro* can be analyzed by a variety of methods. The MTT system enables the measurement of the activity of living cells via the metabolic conversion of the MTT-dye by the reduced pyridine nucleotides NADH and NADPH.^[165] The MTT method is simple, accurate and yields reproducible results. The key component is (3-[4,5-dimethylthiazol-2-yl]-2,5-diphenyl tetrazolium bromide) or MTT. Solutions of MTT, dissolved in medium or balanced salt solutions are yellowish in color. Mitochondrial dehydrogenases of viable cells cleave the tetrazolium ring, yielding purple formazan crystals which are insoluble in aqueous solutions. The crystals can be dissolved in DMSO and the resulting purple solution can be measured spectrophotometrically. An increase or decrease in cell numbers or metabolic activity result in a concomitant change in the amount of formazan formed, indicating the degree of cytotoxicity caused by the test material.

Procedure

The cells were counted (see 5.2.2.2.2) and adjusted to the desired cell density (NIH3T3: 15.000 cells/mL, HaCat: 45.000 cells/mL). For every measurement, 100 μ L of the solution was placed in a well of a 96-well plate. Each measurement was prepared as triplicate. Medium only was used as a blank control. The cells were grown at 37 °C overnight in a gassed (95 % air and 5 % CO₂) humidified incubator. 100x stocks of the respective compounds were prepared as DMSO stocks in different concentrations. 3.5 μ L of the stocks were added to 346.5 μ L of medium to prepare enough of a 1x working solution of the respective compounds for a triplicate measurement. The same amount of DMSO in 346.5 μ L medium was prepared as a negative control. The medium of the overnight cultures was carefully removed using a pipet. 100 μ L of the respective working solution was added to the well and incubated for 24 h at 37 °C in a gassed (95 % air and 5 % CO₂) humidified incubator. After the incubation, 20 μ L of the MTT- solution (5 mg/mL in PBS, sterile filtered) was added

and incubated for 5 min at 300 rpm on a shaker. After incubation at 37 °C in a gassed (95 % air and 5 % CO₂) humidified incubator for 2 h metabolized MTT crystals are visible under light microscope. The supernatant is removed and the violet formazan crystals were dissolved in 200 μ L DMSO by incubation on a shaker at 300 rpm for 5 min at RT. The absorption at 570 nm was measured using a Tecan, plate reader. Background was measured at 630 nm and subtracted as well as the blank control. The DMSO control was set to 100 % cell viability. The values of the different compounds were compared against the DMSO control.

5.2.3 Genomics

5.2.3.1 Materials

5.2.3.1.1 Buffers

Name	Composition
TAE-buffer stock (pH 7,0)	2,0 M Tris-HCl 1,0 M AcOH 0,1 M EDTA
TAE-Gel buffer	20 mL TAE-buffer stock 980 mL ddH ₂ O
TAE-running buffer	10 mL TAE-buffer stock 980 mL ddH ₂ O
TE-Puffer	10 mM Tris Base 1 mM EDTA adjust pH to 8
DNA loading buffer	250 mg Bromphenolblue 250 mg Xylencyanol 33 mL Tris (150 mM) 60 mL Glycerin 7 mL ddH ₂ O
Ethidium bromide stock	dissolve 1 Tab in 1 mL ddH ₂ O dilute 1:10 with ddH ₂ O

5.2.3.1.2 Enzymes

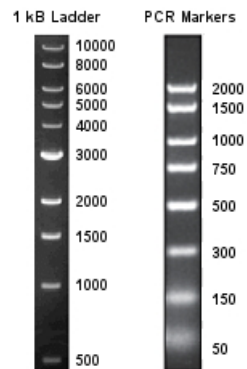
Ezyme	Company
AccuPrime Pfx	Invitrogen, Carlsbad, USA
Platinum Pfx	Invitrogen, Carlsbad, USA
Pfu DNA Polymerase	Promega, Fitchburg, USA
GoTAQ	Promega, Fitchburg, USA
Phusion High Fidelity	New England Biolabs, Ipswich, USA
BP Clonase Mix II	Invitrogen, Carlsbad, USA
LR clonase Mix II	Invitrogen, Carlsbad, USA
DpnI	New England Biolabs, Ipswich, USA
BamHI	Promega, Fitchburg, USA
EcoRI	Promega, Fitchburg, USA
HindIII	Promega, Fitchburg, USA
dTTP	Promega, Fitchburg, USA
dATP	Promega, Fitchburg, USA
T4Ligase	Promega, Fitchburg, USA

5.2.3.2 Plasmids

Name	Source	Res.	Tags	Ind.
pDONR 201	Invitrogen	Kan, Cm	-	-
pDEST 007	Carsten Pieck	Amp, Cm	Strep II	A-Tet
pETG-41K	PEPF	Kan, Cm	N-His ₆ -MBP	IPTG
pNL9164	Sigma Aldrich	Ery, Amp	-	CdCl ₂
pDG148Stu	BGSC	Kan, Bleo	-	IPTG
pRB473XylR	Prof. Ohlsen	Amp, Cm	-	Xylose

5.2.3.2.1 Size standards

Media	Composition
1kB Ladder	New England Biolabs, Ipswich, USA
PCR Markers	Novagen, Darmstadt, Germany



5.2.3.2.2 Primers

Gateway:

β -ketoacyl-ACP synthase III (FabH), S. aureus Mu50:

forward primer: 5'- GGG GAC AAG TTT GTA CAA AAA AGC AGG CTA
CTT TGG TGC ATA TGC ACC AG -3'

reverse primer: 5'- GGG GAC CAC TTT GTA CAA GAA AGC TGG GTG
TAT TGT CAT TGC GCC CCA A -3'

β -ketoacyl-ACP synthase II (FabF), S. aureus Mu50:

forward primer: 5'- GGG GAC AAG TTT GTA CAA AAA AGC AGG CTT
TAT GAG TCA AAA TAA AAG AGT AGT T -3'

reverse primer: 5'- GGG GAC CAC TTT GTA CAA GAA AGC TGG GTG

TTA TGC TTC AAA TTT CTT GAA TAC -3'

Lipoate protein ligase (LPL), *S. aureus* Mu50:

forward primer: 5'- GGG GAC AAG TTT GTA CAA AAA AGC AGG CTT
TAT GAC TGA AAC TTG GAA TTT TAT -3'

reverse primer: 5'- GGG GAC CAC TTT GTA CAA GAA AGC TGG GTG
CTA CTT TCT AAA CAT CCA TTC -3'

HTH-type transcriptional regulator, mgrA *S. aureus* Mu50:

forward primer: 5'- GGG GAC AAG TTT GTA CAA AAA AGC AGG CTT
TAT GTC TGA TCA ACA TAA TTT AAA -3'

reverse primer: 5'- GGG GAC CAC TTT GTA CAA GAA AGC TGG GTG
TTA TTT TTC CTT TGT TTC ATC AA -3'

Diaminopimelat epimerase, DAPE *L. monocytogenes* EGD-e:

forward primer: 5'- GGG GAC AAG TTT GTA CAA AAA AGC AGG CTT
TAT GGA AAC AAT TCA CTT TAC A -3'

reverse primer: 5'- GGG GAC CAC TTT GTA CAA GAA AGC TGG GTG
TCA TTC GGT TGT TTT TAG AAA -3'

SufC, *L. monocytogenes* EGD-e:

forward primer: 5'- GGG GAC AAG TTT GTA CAA AAA AGC AGG CTT
TAT GGC AAC TTT AAA GAT TCA A -3'

reverse primer: 5'- GGG GAC CAC TTT GTA CAA GAA AGC TGG GTG
TTA TTG TTG GTC TAC TGC T -3'

SufB, *L. monocytogenes* EGD-e:

forward primer: 5'- GGG GAC AAG TTT GTA CAA AAA AGC AGG CTT
TAT GAC TGA AAT TCC AGA AAT TGG -3'

reverse primer: 5'- GGG GAC CAC TTT GTA CAA GAA AGC TGG GTG

TTA ACC AAT CGA GCC TTC CA -3'

Targetron:

β-ketoacyl-ACP synthase III (FabH), *S. aureus* Mu50

72/73s-IBS: 5'- AAA AAA GCT TAT AAT TAT CCT TAT ATT TCG AGC
AAG TGC GCC CAG ATA GGG TG -3'

72/73s-EBS1d: 5'- CAG ATT GTA CAA ATG TGG TGA TAA CAG ATA
AGT CGA GCA ATT TAA CTT ACC TTT CTT TGT -3'

72/73s-EBS2: 5'- TGA ACG CAA GTT TCT AAT TTC GGT TAA ATA
TCG ATA GAG GAA AGT GTC T -3'

β-ketoacyl-ACP synthase II (FabF), *S. aureus* Mu50

443/444s-IBS: 5'- AAA AAA GCT TAT AAT TAT CCT TAA CTG GCC
AAG TAG TGC GCC CAG ATA GGG TG -3'

443/444s-EBS1d: 5'- CAG ATT GTA CAA ATG TGG TGA TAA CAG ATA
AGT CCA AGT ATC TAA CTT ACC TTT CTT TGT -3'

443/444s-EBS2: 5'- TGA ACG CAA GTT TCT AAT TTC GAT TCC AGT
TCG ATA GAG GAA AGT GTC T -3'

Homologous overexpression:

β-ketoacyl-ACP synthase III (FabH), *L. monocytogenes* EGD-e:

forward primer: 5'- AAG GAG GAA GCA GGT ATG AAC GCA GGA ATT
TTA GGA G -3'

reverse primer: 5'- GAC ACG CAC GAG GTT TAC TTA CCC CAA CGA
ATG ATT AG -3'

β-ketoacyl-ACP synthase II (FabF), *L. monocytogenes* EGD-e:

forward primer: 5'- AAG GAG GAA GCA GGT ATG GAT AAG AGA AGA
GTA GTT GTT ACT G -3'

reverse primer: 5'-GAC ACG CAC GAG GTT TAG TCT TCT ATT CTT

TTA AAT ACT AAA G -3'

β-ketoacyl-ACP synthase III (FabH), *S. aureus* Mu50:

forward primer: 5'- GCC AGG ATC CAT GAA CGT GGG TAT TAA AGG
TTT TG -3'

reverse primer: 5'- GCC AGA ATT CCT ATT TTC CCC ATT TTA TTG
TCA TTG -3'

β-ketoacyl-ACP synthase II (FabF), *S. aureus* Mu50:

forward primer: 5'- GCC AGG ATC CAT GAG TCA AAA TAA AAG AGT
AGT TAT TAC AG -3'

reverse primer: 5'- GCC AGA ATT CTT ATG CTT CAA ATT TCT TGA
ATA CTA ATA C -3'

Missmatch:

β-ketoacyl-ACP synthase II (FabF) C165A, *S. aureus* Mu50:

forward primer: 5'- AAA TGG TGC AAC AGT TAC AGC AGC TGC AAC
AGG TAC AAA CTC

reverse primer: 5'- GAG TTT GTA CCT GTT GCA GCT GCT GTA ACT
GTT GCA CCA TTT

β-ketoacyl-ACP synthase II (FabF) C220A, *S. aureus* Mu50:

forward primer: 5'- ACA AAT GAT GAC ATT GAA ACA GCA GCT CGT
CCA TTC CAA GAA GG

reverse primer: 5'- CCT TCT TGG AAT GGA CGA GCT GCT GTT TCA
ATG TCA TCA TTT GT

β-ketoacyl-ACP synthase II (FabF) C376A, *S. aureus* Mu50:

forward primer: 5'- TGC GGT AAC AAC AGA CCC AGA AGC TGA TTT
GGA TAT TGT TC

reverse primer: 5'- GAA CAA TAT CCA AAT CAG CTT CTG GGT CTG

GTG TTA CCG CA

β-ketoacyl-ACP synthase III (FabH) C112A, *S. aureus* Mu50:

forward primer: 5'- CCT CTA TGG ATC AAC TTG CAG CAG CTT CTG
GAT TTA TGT ATT CAA TGA

reverse primer: 5'- TCA TTG AAT ACA TAA ATC CAG AAG CTG CTG
CAA GTT GAT CCA TAG AGG

5.2.3.3 Methods

5.2.3.3.1 Extraction of genomic DNA

Genomic DNA was prepared from overnight cultures of the respective Bacteria using the DNeasy Blood & Tissue Kit (Qiagen, Hilden, Germany).

5.2.3.3.2 PCR

General

Since its invention in 1985 the Polymerase chain reaction became one of the most important techniques in the area of molecular biology. The method relies on thermal cycling consisting of cycles of repeated heating and cooling and a heat resistant DNA Polymerase to selectively amplify a single or a few copies of a piece of DNA across several orders of magnitude. The essential components for the reaction are:

- a DNA strand containing the desired sequence
- a small DNA fragment for each strand of the template with a complementary sequence to the target (primer)

- a heat stable DNA-Polymerase (e.g. Taq-Polymerase)
- deoxynucleoside triphosphates (dNTPs), the building-blocks for the DNA polymerase to synthesize a new DNA strand
- divalent cations (e.g. Mg^{2+}), essential for a proper function of the Polymerase
- buffer solution, providing a suitable chemical environment for optimal activity and stability of the DNA polymerase

The PCR reaction is normally done in a Thermocycler, a machine which performs the temperature cycles with great precision. Typically the PCR is often preceded by a single temperature step at a high temperature ($>90\text{ }^{\circ}\text{C}$) followed by a series of 30 repeated temperature changes, called cycles, with each cycle commonly consisting of 2-3 discrete temperature steps shown in fig. Figure 5.2.3.1:

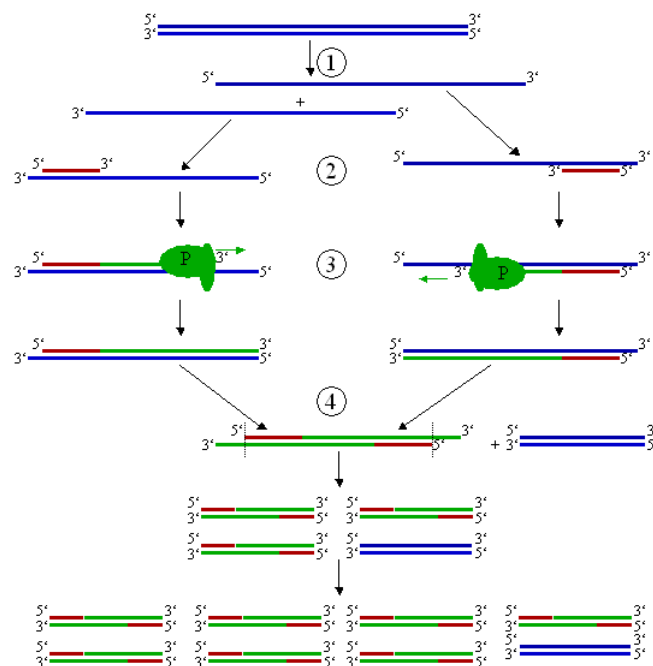


Figure 5.2.3.1: *Schematic figure of a PCR: (1) Melting of the template, (2) annealing, (3) elongation, (4) end of cycle*

1. **Melting:** In the first step the double stranded DNA is melted at 96 °C by breaking the H-bonds holding together the double strands. A longer incubation time (~ 5 min) may be necessary to completely melt template as well as primers.
2. **Annealing:** By reducing the temperature to the so called melting temperature primers specifically bind to the desired target sequence on the DNA template. This temperature can be calculated using different methods (e.g. nearest neighbor) based of the length and the GC content of the primers.
3. **Elongation:** After annealing of the primers the temperature is changed to the optimum of the DNA-Polymerase (e.g. 68 °C for AccuPrime *Pfx*). The enzyme starts at the 3'-End of the Primer-DNA complex synthesizing a new strand using the complementary strand as a template. The elongation time has to be calculated by the length of the desired DNA fragment and the rate of the enzyme. As a rule of thumb the polymerase needs 1 min per kbp.
4. **Repeat cycle:** Continue with melting the resulting new double-stranded DNA. The new DNA can be used as a template effectively doubling the amount of template in each cycle.

PCR for Gateway

The reaction was prepared as follows:

- 11.5 μL ddH₂O
- 2.5 μL 10x reaction buffer
- 1 μL template DNA (conc. between 100 and 1 ng/ μL)
- 4 μL sense primer (10 pM)
- 4 μL anti-sense primer (10 pM)
- 2 μL AccuPrime *Pfx* Polymerase

The following temperature program was used for the Gateway cloning:

1. 96 °C 1:30 min
2. 94 °C 0:10 min
3. $T_m - 2$ °C 0:15 min
4. 68 °C 1:00 min pro 1000 bp
5. Goto 1. 4x
6. 94 °C 0:10 min
7. $T_m - 2$ °C 0:15 min
 $-0,2$ °C pro Zyklus
8. 68 °C 1:00 min pro 1000 bp
9. Goto 6. 6x
10. 96 °C 0:10 min
11. $T_m - 0,5$ °C 0:15 min
12. 96 °C 1:30 min
13. 68 °C 1:00 min pro 1000 bp
14. Goto 10. 30x
15. 68 °C 7:00
16. 4 °C Hold

PCR for Quik change

The reaction was prepared as follows:

- 35.6 μ L ddH₂O

- 10.0 μL 10x reaction buffer
- 1 μL template DNA (conc. between 300 and 100 ng/ μL)
- 0.8 μL sense primer (10 pM)
- 0.8 μL antisense primer (10 pM)
- 1 μL dNTPs (10 mM)
- 1 μL high specificity Polymerase (e.g. *Phusion*)

Problems with the the mismatch PCR could be addressed by either using smaller amounts of template and/or primers, by addition of up to 8 % of DMSO to the reaction solution or by changing the annealing temperature. Additionally the use of special GC buffers (for sequences containing high amounts of G and C bases) could boost the efficiency of the reaction.

The following PCR program was used for the mismatch cloning:

- | | |
|------------|----------------------|
| 1. 95 °C | 5:00 min |
| 2. 95 °C | 1:00 min |
| 3. 59 °C | 1:00 min |
| 4. 72 °C | 1:00 min pro 1000 bp |
| 5. Goto 2. | 30x |
| 6. 72 °C | 7:00 |
| 7. 4 °C | Hold |

PCR for Targetron

A primer mastermix was prepared as follows:

- 100 μM IBS
- 100 μM EBS1d

- 1.5 μL antisense primer (10 pM)
- 1 μL Accu Prime-Pfx Polymerase (Invitrogen)

By increasing the amount of template DNA to 5 μL and the total reaction volume to 100 μL point mutations can be avoided. The following PCR program was used:

- | | |
|-----------------------------|----------|
| 1. 95 °C | 2:00 min |
| 2. 95 °C | 0:30 min |
| 3. 56 °C (FabH) 57 °C(FabF) | 0:30 min |
| 4. 68 °C | 2:00 min |
| 5. Goto 2. | 30x |
| 6. 68 °C | 7:00 |
| 7. 4 °C | Hold |

5.2.3.3.3 Agarose gelelectrophoresis

PCR fragments and plasmids can be analyzed and purified by using agarose gelelectrophoresis. In this method the negatively charged DNA is pulled through an agarose polymer by the application of an electrical field. The longer the DNA, the more it interacts with the polymer making the DNA move slower in the gel. Detection of the DNA in the gel can be achieved by the addition of ethidiumbromide to the buffer. This dye intercalates in the DNA making the DNA visible under UV-Light as orange bands. If DNA is extracted from a gel, one has to be careful not to expose the DNA to UV light for more than 30 secs, otherwise photodamages like thymine-thymine dimers will render the DNA useless.

Agarose gel (1 %): 500 mg of agarose were dissolved in 50 mL TAE-gel buffer (see 5.2.3.1.1) and heated in a microwave until the agarose was completely dissolved. The solution was allowed to cool to ~ 50 °C and 10 μL ethidiumbromide solution (see 5.2.3.1.1) were added. A comb with the appropriate

number of lanes was placed in the gel casting tray and the warm agarose solution was poured in the tray. After 20 min the samples were mixed with loading buffer, loaded onto the gel and run at 95 V, for 30-60 min depending on the size of the desired DNA fragment. Different commercially available standards were used as size standards (see 5.2.3.2.1). The bands were extracted using the E.Z.N.A Gel Extraktion Kit from (Omega Biotek, Germany).

5.2.3.3.4 Gateway cloning

General

To produce clones for the recombinant overexpression of proteins the Gateway Kit (Invitrogen) was used. The gateway system relies on a set of recombination sequences, the ATT-sites and two enzyme mixes (BP and LR Clonase) that enable a fast and efficient transfer DNA-fragments into and between plasmids. The ATT-sites are derived from the site specific recombination sequences of the bacteriophage lambda which enable the virus to insert its DNA into the bacterial chromosome specifically at certain sites. Gateway vectors additionally comprise a *ccdB* control gene which kills off any bacterium containing an unsuccessful clone. Thereby the selection of successful recombinants is simplified greatly. The steps to create a Gateway expression clone are:

1. **Gateway PCR:**

flanking attB sequences are attached to the gene of interest by using specifically designed primers in the PCR.

2. **Cloning in DONR-vector:**

the DONR-vectors are high copy plasmids containing a so called *ccdB* gene (coupled cell division type B) which codes for a topoisomerase II inhibitor which inhibits proper supercoiling of chromosomal DNA. If this protein is expressed it effectively inhibits division of host cells. This gene is flanked by attP sequences which are used as recombination sites for the attB sites in the gene of interest. Additionally the plasmid contains an antibiotic resistance. The BP enzyme mix catalyzes the recombinant

exchange of the PCR fragments with the *ccdB* sequence in the vector, thereby creating the so called attL sites.

3. Transformation in competent cells:

After the recombinant exchange of the DNA sequences catalyzed by the BP enzyme mix, clones can be transformed in competent *E.coli* cells (e.g. TOP10). Cells growing on selective agar can be used for further cloning as cells containing empty plasmid are killed by the *ccdB* protein, whereas cells containing no plasmid will die by the selective antibiotic.

4. Cloning in DEST-vector:

after harvesting the plasmids from *E.coli* the gene of interest can be cloned in different expression plasmids called DEST-vectors. These plasmids contain new recognition sites (attR) which are used to recombinantly exchange the DNA between DONR and the DEST-vectors. This reaction is catalyzed by the LR-enzyme mix. Depending on the purification method preferred different DEST-vectors can be used as a wide variety of plasmids with different Tags are available.

5. Transformation in competent cells:

the new clones can be transformed in competent *E.coli* cells (eg. BL21) and grown on selective medium. As the DONR and DEST-vector have different antibiotic resistances genes, colonies growing on DEST-selection medium only contain successfully cloned DEST-plasmids.

6. Overexpression:

depending on the promotor of the DEST-vector, overexpression can be induced by addition of the respective inducer molecule. (e.g. anhydroteracyclin or Isopropyl β -D-1-thiogalactopyranoside (IPTG))

Primer design

Primers for the gateway system have to be designed specifically for this purpose. According to the Gateway manual primers should consist of 18 to 25 nucleotides. The melting temperature of the sense and the antisense primers should differ by no more than 0.5 – 1 °C. Melting temperatures

were calculated by using the nearest neighbor method^[184]. The best results were achieved in a temperature range between 50 and 65 °C. After the first part of the primers is designed the attB sequences are added (sense: 5'-ggggacaagtttgtacaaaaaagcaggctac, antisense: 5'-ggggaccactttgtacaagaaagctgggtg). The resulting primers were ordered in HPLC grade purity from Metabion, Planegg/Martinsried, Germany. After the PCR (see 5.2.3.3.2) the fragments were purified by agarose gelelectrophoresis (see 5.2.3.3.3).

BP cloning

For the reaction 100 fmol of the PCR products were used. The amount (in mole) of DNA was calculated by the mass using this formula with N being the length of the DNA in base pairs:

$$ng = (fmol)(N)\left(\frac{660 \text{ fg}}{fmol}\right)\left(\frac{1 \text{ ng}}{10^6 \text{ fg}}\right)$$

The reaction was prepared as follows:

- 1 μL PCR-fragment (100 fmol/ μL)
- 1 μL pDONR (150 ng/ μL)
- 6 μL TE-Buffer
- 2 μL BP-Clonase Mix II

The reaction was incubated for 2-12 h at RT. A Protease K incubation is not necessary.

LR cloning

The reaction was prepared as follows:

- 1 μL PCR-fragment (100 fmol/ μL)
- 1 μL pDONR (150 ng/ μL)
- 6 μL TE-Buffer
- 2 μL BP-Clonase Mix II

The reaction was incubated for 2-12 h at RT. A protease K incubation as mentioned in the manual is not necessary.

5.2.3.3.5 Ligation independent cloning

General

Conventional cloning uses restriction sites present in the PCR product or blunt ends for the insertion of the PCR products into a plasmid. However, the cloning of small DNA molecules does often prove to be difficult and a sizeable fraction of the clones will lack inserts. This may not present a major problem if a convenient screening procedure or selection method (like the *ccdB* gene in the Gateway system) is available, but in most cases laborious PCR screens are necessary. *Joseph et al* have developed a more effective method for the cloning of PCR products, that does not involve restriction enzymes or DNA ligase.^[180] In essence, long single-stranded tails are created at the ends of the PCR products and the linear plasmid vector. The single strand-ends present at the PCR fragments are complementary to those attached to the vector, thus permitting non-covalent bi-molecular associations e.g. circularization between two molecules. The vector has identical, non-complementary tails at either end, preventing the formation of circular forms consisting of vector only. The recombinant forms are used for transformation in *E.coli*; non-recombinant transformants are strongly reduced due to the poor transformation efficiency of linear plasmid DNA in *E.coli* (10^2 - 10^4 times less than circularized DNA^[185]).

Procedure

Two reaction mixes were prepared as follows: Solution 1:

- 150 ng StuI digested blunt end vector
- 5 μ L T4 Polymerase (1:100)
- 2 μ L Pol-Buffer
- 2 μ L dTTP (10 mM)
- ad 20 μ L ddH₂O

Solution 2:

- 1500 ng Insert
- 0.55 μ L T4 Pol (undiluted)
- 2 μ L Pol-Buffer
- 2 μ L dATP (10 mM)
- ad 20 μ L ddH₂O

After incubation for 15 min at 37 °C both solutions were pooled and incubated for 30 min at RT. The resulting vector can be transformed into chemically competent TOP10 cells (see 5.2.3.3.7).

5.2.3.3.6 Ligation

The reaction was prepared as follows:

- 100 ng vector
- 50-100 ng insert (49 ng FabH, 65 ng FabF)
- 1 μ L Buffer
- 1 μ L Ligase
- ad 10 μ L ddH₂O

Reaction mixture was mixed and incubated for 3 h at RT or overnight at 4 °C

5.2.3.3.7 Transformation

General

Transformation is the genetic alteration of a cell resulting from the direct uptake, incorporation and expression of exogenous genetic material (exogenous DNA) from its surrounding and taken up through the cell membrane(s).^[186] This mechanism can be used to insert, amplify and express artificial genes in bacteria, using plasmids a shuttle. Plasmids are circular double stranded DNA molecules that can replicate independent of chromosomal DNA, responsible for horizontal gen transfer in bacteria. Plasmids used in genetic engineering are called vectors and are commercially available in a broad variety. Bacteria that are capable of being transformed, whether naturally or artificially, are called competent. Artificial competence is induced by laboratory procedures and involves making the cell passively permeable to DNA by exposing it to conditions that do not normally occur in nature (see 5.2.1.2.2). Depending on the previous treatment of the cells their membrane can either be opened by a short heat shock (42 °C, 30 sec) or by application of an electric field (10-20 kV/cm) for a short time. While the holes are quickly repaired by the cell, the plasmids enter the cell. Most vectors carry genes that make cells resilient to a particular antibiotic. If the transformed bacteria are grown in selective medium only the bacteria which took up copies of the plasmid will survive.

Procedure for chemically competent *E.coli*

One aliquot of the cells were thawed on ice for 10 min. 4 μ L of the cloning reaction (or DpnI digest) were added and the suspension was mixed by inversion of the tube and incubated for 30 min on ice. The transformation was initiated by a heatshock at 42 °C for 35 sec. 200 μ L of prewarmed LB or SOC (see 5.2.1.1.3) were added and placed sideways in a shaker at 37 °C for 1-2 h. 100 μ L and the rest of the suspension was plated each on an selective agar plate (DONR: 25 μ L Kanamycin, DEST: 100 mg/mL Carbenicillin/Ampicillin) as a selective medium. After 14 h at 37 °C single colonies were picked and grown

in a liquid LB-overnight culture containing the respective antibiotic. A cryo-stock was prepared from the cells (see 5.2.1.2.1). Cells were spun down at 4000 g and 4 °C for 10 min and the plasmids were isolated using the Plasmid extraction Kit (Omega BitoTek, Germany). Concentrations were determined using a Tecan Image reader.

- DONR vectors: chemically competent OneShotR TOP10 E. coli (see 5.2.1.2.2)
- DEST vectors: chemically competent BL21 E. coli (see 5.2.1.2.2)
- Quik change: chemically competent XL1 Blue E. coli (see 5.2.1.2.2)

Procedure for electro-competent cells

Protocol for *Listeria monocytogenes* EGD-e: One aliquot of electrocompetent cells (see 5.2.1.2.2) as well as the DNA and the electroporation cuvettes (2 mm) were placed on ice for 30 min. 5 μ L of plasmid DNA (4-5 μ g of DNA) were added to the cells, mixed by inversion of the tube, cautiously transferred to the poration cuvette and incubated on ice for another minute. The outside surface of the cuvette were wiped dry and the following exponential electroporation protocol was used:

- 2,5 kV
- 200 Ω
- 25 μ F

The exponential decay of the pulse should be around 3.6 ms. After the pulse immediately 1 mL of prewarmed BHB was added to the cells, and mixed by inversion of the tube. The cells were carefully transferred into a sterile 1.5 mL tube and incubated for 6 h at either 30 °C or 37 °C depending on the plasmid. By plating on selective BHB agar plates, single clones can be picked after 48 h. Plasmids were isolated using the Plasmid extraction Kit (Omega BitoTek, Germany). DNA-concentrations were determined using a Tecan Image reader.

Protocol for *Staphylococcus aureus* RN4220/Mu50: One aliquot of electrocompetent cells (see 5.2.1.2.2) were thawed at RT. 5 μ L of plasmid DNA

(4-5 μg of DNA) were added to the cells, mixed by inversion of the tube, cautiously transferred to the poration cuvette and incubated at RT for 15 min. The following exponential electroporation protocols were used:

1 mm cuvettes:

- 2 kV
- 100 Ω
- 25 μF

The exponential decay of the pulse should be around 1.9 ms.

2 mm cuvettes:

- 3 kV
- 100 Ω
- 25 μF

The exponential decay of the pulse should be around 2.4 ms. Immediately after the pulse, 1 mL of prewarmed BHB was added to the cells, and mixed by inversion of the tube. The cells were carefully transferred into a sterile 1.5 mL tube and incubated for 2 h at 37 °C. By plating on selective BHB agar plates, single clones can be picked after 24-48 h. Plasmid were isolated using the Midi Plus Prep(Qiagen) from 75 mL RN4220 culture. According to manufacturer's protocol, high yield buffer volumes were used. The additional resuspension in buffer P1 containing 50 μL (2 mg/mL) lysostaphin (Sigma-Aldrich) and incubation for 20-30 min at 37 °C further increased the yield. DNA-concentrations were determined using a Tecan Image reader.

5.2.3.3.8 Site directed mutagenesis

General

Site-directed mutagenesis is a molecular biology technique by which a mutation can be created at a defined site in a known DNA sequence. This can be used to disable enzymes by changing vital amino acids of their actives

sites to inactive counterparts (e.g. Cys to Ala). In this thesis the mutation were introduced by employing the QuikChange II Site-Directed Mutagenesis kit (Agilent Technologies). The first step in this procedure requires two short synthetic DNA primers (sense and antisense) specially designed for the desired base change. This primer is then hybridized with a double-stranded plasmidic DNA containing the gene of interest. A DNA polymerase is used to extended the primer, which copies the rest of the gene in a PCR like fashion(see 5.2.3.3.2). Incorporation of the oligonucleotide primers generates a mutated linearized plasmid containing staggered nicks. Following temperature cycling, the product is treated with a DpnI endonuclease which is specific for methylated and hemi-methylated DNA. It can be used to digest the parental DNA template and to select for mutation-containing synthesized DNA. The nicked vector DNA containing the desired mutations can then be transformed in competent cells, which are able to repair nicked plasmid DNA (see 5.2.3.3.7).

Procedure

The mutation was introduced by mismatch PCR (see 5.2.3.3.2). After purification by agarose gel electrophoresis (see 5.2.3.3.3) 5 μL of the DNA ($\sim 15 \text{ ng}/\mu\text{L}$) were mixed with 0.5 μL of reaction Buffer 4 (New England Bio-Labs). 1 μL of DpnI was added, vortexed and spinned down. After incubation for 2 h at 37 °C the reaction solution is added to chemically competent XL1 Blue cells on ice. The cells were transformed using the standard protocol (see 5.2.3.3.7) and 50 μL as well as 150 μL were plated on the adequate selection agar for the plasmid. Colonies were picked and grown in a liquid overnight culture. After a plasmid extraction the identity of the point-mutations can be confirmed by sequence analysis. If a DONR vector was used as a template, normal LR-Gateway cloning was used to place the mutated gene in an Expression vector (see 5.2.3.3.4).

5.2.3.3.9 Gene knockout

General

A gene knockout is a genetic method by which one or more genes of an organism are disabled ("knocked out" of the organism). This can be used in learning about the function of a gene in a specific organism by drawing inferences from the different phenotypes of the knockout organism and normal 'wildtype' individuals. To establish a knockout three different methods have emerged in the last decades. The first approach to knockout bacterial genes was the use of transposon mutagenesis. Transposons are relatively short pieces of DNA that replicate by inserting into other pieces of DNA (plasmids, chromosomes, viruses). These transpositions are catalyzed by various types of transposase enzymes which make a staggered cut at the target site producing sticky ends. Then the transposon is cut out and ligated into the target site which disrupts the gene and almost always completely inactivates it. There are, however, some drawbacks to transposon mutagenesis. As transposons are not site specific, so laborious screens are required to find a knockout in the gene of interest.

This problem can be overcome by the TargeTron Gene Knockout System (Sigma Aldrich) which provides a rapid and specific disruption of bacterial genes by insertion of group II introns. These introns consist of an autocatalytic RNA and a multifunctional, intron-encoded protein (IEP), which has reverse transcriptase activity. Insertion in the target gene occurs by a DNA-primed reverse transcription in which the excised intron RNA reverse splices directly into a DNA target site and is then reverse transcribed by the IEP.^[187] The process of using the TargeTron system is divided in three key steps. First a computer algorithm is used to identify target sites in the gene of interest. This algorithm also outputs primer sequences, which are used to customize the intron RNA by changing the coding DNA sequence by PCR. Next, the mutated PCR fragment is ligated into a linearized vector that contains the remaining intron components. The ligation reaction is transformed into the host followed by expression of the re-targeted intron. The intron will then insert in the target sequence disrupting the gene. Knockouts are then selected

using a kanamycin marker that is activated upon chromosomal insertion.^[178]

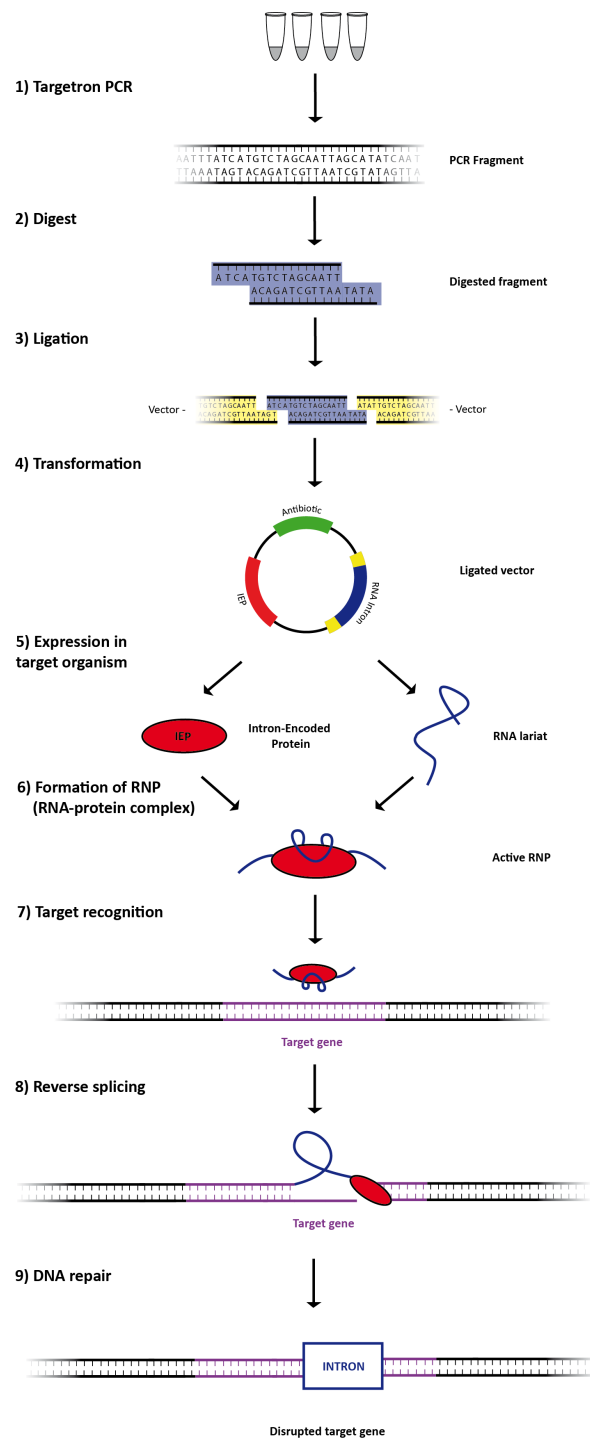


Figure 5.2.3.2: Schematic workflow of the Targetron system

Using gene specific primers, kanamycin resistant colonies are PCR screened to confirm insertion. This streamlined process can yield the desired mutation within a few weeks without the need for huge screens to yield the knockout of interest. However problematic is that in most cases insertions cause polar mutations, meaning that genes lying on the same transcript downstream of the inserted intron will not be expressed efficiently. Thus, it is possible to unintentionally influence a whole set of genes, which may lead to wrong conclusions about the function of your target gene.

A third technique called 'recombineering' combines the strengths of both methods mentioned above. Recombeneering relies on a site specific homologous recombination *in vivo*, a process bacteriophages utilize to insert their DNA in the host genome. The method can be used to either exchange or to delete genes. The DNA which is to be inserted in recombineering can either be a double-stranded PCR product^[188,189,190] or a single-stranded oligonucleotide^[191] carrying short sequences of DNA (cassette) homologous to DNA surrounding the gene of interest. By transformation of this DNA into recombination-competent cells and induction of the recombinases the gene of interest is excised and replaced by the DNA surrounded by the cassette. As examples, the cassette can be inserted between two adjacent bases, can be designed to replace the coding sequence of a gene by creating an in-frame, nonpolar knockout, or can be used to remove a whole operon and even more. The region deleted can be at least 50kb.^[192] Traditionally the inserted DNA carries an antibiotic resistance by which successful clones can be selected later on.

This method however selective and powerful has disadvantages on its own. The design of the cassettes is often problematic and time consuming. Additionally the need for recombination-competent cells limits the method to a handful of organisms or encompasses the laborious process of designing competent cells yourself.

For this reason the streamlined TargeTron system was used in this thesis to create knockouts.

Procedure

The PCR fragment for the TargeTron system was created by using the TargeTron PCR protocol (see 5.2.3.3.2). The 350 bp fragment was purified by Agarose gelelectrophoresis (see 5.2.3.3.3), digested with the restriction enzymes DpnI, BsrGI and HindIII according to the enzyme manual. The addition of DpnI is required only when using the vector pNL9164 (see 5.2.3.2). The digestion is necessary to produce cohesive ends for the ligation into the vector. If the vector is not linearized (e.g. pNL9164) a double digest with BsrGI and HindIII is obligatory. After heat inactivation of the restriction enzymes ligation reaction is started by mixing 2 μL of the linearized vector (40 ng), 6 μL of the digested PCR-product, 9 μL of ddH₂O, 2 μL 10x Ligase Buffer and 1 μL of a T4 Ligase. The solution was vortexed, spinned down and incubated for 14 h at 16 °C. 4 μL of the solution were used for the transformation in Top10 cells (see 5.2.3.3.7). The bacteria were grown on Ampicillin LB Agar plates. Single colonies were picked and grown in a liquid LB-Ampicillin overnight culture. A cryostock was prepared (see 5.2.1.2.1) and the rest of the cells were spinned down at 4000 g and 4 °C for 10 min to isolate the vector by using the Plasmid extraction Kit (Omega BitoTek, Germany). The DNA concentration was determined using a Tecan Image reader.

The vector was transformed in the target organism using electroporation (see 5.2.3.3.7). In case of a desired knockout in *Staphylococcus aureus* a transformation in *Staphylococcus aureus* RN4220 a restriction deficient mutant of *Staphylococcus aureus* 8325 is necessary. This additional step provides DNA derived from *E.coli* with the correct methylation pattern to be accepted in other, non deficient strains like Mu50 or NCTC8325. After electroporation the cells were grown in BHB for 2 h, plated on selective medium and grown overnight in a shaker. In case of the vector pNL9164 cells have to be grown at 32 °C as higher temperatures will cure the cells from the plasmid. Single colonies were picked and grown in a liquid BHB-Erythromycin overnight culture. Fresh 5 mL BHB cultures were inoculated 1:1000 with the overnight cultures, grown to OD₆₀₀ \sim 0.5 at 32 °C on a shaker. Expression of the group II Intron was induced by the addition of 10 μM CdCl₂. Cells were incubated at 32 °C for 90 min plated on selective medium and grown overnight. The identity of knockout clones can be determined by colony PCR, using either the EBS

Universal primer, the EBS2 primer or primers for the gene of interest. The total size of the colony PCR product using the EBS Universal primer will be 219 bp plus adjacent gene sequence determined by the location of your gene specific primer. The total size of the colony PCR product using the EBS2 primer will be 2059 bp plus adjacent gene sequence. When using gene specific primers, the size of the PCR product will be the original sequence plus the insert. (see 5.2.3.3.2)

5.2.3.3.10 Gene overexpression

General

Gene expression is the process by which genetic information is used to produce a functional gene product, in most cases proteins. Several steps in the gene expression process may be modulated, giving the organism control over quantities and functional states of the expression products. By exchanging the control sequences responsible for the translation of a gene, it is possible to increase the production of a desired gene by several magnitudes. In this work, plasmidic DNA was used to insert heterologous genes into bacteria. The genes incorporated in the plasmids are controlled by a promotor, which can be regulated by the addition of the respective inductor, a chemical compound that binds to the promotor and thereby activating the expression of the desired gene. In bacterial systems the so produced proteins can make up to 50 % of protein content in the cell. These quantities however can be toxic for the bacterial host, which leads to cell death, or the bacteria stack missfolded proteins in insoluble inclusion bodies. Therefore the conditions for every overexpression should be optimized individually, depending on the promotor, the host bacterium and the protein properties (e.g. solubility, toxicity, proteolytic or oxidative stability).

Procedure for anhydrotetracyclin-Promotor

Bacterial cells are grown in selective medium over night. Fresh selective medium (small scale: 5 mL; large scale: up to 3 L) is inoculated 1:1000 with

the overnight culture and grown to an O.D.₆₀₀: 0.5-0.7 at 37 °C and 225 rpm in a shaker. The inductor was applied (ATet: 200 ng/ μ L; IPTG: 2 mM; CdCl₂: 10 μ M) and incubated for 1-6 h depending on the protein. After incubation cells were harvested at 3000 x g

5.2.4 Proteomics

5.2.4.1 Materials

5.2.4.1.1 Devices

Device	Company
SDS Gelstation	Pequlab, Erlangen
Fujifilm Las-4000 Lum. Image Analyzer	Fujifilm, Düsseldorf
Fujifilm Las-3000 Fluorescence Darkbox	Fujifilm, Düsseldorf
Sonopuls HD 2070	Bandelin, Berlin
Ultraschallbad Ultrasonic Cleaner	VWR, Darmstadt
Speedvac AVC 2-33 IR	Christ
Lyophille Alpha 2-4 LD plus	Christ
HPLC 2695 Separation Module	Waters, Eschborn
HPLC XBridge BEH130 C18 5 μ M Columns	Waters, Eschborn
Dionex Ultimate 3000	Dionex, Sunnyvale, USA
Dionex C18 Nano Trap column (100 μ m)	Dionex, USA
Dionex C18 PepMap 100 (3 μ m) column	Dionex, USA
LTQ Orbitrap XL	Thermo Scientific, USA

5.2.4.1.2 Buffers

Name	Composition
PBS	8,00 g NaCl 0,20 g KCl 1,44 g Na ₂ HPO ₄ 0,24 g KH ₂ PO ₄

	Ad 700 mL H ₂ O adjust pH to = 7,4 Ad 1 l H ₂ O
APS-Solution	10 % (w/v) Ammoniumpersulfate in H ₂ O
10 % SDS-Solution	10 % (w/v) Sodiumdodecylsulfate in H ₂ O
0,2 % SDS in PBS	1 mL 10 % SDS-Lösung Ad 50 mL PBS
SDS-stacking gel buffer (10x)	0,50 M Tris Base in H ₂ O adjust pH to 6,8
SDS-resolving gel buffer (10x)	3,00 M Tris Base in H ₂ O adjust pH to 8,8
SDS-Buffer (10x)	0,25 M Tris Base in H ₂ O 1,92 M Glycin in H ₂ O 1 % w/v SDS in H ₂ O
SDS loading buffer (2x)	496,00 mg Tris HCl 5,00 mL Glycerine 1,25 mg Bromphenol blue 1,00 g Sodiumdodecylsulfate Ad 40 mL H ₂ O 2,50 mL Mercaptoethanol Ad 50 mL H ₂ O
Coomassie-stain	0,24 % (w/v) Coomassie Brilliant Blue 9,20 % (v/v) Acetic acid 45,4 % (v/v) biochemical Ethanol
Coomassie-destainer	20,0 % (v/v) biochemical Ethanol

	10,0 % (v/v) Acetic acid
RhN ₃ -Stock (300x)	9,9 mg RhN ₃ Ad 100 μ L MeOH
RhN ₃ -working stock (1x)	1 μ L RhN ₃ -Stock 295 μ L DMSO
TCEP-Solution	7,5 mg tris(2-Carboxyethylphosphin) 500 μ L H ₂ O
TBTA Ligand-Stock (50x)	8,85 mg TBTA Ligand 200,00 μ L DMSO
TBTA Ligand (1x)	20 μ L 50x Ligand-Stock 800 μ L <i>t</i> Butanol 180 μ L DMSO
50 mM CuSO ₄	12,5 mg CuSO ₄ x 5 H ₂ O 1,0 mL H ₂ O
Trifunctional linker (1x)	10 mM in DMSO
50 mM AHC solution	4 mg NH ₄ HCO ₃ 1,0 mL H ₂ O
10 mM DTT solution	1,54 mg Dithiotreitol 1,0 mL 50 mM AHC
55 mM IAA solution	10,2 mg Iodacetamid 1,0 mL 50 mM AHC
Trypsin solution	dissolve 1 batch of Trypsin in 40 μ L Tryp Buffer

dilute 1:100 in 25 mM AHC

Chymotrypsin solution

dissolve 1 batch of Chymotrypsin
in 50 μ L 1M HCl

dilute 1:100 in 25 mM AHC

5.2.4.1.3 Fluorescent dyes, ligands and linkers for click-chemistry

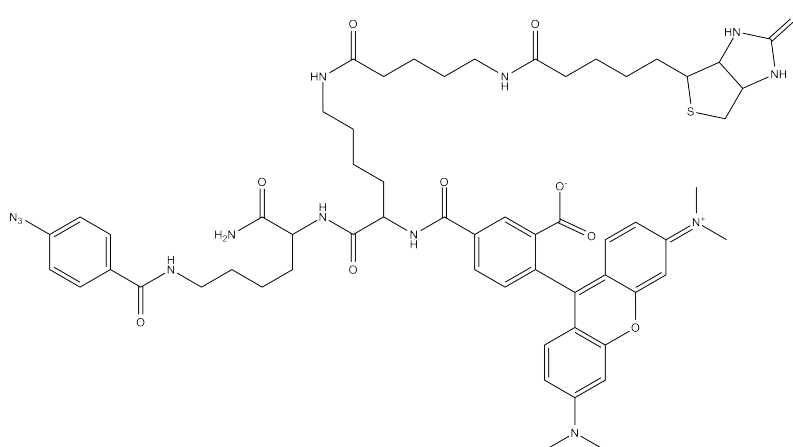


Figure 5.2.4.1: *Trifunctional linker*

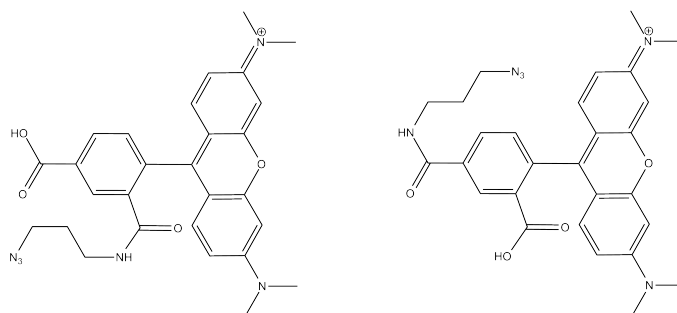


Figure 5.2.4.2: *Isomers of rhodamineazid*

5.2.4.2 Methods

5.2.4.2.1 SDS-PolyAcrylamid-Gel Electrophoresis (SDS-Page)

Gelectrophoresis is a method which enables the separation of molecules based on size and charge. Using an electric field, the molecules are forced to move through a Polymer gel, at different rates, determined by their size and charge. The problem in protein separation is that proteins, unlike DNA, can have varying charges and complex shapes, therefore they may not migrate into the polyacrylamide gel at similar rates. In protein separation SDS (Sodium dodecyl sulfate) is used as a negatively charged surfactant, which binds to proteins at a fixed rate (1,4 g SDS g⁻¹ protein). This forces the proteins to unfold and creates a constant charge on the protein surface, masking the charges that derive from the individual amino acid sequence. When an electric field is applied, the rate at which the resulting SDS coated proteins migrate in the gel, is relative only to its size and not its charge or shape. The speed is determined by the interaction with the polyacrylamid network, so that smaller molecules move faster through the gel. To maximize resolution, proteins must enter the gel as a distinct stack. This can be achieved by the use of two gels. A stacking gel which has large pores and a pH of 6.8 and a resolving gel, characterized by small pores and a pH of 8.8. Both gels contain Cl⁻ as their mobile anion, while running buffer (pH 8.8) contains anionic glycine. When electrophoresis begins, glycine enters the stacking gel, where most of glycine is protonated to its zwitterionic form with zero net charge. The glycine front moves slowly through the stacking gel, lagging behind the strongly charged, highly mobile Cl⁻ ions. Between the leading Cl⁻ ions and the following glycine zwitterions, a region of low conductivity, with a consequent high voltage drop, is formed. This so called Kohlrausch discontinuity pulls the proteins rapidly through the large pores of the stacking gel, concentrating the sample and depositing it at the top of the resolving gel in a focused narrow band. When the stack enters the resolving gel, the increase in pH leads to a deprotonation of glycine to its anionic form increasing its speed in the gel, dissipating the discontinuity. This allows the proteins to unstack and separate through the small pore resolving gel.

The gels were prepared according to the following method and run at 300 V for about 4 h. (for Buffers and solutions see section 5.2.4.1.2):

Large stacking gel:

Acryl. [%]	H ₂ O [mL]	Rotiph. [mL]	S. gel buf. [mL]	10% SDS-soln. [μ L]	APS-soln. [μ L]	TEMED [μ L]
3,75	11	2,25	4,5	180	90	18

Large resolving gel:

Acryl. [%]	H ₂ O [mL]	Rotiph. [mL]	R. gel buf. [mL]	10% SDS-soln. [μ L]	APS-soln. [μ L]	TEMED [μ L]
10,0	21,6	18,0	13,5	540	225	22,5
12,5	17,1	22,5	13,5	540	225	22,5
15,0	12,6	27,0	13,5	540	225	22,5

Small stacking gel:

Acryl. [%]	H ₂ O [mL]	Rotiph. [mL]	S. gel buf. [mL]	10% SDS-soln. [μ L]	APS-soln. [μ L]	TEMED [μ L]
3,75	3,7	0,75	1,5	60	30	6

Large resolving gel:

Acryl. [%]	H ₂ O [mL]	Rotiph. [mL]	R. gel buf. [mL]	10% SDS-soln. [μ L]	APS-soln. [μ L]	TEMED [μ L]
10,0	7,2	6,0	4,5	180	75	7,5
12,5	5,7	7,5	4,5	180	75	7,5
15,0	4,2	9,0	4,5	180	75	7,5

5.2.4.2.2 Coomassie-staining

The Coomassie Brilliant Blue G-250 is a disulfonated Triphenylmethane dye which can form complexes with basic (Arg, His) and hydrophobic (Phe, Trp, Tyr) residues of proteins under acidic conditions. Upon binding its absorption maximum changes from 470 nm to 595 nm. This fact is used in the quantification (Bradford assay, see 5.2.4.2.3) as well as in the qualitative analysis of proteins. After separation by SDS-Page one incubates the gel with the stain for 2 min at $\sim 95\text{ }^{\circ}\text{C}$ or overnight at RT. The stain is removed, the gel is two times washed with water and covered in destainer for several hours. Unbound dye will be dissolve in the ethanolic solution and therefore be washed out of the gel. Only the protein-dye complex will remain in the gel, resulting in visible protein bands in the gel. The detection limit for proteins stained with this method lies at around 50-100 ng.

5.2.4.2.3 Bradford Assay

The Bradfor Assay is a photometric method for the quantification of proteins. It uses the Coomassie Brilliant Blue G-250 dye which is described above. To deduce the amount of protein from the absorption level at 595 nm, one has to set up a calibration curve with a known enzyme. In most cases bovine serum albumine (BSA) is used as the standard. However the complex building properties of different enzymes with the dye vary greatly. This may lead to aberrations up to 40 % which makes this assay a quick but only semiquantitative method. To set up the calibration curve a BSA-solution ($2\text{ mg}^{-1}\text{L}$ in ddH₂O) was prepared. The RotiQuantTM from Roth stock solution was diluted 1:4 with ddH₂O and filtered. The following BSA dilutions were prepared:

Table 5.2.4.3: *Dilution series for a Bradford-Assay*

Conc. BSA [$\mu\text{g}/\mu\text{L}$]	Volume H ₂ O [μL]	Volume BSA-soln. [μL]
0,00	40	0
0,25	35	5
0,50	30	10
0,75	25	15
1,00	20	20
1,50	10	30

2 mL of the Bradford solution were added to each concentration and mixed by inverting the tube. The solutions were incubated for 1 min to form a stable complex, prior to plotting the curve. The protein samples were diluted 1:5 with ddH₂O and 2 mL of the Bradford solution was added to 40 μL of the protein dilution. After 1 min incubation time the absorption was measured. Protein concentration could then be extrapolated. If the absorption values lie outside the calibration range (0.1 and 1.0 g m/L) the samples should be used in higher or lower concentrations.

5.2.4.2.4 Preparation of proteomes

Proteomes of the bacterial strains *Escherichia coli* K12, *Bacillus licheniformis* ATCC 14580, *Bacillus subtilis* 168, *Listeria welshimeri* SLCC 5334 serovar 6b and *Pseudomonas putida* KT2440 were prepared from 1 L liquid cultures harvested 1 h after transition in the stationary phase by centrifugation at 4000 g. All strains were grown in LB (Luria-Bertani broth) medium except *Listeria welshimeri*, which was maintained in BHB (brain-heart broth) medium. The bacterial cell pellets were washed with 50 mL PBS, resuspended in 20 mL PBS and lysed by sonication with a Bandelin Sonopuls with 8 x 10 sec. pulsed at 70% max.power and 4 °C.

5.2.4.2.5 Heat control

To prove selective binding of probes, heat controls can be performed. The heat denaturation of the active site should prevent any selective interaction with the probe, resulting in a lacking fluorescent signal in the gel. To proteome samples SDS in PBS was added to a final concentration of 1% (w/v). The samples were incubated at 96 °C for 10 min in a Shaker. After incubation the samples were allowed to cool to room temperature for at least 10 min before continuing with probe incubation in *in vitro* ABPP experiments.

5.2.4.2.6 Analytic proteome labeling *in vitro*

Proteome samples were adjusted to a final concentration of 1 mg/mL protein by dilution in PBS prior to probe labeling. Probes were prepared as DMSO-stocks (Acetone stocks in case of the thiiranes). The following concentrations are end concentrations in solution. The experiments were carried out in 43 μ L total volume such that once CC reagents were added, the total reaction volume was 50 μ L. Reactions were initiated by addition of the probe and allowed to incubate for 60 min at RT. For the heat controls the proteomes were denatured with 2 μ L of 21.5 % SDS at 96 °C for 5 min and were allowed to cool to room temperature before the respective probe was applied. Following probe incubation, 100 μ M of rhodamine-azide were added followed by 1 mM TCEP and 100 μ M ligand. Samples were vortexed and 1 mM CuSO₄ was added to start click reaction. The reactions were incubated at room temperature for 1 h. 50 μ L 2x SDS loading buffer were added and 50 μ L of this solution were applied to a Acrylamide-gel and a SDS-PAGE (see 5.2.4.2.1) was run. The gels were then analyzed by a Fujifilm Las-4000 Luminescent Image Analyzer (equipped with a Fujinon VRF43LMD3 lens and a 575DF20 Filter) or a Fujifilm Las-3000 Fluorescence Darkbox (equipped with a Fujinon VRF43LMD lens and a 605DF40 Filter) at 520 nm excitation light.

5.2.4.2.7 Analytic proteome labeling *in situ*

Probes were prepared as DMSO-stocks (Acetone stocks in case of the thii-
ranes). The following concentrations are end concentrations in solution. Bac-
terial cultures were grown in their respective medium at 37 °C to stationary
phase. Samples were adjusted to an OD₆₀₀ of 2 m/L and 1 mL of the respec-
tive culture spinned down at 5000 g at 4 °C for 10 min. The supernatant was
discarded and the pellet was resuspended in 99 μL PBS. 1 μL of the respective
probe-stock was added and incubated for 1 h at RT. The cells were spinned
down at 5000 g at 4 °C for 10 min and washed with 1 mL PBS two times. The
pellet was resuspended in 100 μL PBS and lysed by sonication with a Bandelin
Sonopuls with 8 x 10 sec. pulsed at 80% max. power and 4 °C. Unlysed cells
and membrane fraction were separated by centrifugation at 10.000 g. The
supernatant was transferred to a new Tube. 100 μM of rhodamine-azide were
added followed by 1 mM TCEP and 100 μM ligand. Samples were vortexed
and 1 mM CuSO₄ was added. The reactions were incubated at room tempe-
rature for 1 h. 50 μL 2x SDS loading buffer were added and 50 μL of this
solution were applied to a Acrylamide-gel and a SDS-PAGE (see 5.2.4.2.1)
was run. The gels were then analyzed by a Fujifilm Las-4000 Luminescent
Image Analyzer (equipped with a Fujinon VRF43LMD3 lens and a 575DF20
Filter) or a Fujifilm Las-3000 Fluorescence Darkbox (equipped with a Fujinon
VRF43LMD lens and a 605DF40 Filter) at 520 nm excitation light.

5.2.4.2.8 Preparative proteome labeling *in situ*

Probes were prepared as DMSO-stocks (Acetone stocks in case of the thii-
ranes). The following concentrations are end concentrations in solution. In
this experiment, negative controls are done to enable subtraction of back-
ground signals in the mass data, which are caused by unspecific enrichment
on the Streptavidin-beads. Bacterial cultures were grown in their respective
medium at 37 °C to stationary phase. Samples were adjusted to an OD₆₀₀ of
2 m/L and 5 mL of the respective culture spinned down at 5000 g at 4 °C
for 10 min. The supernatant was discarded and the pellet was resuspended in
500 μL PBS. 1 μL of the respective probe-stock was added and incubated for

1 h at RT. Negative controls were incubated with the same amount of DMSO (Acetone in case of thiiranes). The cells were then spun down at 5000 g at 4 °C for 10 min and washed with 1 mL PBS two times. The pellet was resuspended in 500 μ L PBS and lysed by sonication with a Bandelin Sonopuls with 8 x 10 sec. pulsed at 80% max. power and 4 °C. Unlysed cells and membrane fraction were separated by centrifugation at 10.000 g. The supernatant was transferred to a new Tube. If the membrane fraction was used, it was washed three times with PBS, and resuspended in 500 μ L PBS.

100 μ M of trifunctional linker (see 5.2.4.1.3) were added followed by 1 mM TCEP and 100 μ M ligand. Samples were vortexed and 1 mM CuSO_4 was added. The reactions were incubated at room temperature for 1 h. 500 μ L of ice cold Acetone were added and the solutions were allowed to precipitate for 15 min on ice. The samples were spun down for 30 min at 10.000 g and 4 °C. The supernatant was discarded and the pellet was resuspended in 500 μ L ice-cold MeOH by sonication (4 sec. 80% max. power, 4 °C) followed by centrifugation at 10.000 g for 30 min at 4 °C. The supernatant was discarded and the washing step was repeated. The pellet was resuspended in 0.2% SDS in PBS by sonication (4 sec. 80% max. power, RT). 50 μ L of the samples labeled with probes were transferred into new tubes as controls for the enrichment and stored at -20 °C. For every sample 50 μ L of the Agarose-bead stock solution were washed with 1 mL 0.2% SDS in PBS three times. The centrifugation steps have to be done carefully as the beads can be damaged at forces > 0.5 g. The SDS-protein solutions were added to the washed beads and were incubated on a rocking platform for 1 h at RT. The supernatant was discarded and the beads were washed three times each with 1 mL 0.2% SDS in PBS, 6M (aq.) Urea and PBS. 50 μ L of 2x SDS-loading buffer were added and the samples were incubated at 99 °C for 10 min to cleave the labeled enzymes from the avidin beads. The supernatant was applied to a Acrylamide-gel in the order: analytical control, enriched samples, negative control. The SDS-PAGE (see 5.2.4.2.1) was run and the gels were then analyzed by a Fujifilm Las-4000 Luminescent Image Analyzer (equipped with a Fujinon VRF43LMD3 lens and a 575DF20 Filter) or a Fujifilm Las-3000 Fluorescence Darkbox (equipped with a Fujinon VRF43LMD lens and a 605DF40 Filter) at 520 nm excitation light. If the enrichment worked the analytical controls showed weak signals, whereas the enriched samples

showed strong labeling events. The enriched bands and the negative controls were cut out of the gel by using the fluorescent readout as a template. The gel pieces were cut in small cubes and transferred in a new 500 μL tube. 500 μL ddH₂O were added and incubated for 15 min at RT in an ultrasonic bath. The supernatant was removed and 200 μL of a 1:1 (v/v) mixture of 50 mM AHC (see 5.2.4.1.2) and Acetonitrile were added to the gel pieces. The tube was incubated for 15 min at RT in an ultrasonic bath. The supernatant was discarded and 100 μL Acetonitrile were added to the gel pieces and incubated for 10 min at RT. The pieces shrink and turn white. The supernatant was discarded and 100 μL 50 mM AHC were added. After incubation for 5 min at RT, 100 μL Acetonitrile were added. After incubation for 15 min at RT supernatant was discarded and 100 μL Acetonitrile were added. After incubation for 15 min at RT the supernatant was discarded and the gel pieces were dried in a Speed-Vac for 15 min. A 10 mM DTT solution (see 5.2.4.1.2) was freshly prepared and 100 μL were added to the dried gel pieces and incubated for 45 min at 56 °C. The samples were allowed to cool down, the supernatant was removed and 100 μL of freshly prepared IAA solution (see 5.2.4.1.2) were added and incubated in the dark for 30 min at RT. The supernatant was discarded and the gel pieces were washed with 200 μL of a 1:1 (v/v) mixture of 50 mM AHC and Acetonitrile. The supernatant was removed and 100 μL Acetonitrile were added. After incubation for 10 min at RT the supernatant was removed and the gel pieces were dried in a Speed-Vac for 10 min. 100 μL of a protease solution (Trypsin or Chymotrypsin, see 5.2.4.1.2) were added and incubated at 37 °C (Trypsin) or 25 °C (Chymotrypsin) over night. The supernatant was transferred in a new tube and 100 μL of 25 mM AHC were added to the gel pieces. After incubation for 15 min on an ultrasonic bath another 100 μL Acetonitrile were added. After incubation for 15 min the 200 μL supernatant were combined with the supernatant from the previous step. 100 μL of a 5 % (v/v) formic acid solution (aq.) were added to the gel pieces and incubated for 15 min on an ultrasonic bath. Another 100 μL Acetonitrile were added and incubated on an ultrasonic bath for 15 min. The 200 μL supernatant were combined with the other supernatants. About 2 L of sheared salmon sperm DNA was added. The tubes with the combined solutions were concentrated on a Speed-Vac to a volume of $\sim 20 \mu\text{L}$. If samples dry up they can be dissolved in 1 % formic acid (aq.). samples were filtered

over centrifugal filters (VWR, modified Nylon, 0.2 μm pore size) at 10.000 g for 10 mins at RT. The solution can then be applied to ESI-mass spec analysis.

5.2.4.2.9 Bioinformatics

The digested peptides were analyzed by tandem mass spectrometry. The datasets were compared to respective databases of the sequenced organisms by the SEQUEST algorithm using the BioWorks software of Thermo Scientific which had been used in the workgroup to great success before. The search was limited to fragments of the respective digest method (Trypsin or Chymotrypsin) with not more than 3 missed cleavage sites, monoisotopic precursor ions and a mass tolerance of <10 ppm. The following additional filters were applied to find the best results according to literature:

- Xcorr values: 1.5, 2.0 and 2.5
- Number of peptides: 2
- peptide probability: $< 0,001$
- Databases: Sequenced genomes transcribed *in silico*

Curriculum vitae

Personal Data:

Date of birth: 5th of July 1983

Place of birth: München

Nationality: German

Research Experience:

04/2008 to present: **PhD thesis.**

Ludwig-Maximilians University Munich (LMU)
and Technical University Munich (TUM).

Supervisor: Prof. Dr. Stephan A. Sieber.

Title: 'Three membered rings as probes in the
activitybased protein profiling.'

09/2007 – 02/2008: **Masters thesis.**

Ludwig-Maximilians University Munich.

Supervisor: Prof. Dr. Thomas Carell.

Title: 'Synthese chemischer Sonden zur
Markierung bakterieller Phosphatasen
und Untersuchung der Dynamik von
Peptid-Deformylasen.'

08/2005 – 12/2005: **Bachelor thesis.**

Ludwig-Maximilians University Munich.

Supervisor: Prof. Dr. Thomas Carell.

Title: 'A new synthesis of the hyper-
modification queuosin'.

Education:

10/2002 – 07/2007: **Undergraduate studies, graduate studies and Master exams in chemistry and biochemistry.**
Ludwig-Maximilians University Munich.

06/2002: **Abitur**
Günter-Stöhr-Gymnasium in Munich.

Publications

Pitscheider, M., Sieber, S. A. *Chem. Comm.* **25**, 3741–3743 (2009)

Böttcher, T., Pitscheider, M. and Sieber, S.A. *Angewandte Chemie* **49**(15), 2680–2698 (2010)

Orth, R., Pitscheider, M. and Sieber, S.A. *Synthesis* **13**, 2201–2206 (2010)

List of abbreviations

ABC	ATP-binding cassette
ACN	Acetonitrile
AHC	Ammonium bicarbonate
AcOH	Acetic acid
ABPP	Activity-based protein profiling
Ala	Alanine
ATT	Attachment-sites
ATet	Anhydrotetracyclin
BHI	Brain-Heart-Infusion
BHB	Brain-Heart-broth
Boc	^t Butyl-Oxycarbonyl
Boc ₂ O	^t Butyl-Oxycarbonyl anhydride
bp	Basepairs
BSA	Bovine serum albumin
calc.	Calculated
CC	Click-Chemistry
CHCl ₃	Chloroform
CoA	Coenzyme A
Cys	Cysteine
d	Doublet
DCM	Dichloromethane
DAPE	Diaminopimelat-epimerase
DCC	Dicyclohexylcarbodiimid
DIC	Diisopropylcarbodiimid
DIPEA	Diisopropylethylamine

DMAP	4-Dimethyl-aminopyridine
DMEM	Dulbecco's Modification of Eagle's Medium
DMF	Dimethylformamid
DMSO	Dimethylsulfoxid
DNA	Deoxyribonucleic acid
dNTP	Deoxyribonucleotide triphosphate
DTT	Dithiothreitol
EARSS	European Antimicrobial Resistance Surveillance System
EDTA	Ethylen-diamine-tetraacetat
e.g.	Exempli gratia
EI-MS	Electron impact ionisation mass-spectrum
ESI-MS	Electrospray ionisation mass-spectrum
eq.	Equivalentents
EtOAc	Ethylacetate
EtOH	Ethanol
Et ₂ O	Diethylether
Et ₃ N	Triethylamine
μF	Micro-Faraday
Fab	Ketoacyl-acyl carrier protein synthase
FAS	Fatty acid biosynthesis
FCS	Fetal calf serum
FMOC	Fluorenylmethoxycarbonyl
g	Gram
h	Hour
HACAT	Human adult high calcium low temperature keratinocytes
HCl	Hydrochloric acid
HEPES	4-(2-hydroxyethyl)-1-piperazine-ethane- sulfonic acid
HOBt	N-Hydroxybenzotriazol
HPLC	High-pressure liquid-chromatography
Hz	Hertz
IEP	Intron-encoded protein

IGFS	In-gel fluorescence scanning
iPr	Isopropyl
KAS	β -ketoacyl-ACP synthases
kV	Kilo-Volt
KOH	Potassium hydroxyde
KSCN	Potassium thiocyanate
L	Liter
LB	Luria-broth
LPL	Lipoate protein ligase
LTQ	Linear trap quadrupole
m	Multiplett
mass-spec	Mass spectrometry
MALDI-MS	Matrix-assisted laser-desorption/ionization
MATE	Multidrug and toxic compound extrusion
max.	Maximal
MCPBA	Meta-chloroperoxybenzoic acid
MeOH	Methanol
mgrA	MarR family transcriptional regulator
MHz	Megahertz
MIC	Minimal inhibitory concentration
min	Minutes
mL	Milliliter
mmol	Millimole
mM	Millimolar
μ M	Micromolar
MRSA	Methicillin-resistant <i>Staphylococcus aureus</i>
MS	Mass spectrometry
MudPIT	Multidimensional protein identification technology
MTT	Methylthiazol-tetrazoliumbromid
MW	Molecular weight
NADH	Nicotinamide adenine dinucleotide
NADH	Nicotinamide adenine dinucleotide phosphate
NMR	Nuclear magnetic resonance

NaOH	Sodium hydroxide
PAGE	Polyacrylamide gel electrophoresis
PBP	Penicillin binding proteins
PCR	Polymerase chain-reaction
PDA	Photodiode Array
ppm	Parts per million
PSMF	Phenylmethyl-sulfonyl fluoride
rpm	Rotations per minute
RND	Resistance-nodulation-division
RT	Room temperature
s	Singulett
SDS	Sodiumdodecylsulfate
SCCmec	Staphylococcal chromosomal cassette mec
sec	Second
SOCl ₂	Thionyl chloride
SufC	Sulfur mobilizing ABC protein
t	Triplet
TAMRA	Carboxy-tetramethyl-rhodamine
TBTA	Tris-(5-benzyl-1H-triazol-4-yl)-methanamine
TCEP	Tris(2-Carboxyethyl)phosphine
TFA	Trifluoroacetic acid
Tris	Tris(hydroxymethyl)-aminomethane
TOF	Time of Flight
TOP	Tandem orthogonal proteolysis
TLC	Thin-layer chromatography

Bibliography

- [1] Klevens, R. M., Morrison, M. A., Nadle, J., Petit, S., Gershman, K., Ray, S., Harrison, L. H., Lynfield, R., Dumyati, G., Townes, J. M., Craig, A. S., Zell, E. R., Fosheim, G. E., McDougal, L. K., Carey, R. B., Fridkin, S. K., and for the Active Bacterial Core surveillance (ABCs) MRSA Investigators. *JAMA: The Journal of the American Medical Association* **298**(15), 1763–1771 (2007).
- [2] Rock, C., O. and Cronan, J., E. J. *Biochim. Biophys. Acta* **1302**, 1–16 (1996).
- [3] He, X. and Reynolds, K. A. *Antimicrob Agents Chemother* **46**(5), 1310–1318 (2002).
- [4] Qiu, X., Janson, C. A., Konstantinidis, A. K., Nwagwu, S., Silverman, C., Smith, W. W., Khandekar, S., Lonsdale, J., and Abdel-Meguid, S. S. *THE JOURNAL OF BIOLOGICAL CHEMISTRY* **274**(51), 36465–36471 (1999).
- [5] Miller, D., J., Zhang, Y., M., Rock, C., O., and White, S., W. Journal: To be Published.
- [6] Wang, J., Kodali, S., Lee, S. H., Galgoci, A., Painter, R., Dorso, K., Racine, F., Motyl, M., Hernandez, L., Tinney, E., Colletti, S. L., Herath, K., Cummings, R., Salazar, O., González, I., Basilio, A., Vicente, F., Genilloud, O., Pelaez, F., Jayasuriya, H., Young, K., Cully, D. F., and Singh, S. B. *Proc Natl Acad Sci U S A* **104**(18), 7612–7616 (2007).
- [7] Kutchma, A. J., Hoang, T. T., and Schweizer, H. P. *J. Bacteriol.* **181**(17), 5498–5504 (1999).
- [8] Livermore, D. M. *Int J Antimicrob Agents* **16 Suppl 1**, 3–10 (2000).

-
- [9] Marschall, L. *Im Schatten der chemischen Synthese: Industrielle Biotechnologie in Deutschland (1900-1970)*. Campus Verlag, 1 edition, (2000).
- [10] Livermore, D. M., Mushtaq, S., James, D., Potz, N., Walker, R. A., Charlett, A., Warburton, F., Johnson, A. P., Warner, M., and Henwood, C. J. *Int J Antimicrob Agents* **22**(1), 14–27 (2003).
- [11] Bachmann, G., Sulak, P. J., Sampson-Landers, C., Benda, N., and Marr, J. September (2004).
- [12] Johnson, A. P., Pearson, A., and Duckworth, G. *Journal of Antimicrobial Chemotherapy* **56**(3), 455–462 (2005).
- [13] (EARSS), E. A. R. S. S. Technical report, Euro Antimicrobial Resistance Surveillance System, (2008).
- [14] Clatworthy, A. E., Pierson, E., and Hung, D. T. *Nat Chem Biol* **3**(9), 541–548 (2007).
- [15] Cohen, M. L. *Science* **257**(5073), 1050–1055 (1992).
- [16] Arnold, Sandra, R. and Straus, Sharon, E. *Cochrane Database of Systematic Reviews* **4** (2005).
- [17] Pechere, J.-C., Hughes, D., Kardas, P., and Cornaglia, G. *Int J Antimicrob Agents* **29**(3), 245–253 (2007).
- [18] Martinez, J. L. *Science* **321**(5887), 365–367 (2008).
- [19] UCS. Technical report, UCS, (2001).
- [20] Neu, H. C. *Science* **257**(5073), 1064–1073 (1992).
- [21] Walsh, C. *Nat Rev Micro* **1**(1), 65–70 (2003).
- [22] Fuda, C., Fisher, J., and Mobashery, S. *Cellular and Molecular Life Sciences* **62**, 2617–2633 (2005).
- [23] Mwangi, M. M., Wu, S. W., Zhou, Y., Sieradzki, K., de Lencastre, H., Richardson, P., Bruce, D., Rubin, E., Myers, E., Siggia, E. D., and Tomasz, A. *Proceedings of the National Academy of Sciences* **104**(22), 9451–9456 (2007).

-
- [24] Ito, T., Okuma, K., Ma, X. X., Yuzawa, H., and Hiramatsu, K. February (2003).
- [25] Katayama, Y., Ito, T., and Hiramatsu, K. *Antimicrob. Agents Chemother.* **45**(7), 1955–1963 (2001).
- [26] Heisig, P. *Pharmazie in unserer Zeit* **35**(5), 400–408 (2006).
- [27] Lubelski, J., Konings, W. N., and Driessen, A. J. M. *Microbiol Mol Biol Rev* **71**(3), 463–476 (2007).
- [28] Kuroda, T. and Tsuchiya, T. *Biochimica et Biophysica Acta* **1794**(5), 763–768 (2009).
- [29] Li, X.-Z. and Nikaido, H. *Drugs* **69**(12), 1555–1623 (2009).
- [30] Li, X.-Z. and Nikaido, H. *Drugs* **64**(2), 159–204 (2004).
- [31] Nikaido, H. and Takatsuka, Y. *Biochim Biophys Acta* **1794**(5), 769–781 (2009).
- [32] Tseng, T. T., Gratwick, K. S., Kollman, J., Park, D., Nies, D. H., Goffeau, A., and Saier, Jr, M. *J Mol Microbiol Biotechnol* **1**(1), 107–125 (1999).
- [33] Hanaki, H., Kuwahara-Arai, K., Boyle-Vavra, S., Daum, R. S., Labischinski, H., and Hiramatsu, K. *Journal of Antimicrobial Chemotherapy* **42**(2), 199–209 (1998).
- [34] Rose, W. E., Knier, R. M., and Hutson, P. R. *Journal of Antimicrobial Chemotherapy* **65**(10), 2149–2154 (2010).
- [35] Jacoby, G. A. and Munoz-Price, L. S. *New England Journal of Medicine* **352**(4), 380–391 (2005).
- [36] Abraham, E. P. and Chain, E. *Nature* **146**, 837–837 (1940).
- [37] Ghuysen, J. M. *Annu Rev Microbiol* **45**, 37–67 (1991).
- [38] Bush, K. *Clin Microbiol Rev* **1**(1), 109–123 (1988).
- [39] Fields, S. *Science* **291**, 1221–1224 (2001).

-
- [40] Taniguchi, Y., Choi, P. J., Li, G.-W., Chen, H., Babu, M., Hearn, J., Emili, A., and Xie, X. S. *Science* **329**(5991), 533–538 (2010).
- [41] Evans, M. and Cravatt, B. *Chem Rev.* **106**(8), 3279–3301 (2006).
- [42] Cravatt, B. F., Wright, A. T., and Kozarich, J. W. *Annu Rev Biochem* **77**, 383–414 (2008).
- [43] Joyce, J. A., Baruch, A., Chehade, K., Meyer-Morse, N., Giraudo, E., Tsai, F.-Y., Greenbaum, D. C., Hager, J. H., Bogoy, M., and Hanahan, D. *Cancer Cell* **5**(5), 443–453 (2004).
- [44] Fonovic, M. and Bogoy, M. *Curr Pharm Des* **13**(3), 253–261 (2007).
- [45] Sieber, S., Niessen, S., Hoover, H., and Cravatt, B. *Nat. Chem Biol.* **2**(5), 274–281 (2006).
- [46] Saghatelian, A., Jessani, N., Joseph, A., Humphrey, M., and Cravatt, B. F. *Proc Natl Acad Sci U S A* **101**(27), 10000–10005 (2004).
- [47] Dorman, G. and Prestwich, G. *Biochemistry* **33**(19), 5661–5673 (1994).
- [48] Hein, J., E. and Fokin, V., V. *Chem. Soc. Rev.* **39**, 1302–1315 (2010).
- [49] Kidd, D., Liu, Y., and Cravatt, B. F. *Biochemistry* **40**(13), 4005–4015 (2001).
- [50] Patricelli, M. P., Giang, D. K., Stamp, L. M., and Burbaum, J. J. *Proteomics* **1**(9), 1067–1071 (2001).
- [51] Adam, G. C., Cravatt, B. F., and Sorensen, E. J. *Chem Biol* **8**(1), 81–95 (2001).
- [52] Drahl, C., Cravatt, B., and Sorensen, E. *Angew. Chem.* **44**, 5788–5809 (2005).
- [53] Böttcher, T. and Sieber, S. A. *Angewandte Chemie* **47**, 4600–4603 (2008).
- [54] Böttcher, T. and Sieber, S. A. *ChemBioChem* **10**(4), 663–666 (2009).
- [55] Barrett, A. J., Kembhavi, A. A., Brown, M. A., Kirschke, H., Knight, C. G., Tamai, M., and Hanada, K. *Biochem J* **201**(1), 189–198 (1982).

-
- [56] Weerapana, E., Simon, G. M., and Cravatt, B. F. *Nat Chem Biol* **4**(7), 405–407 (2008).
- [57] Pitscheider, M. and Sieber, S. A. *Chem Commun (Camb)* (25), 3741–3743 (2009).
- [58] Böttcher, T. and Sieber, S. A. *Journal of the American Chemical Society* **132**(20), 6964–6972 (2010).
- [59] Adam, G. C., Sorensen, E. J., and Cravatt, B. F. *Nat Biotechnol* **20**(8), 805–809 (2002).
- [60] Böttcher, T. and Sieber, S. A. *Journal of the American Chemical Society* **130**(44), 14400–14401 (2008).
- [61] Liu, Y., Patricelli, M. P., and Cravatt, B. F. *Proc Natl Acad Sci U S A* **96**(26), 14694–14699 (1999).
- [62] Staub, I. and Sieber, S. A. *J Am Chem Soc* **131**(17), 6271–6276 (2009).
- [63] Staub, I. and Sieber, S. A. *J Am Chem Soc* **130**(40), 13400–13409 (2008).
- [64] Li, K.-Y., Tu, H., and Ray, A. K. *Langmuir* **21**(9), 3786–3794 (2005).
- [65] Kebarle, P. and Verkerk, U. H. *Mass Spectrometry Reviews* **28**(6), 898–917 (2009).
- [66] Cottrell, J. S. and Greathead, R. J. *Mass Spectrometry Reviews* **5**(3), 215–247 (1986).
- [67] Wollnik, H. *Mass Spectrometry Reviews* **12**(2), 89–114 (1993).
- [68] Hu, Q., Noll, R. J., Li, H., Makarov, A., Hardman, M., and Graham Cooks, R. *Journal of Mass Spectrometry* **40**(4), 430–443 (2005).
- [69] Comisarow, M. B. and Marshall, A. G. *Chemical Physics Letters* **25**(2), 282–283 (1974).
- [70] Marshall, A. G., Hendrickson, C. L., and Jackson, G. S. *Mass Spectrometry Reviews* **17**(1), 1–35 (1998).

-
- [71] Eng, J. K., Fischer, B., Grossmann, J., and Maccoss, M. J. *J Proteome Res* **7**(10), 4598–4602 (2008).
- [72] Koenig, T., Menze, B. H., Kirchner, M., Monigatti, F., Parker, K. C., Patterson, T., Steen, J. J., Hamprecht, F. A., and Steen, H. *Journal of Proteome Research* **7**(9), 3708–3717 (2008).
- [73] Cragg, G. M., Newman, D. J., and Snader, K. M. *Journal of Natural Products* **60**(1), 52–60 (1997).
- [74] Cragg, G. M. and Newman, D. J. *Expert Opin Investig Drugs* **9**(12), 2783–2797 (2000).
- [75] Newman, D. J., Cragg, G. M., and Snader, K. M. *J Nat Prod* **66**(7), 1022–1037 (2003).
- [76] Breinbauer, R., Vetter, I. R., and Waldmann, H. *Angewandte Chemie International Edition* **41**(16), 2878–2890 (2002).
- [77] Simmons, H. E. and Smith, R. D. *Journal of the American Chemical Society* **81**(16), 4256–4264 (1959).
- [78] Charette, A., B. and Beauchemin, A. *Simmons-Smith Cyclopropanation Reaction*. John Wiley & Sons, Inc. (2004).
- [79] Simmons, H., E., Cairns, T., L., Vladuchick, S., A., and Hoiness, C, M. *Organic Reactions* **20** (1973).
- [80] Grieco, P. A., Oguri, T., Wang, C.-L. J., and Williams, E. *The Journal of Organic Chemistry* **42**(25), 4113–4118 (1977).
- [81] Paulissen, R., Hubert, A. J., and Teyssie, P. *Tetrahedron Letters* **13**(15), 1465–1466 (1972).
- [82] Mende, U., Radüchel, B., Skuballa, V., and Vorbrüggen, H. *Tetrahedron Letters* **16**(9), 629–632 (1975).
- [83] Corey, E. J. and Chaykovsky, M. *Journal of the American Chemical Society* **87**(6), 1353–1364 (1965).
- [84] McCoy, L. L. *Journal of the American Chemical Society* **80**(24), 6568–6572 (1958).

-
- [85] Knunyants, I. *Voltage molecules*, volume Chemical Encyclopedia. 3. Soviet encyclopedia, (1988).
- [86] Grabowsky, S., Schirmeister, T., Paulmann, C., Pfeuffer, T., and Luger, P. *The Journal of Organic Chemistry* **76**(5), 1305–1318 (2011).
- [87] Prilezhaev, N. *Ber. Dtsch. chem. Ges.* **42**, 4811–48 (1909).
- [88] Bartlett, P. D. *Rec. Chem. Prog.* **11**, 47–51 (1950).
- [89] Katsuki, T. and Sharpless, K. B. *Journal of the American Chemical Society* **102**(18), 5974–5976 (1980).
- [90] Jacobsen, E. N., Zhang, W., Muci, A. R., Ecker, J. R., and Deng, L. *Journal of the American Chemical Society* **113**(18), 7063–7064 (1991).
- [91] Garcia-Bosch, I., Company, A., Fontrodona, X., Ribas, X., and Costas, M. *Organic Letters* **10**(11), 2095–2098 (2008).
- [92] Wang, Z.-X., Tu, Y., Frohn, M., Zhang, J.-R., and Shi, Y. *Journal of the American Chemical Society* **119**(46), 11224–11235 (1997).
- [93] Mori, K. and Iwasawa, H. *Tetrahedron* **36**, 87–90 (1980).
- [94] Saito, S., Komada, K., and Moriwake, T. *Org. Synth. Coll.* **9**, 220 (1998).
- [95] Staudinger, H. and Siegwart, J. *Helvetica Chimica Acta* **3**(1), 833–840 (1920).
- [96] Chew, W. and Harpp, D., N. *Journal of Sulfur Chemistry* **15:1**, 1–39 (1993).
- [97] Cox, J. D. *Tetrahedron* **19**(7), 1175–1184 (1963).
- [98] Katritzky, Alan, R. *Comprehensive Heterocyclic Chemistry III: Aziridines and Azirines: Monocyclic*, volume 1. Elsevier Books, (2008).
- [99] Warren, C. and Harp, D. N. *Sulfur reports* **15**, 1–39 (1993).
- [100] Ismail, F. M., Levitsky, D. O., and Dembitsky, V. M. *European Journal of Medicinal Chemistry* **44**(9), 3373–3387 (2009).

-
- [101] Eicher, T., Hauptmann, S., and Speicher, A. *The Chemistry of Heterocycles: Structure, Reactions, Syntheses, and Applications, Second Edition*. Wiley-VCH Verlag GmbH & Co. KGaA, (2004).
- [102] Hassner, A. *The Chemistry of Heterocyclic Compounds, Small Ring Heterocycles: Aziridines, Azirines, Thiiranes, Thiirenes: Aziridines, Azirines, Thiiranes, Thiirenes Pt. 1*. John Wiley & Sons, (1983).
- [103] Peppard, T., L., Sharpe, F., R., and Elvidge, J., A. *J. Chem. Soc., Perkin Trans.* **1**, 311–313 (1980).
- [104] Chuang, H. L., Mukhtar, H., and Bresnick, E. *J. Natl. Cancer Inst.* **60**, 321–325 (1978).
- [105] Tookey, H., L. *Can. J. Biochem.* **51**(12), 1654–60 (1973).
- [106] Cole, R., A. *Phytochem.* **17**, 1563–1565 (1978).
- [107] Adams, E., P., Ayad, K., N., Doyle, F. P., Holland, D. O., Hunter, W. H., Nayler, J., H. C., and Queen, A. *J. Chem. Soc.* , 2665–2673 (1960).
- [108] Adlgasser, K., Hahn, H., and Zenk, R. *Liebigs Annalen der Chemie* **4**(4), 283–288 (1987).
- [109] Strausz, O., P. and Gunning, H., E. *J. Am. Chem. Soc.* **84**, 4080 (1962).
- [110] Christensen, J. E. and Goodman, L. *Journal of the American Chemical Society* **82**(17), 4738–4739 (1960).
- [111] Creighton, A. M. and Owen, L. N. *J. Chem. Soc.* , 1024–1029 (1960).
- [112] Harding, J. S. and Owen, L. N. *J. Chem. Soc.* , 1528–1536 (1954).
- [113] Colthoff, W., (1939).
- [114] Doyle, F. P., Holland, D. O., Mansford, K. R. L., Nayler, J. H. C., and Queen, A. *J. Chem. Soc.* , 2660–2665 (1960).
- [115] Dachlauer, K. and Jackel, L., (1936).
- [116] Price, C. C. and Kirk, P. F. *Journal of the American Chemical Society* **75**(10), 2396–2400 (1953).

-
- [117] Bordwell, F. G. and Andersen, H. M. *Journal of the American Chemical Society* **75**(20), 4959–4962 (1953).
- [118] Bordwell, F. G., Andersen, H. M., and Pitt, B. M. *Journal of the American Chemical Society* **76**(4), 1082–1085 (1954).
- [119] Chan, T. H. and Finkenbine, J. R. *Journal of the American Chemical Society* **94**(8), 2880–2882 (1972).
- [120] Riedel. *Anorganische Chemie*. de Gruyter ;Berlin, New York, 4. ed. edition, (1999).
- [121] Vedeneyev, L., Gurvich, V., Kondrat'yev, V., Medvedev, and Frankevich, Y. *Bond energies, ionization potentials and electron affinities*. St. Martin's Press, New York, (1966).
- [122] Coleman, R., S., Burk, C., H., Navarro, A., Brueggemeier, R., W., and Diaz-Cruz, E. S. *Org. Lett.* **4**, 3545–3548 (2002).
- [123] Reusser, F. *Biochemistry* **16**(15), 3406–12 (1977).
- [124] Argoudelis, A., D., Reusser, F., and Whaley, H., A. *Journal of Antibiotics* **29**(10), 1001–1006 (1976).
- [125] Tomasz, M. *Chemistry & Biology* **2**(9), 575–579 (1995).
- [126] Mayer, M. F. and Hossain, M. M. *The Journal of Organic Chemistry* **63**(20), 6839–6844 (1998).
- [127] Davis, F. A., Liu, H., Zhou, P., Fang, T., Reddy, G. V., and Zhang, Y. *The Journal of Organic Chemistry* **64**(20), 7559–7567 (1999).
- [128] Legters, J., Thijs, L., and Zwanenburg, B. *Tetrahedron Letters* **30**(36), 4881–4884 (1989).
- [129] Zamboni, R. and Rokach, J. *Tetrahedron Letters* **24**(4), 331–334 (1983).
- [130] Staudinger, H. and Meyer, J. *Helvetica Chimica Acta* **2**(1), 635–646 (1919).
- [131] Wenker, H. *Journal of the American Chemical Society* **57**(11), 2328–2328 (1935).

-
- [132] Gabriel, S. *Berichte der deutschen chemischen Gesellschaft* **21**(1), 1049–1057 (1888).
- [133] Osborn, H. M. I. and Sweeney, J. *Tetrahedron: Asymmetry* **8**(11), 1693–1715 (1997).
- [134] Dauban, P., SaniÁlre, L., Tarrade, A., and Dodd, R. H. *Journal of the American Chemical Society* **123**(31), 7707–7708 (2001).
- [135] Han, H., Park, S., B., Kim, S., K., and Chang, S. *J. Org. Chem* **73**, 2862–2870 (2008).
- [136] McConaghy, J. S. and Lwowski, W. *Journal of the American Chemical Society* **89**(10), 2357–2364 (1967).
- [137] Oae, S. and Furukawa, N. *Synthesis* **1**, 30–32 (1976).
- [138] Zimmerman, H., E., Singer, L., and Thyagarajan, B. S. *Journal of the American Chemical Society* **81**(1), 108–116 (1959).
- [139] Breuning, A., Vicik, R., and Schirmeister, T. *Tetrahedron: Assymetry* **14**, 3301–3312 (2003).
- [140] Moisan, B., Robert, A., and Foucaud, A. *Tetrahedron* **30**(16), 2867–2872 (1974).
- [141] Schiess, P. and Wisson, M. *Helvetica Chimica Acta* **57**(6), 1692–1703 (1974).
- [142] Bartók, M. and Láng, K., L. *Chemistry of Heterocyclic Compounds: Small Ring heterocycles, Part III*. Interscience, John Wiley & Sons, Inc., (1985).
- [143] Haddadin, M. J. and Hassner, A. *The Journal of Organic Chemistry* **38**(20), 3466–3471 (1973).
- [144] Haire, M. J. and Boswell, G. A. *The Journal of Organic Chemistry* **42**(26), 4251–4256 (1977).
- [145] Bartók, M. and Láng, K., L. *Chemistry of Heterocyclic Compounds: Small Ring heterocycles, Part I*. Interscience, John Wiley & Sons, Inc., (1985).

-
- [146] Birchall, J., M., Fields, R., Haszeldine, Robert, N., , and Kendall, Norman, T. *J. Chem. Soc., Perkin Trans.* **1**, 1 (1973).
- [147] Tomilov, Y. V., Shulishov, E. V., Yarygin, S. A., and Nefedov, O. M. *Russian Chemical Bulletin* **44**, 2109–2113 (1995).
- [148] Berson, J., A. *Annual Review of Physical Chemistry* **28**, 111–132 (1977).
- [149] Kalwisch, I., Xingya, L., Gottstein, J., and Huisgen, R. *Journal of the American Chemical Society* **103**(23), 7032–7033 (1981).
- [150] Korchevin, N., A., Usov, V., A., and Voronkov, M., G. *Chem. Heterocycl. Cmpds.* **10**, 623 (1974).
- [151] Chew, W., Hynes, R. C., and Harpp, D. N. *The Journal of Organic Chemistry* **58**(16), 4398–4404 (1993).
- [152] Chew, W. and Harpp, D. N. *Tetrahedron Letters* **33**(1), 45–48 (1992).
- [153] Ohta, T., Hirakawa, H., Morikawa, K., Maruyama, A., Inose, Y., Yamashita, A., Oshima, K., Kuroda, M., Hattori, M., Hiramatsu, K., Kuhara, S., and Hayashi, H. *DNA Research* **11**(1), 51–56 (2004).
- [154] Chatterjee, S. S., Hossain, H., Otten, S., Kuenne, C., Kuchmina, K., Machata, S., Domann, E., Chakraborty, T., and Hain, T. *Infection and Immunity* **74**(2), 1323–1338 (February 2006).
- [155] Perkins, D. N., Pappin, D. J. C., Creasy, D. M., and Cottrell, J. S. *ELECTROPHORESIS* **20**(18), 3551–3567 (1999).
- [156] McHugh, L. and Arthur, J. W. *PLoS Comput Biol* **4**(2), e12 02 (2008).
- [157] Yates, John, R. and Eng, Jimmy, K. (2000).
- [158] Institute, T. T. E. T. *BioWorks 3.0 Manual*. Thermo Electron Training Institute, (2011).
- [159] Kim, D. J., Kim, K. H., Lee, H. H., Lee, S. J., Ha, J. Y., Yoon, H. J., and Suh, S. W. *Journal of Biological Chemistry* **280**(45), 38081–38089 (2005).

-
- [160] Born, T. L. and Blanchard, J. S. *Current Opinion in Chemical Biology* **3**(5), 607 – 613 (1999).
- [161] Layer, G., Gaddam, S. A., Ayala-Castro, C. N., Ollagnier-de Choudens, S., Lascoux, D., Fontecave, M., and Outten, F. W. *Journal of Biological Chemistry* **282**(18), 13342–13350 (2007).
- [162] Ravcheev, D. A., Best, A. A., Tintle, N., DeJongh, M., Osterman, A. L., Novichkov, P. S., and Rodionov, D. A. *Journal of Bacteriology* **193**(13), 3228–3240 (2011).
- [163] Mosmann, T. *J Immunol Methods* **65**(1-2), 55–63 (1983).
- [164] Berridge, M., V. and Tan, A., S. *Archiv. Biochem. Biophys* **303**, 474–482 (1993).
- [165] Berridge, M., V., Tan, A., S., McCoy, K., D., and Wang, R. *Biochemica* **4**, 14–19 (1996).
- [166] Pizer, E. S., Wood, F. D., Pasternack, G. R., and Kuhajda, F. P. *Cancer Research* **56**(4), 745–751 (1996).
- [167] Elias, J. E., Haas, W., Faherty, B. K., and Gygi, S. P. *Nat Meth* **2**(9), 667–675 September (2005).
- [168] Moore, R. E., Young, M. K., and Lee, T. D. *Journal of the American Society for Mass Spectrometry* **13**(4), 378 – 386 (2002).
- [169] Kislinger, T., Rahman, K., Radulovic, D., Cox, B., Rossant, J., and Emili, A. *Molecular & Cellular Proteomics* **2**(2), 96–106 (2003).
- [170] Elias, J. E. and Gygi, S. P. *Nat Meth* **4**(3), 207–214 March (2007).
- [171] Gupta, N., Bandeira, N., Keich, U., and Pevzner, P. *Journal of The American Society for Mass Spectrometry* **22**, 1111–1120 (2011). 10.1007/s13361-011-0139-3.
- [172] ThermoFischer. *Database search with Sequest and Mascot*. ThermoFischer, (2011).
- [173] Gajiwala, K. S., Margosiak, S., Lu, J., Cortez, J., Su, Y., Nie, Z., and Appelt, K. *FEBS Letters* **583**(17), 2939–2946 (2009).

-
- [174] Allen, E. E. and Bartlett, D. H. *J. Bacteriol.* **182**(5), 1264–1271 (2000).
- [175] Lai, C.-Y. and Cronan, J. E. *Journal of Biological Chemistry* **278**(51), 51494–51503 (2003).
- [176] Campbell, J. W. and Cronan, J. E. *Annual Review of Microbiology* **55**(1), 305–332 (2001).
- [177] Wang, J., Soisson, S. M., Young, K., Shoop, W., Kodali, S., Galgoci, A., Painter, R., Parthasarathy, G., Tang, Y. S., Cummings, R., Ha, S., Dorso, K., Motyl, M., Jayasuriya, H., Ondeyka, J., Herath, K., Zhang, C., Hernandez, L., Allocco, J., Basilio, n., Tormo, J. R., Genilloud, O., Vicente, F., Pelaez, F., Colwell, L., Lee, S. H., Michael, B., Felcetto, T., Gill, C., Silver, L. L., Hermes, J. D., Bartizal, K., Barrett, J., Schmatz, D., Becker, J. W., Cully, D., and Singh, S. B. *Nature* **441**(7091), 358–361 (2006).
- [178] Sigma Aldrich. *TargeTron Gene Knockout System*, (2011).
- [179] Aslanidis, C. and de Jong, P. J. *Nucleic Acids Research* **18**(20), 6069–6074 (1990).
- [180] Joseph, P., Fantino, J. R., Herbaud, M. L., and Denizot, F. *FEMS Microbiol Lett* **205**(1), 91–97 (2001).
- [181] Korn, A. C. and Moroder, L. *J Chem Res (S)* **3**, 102–103 (1995).
- [182] Bezmenova, T. ., Tukhar', A. A., Bezuglyi, Y. V., Slutskii, V. I., and Nosova, V. M. *Chemistry of Heterocyclic Compounds* **19**, 1287–1288 (1983).
- [183] Csuk, R. and von Scholz, Y. *Tetrahedron* **50**, 10431–10442 (1994).
- [184] Breslauer, K. J., Frank, R., Blocker, H., and Marky, L. A. *Proc. Nat. Acad. Sci.* **83**, 3746–50 (1986).
- [185] Conley, L., C. and Saunders, J., R. *Mol. Gen. Genet.* **194**(1-2), 211–218 (1984).
- [186] Alberts, B. *Molecular Biology of the Cell*. New York: Garland Science, (2002).

-
- [187] Lambowitz, A. M. and Zimmerly, S. *Annu Rev Genet* **38**, 1–35 (2004).
- [188] Murphy, K. C., Campellone, K. G., and Poteete, A. R. *Gene* **246**(1-2), 321–330 (2000).
- [189] Lee, E. C., Yu, D., de Velasco, J. M., Tessarollo, L., Swing, D. A., Court, D. L., Jenkins, N. A., and Copeland, N. G. *Genomics* **73**(1), 56–65 (2001).
- [190] Court, D. L., Sawitzke, J. A., and Thomason, L. C. *Annu Rev Genet* **36**, 361–388 (2002).
- [191] Ellis, R. W. *J Antimicrob Chemother* **51**(3), 739–740 (2003).
- [192] Sawitzke, J. A., Costantino, N., Li, X.-T., Thomason, L. C., Bubunencko, M., Court, C., and Court, D. L. *J Mol Biol* **407**(1), 45–59 (2011).